



National Library
of Canada

Bibliothèque nationale
du Canada

Canadian Theses Service

Service des thèses canadiennes

Ottawa, Canada
K1A 0N4

NOTICE

The quality of this microform is heavily dependent upon the quality of the original thesis submitted for microfilming. Every effort has been made to ensure the highest quality of reproduction possible.

If pages are missing, contact the university which granted the degree.

Some pages may have indistinct print especially if the original pages were typed with a poor typewriter ribbon or if the university sent us an inferior photocopy.

Reproduction in full or in part of this microform is governed by the Canadian Copyright Act, R.S.C. 1970, c. C-30, and subsequent amendments.

AVIS

La qualité de cette microforme dépend grandement de la qualité de la thèse soumise au microfilmage. Nous avons tout fait pour assurer une qualité supérieure de reproduction.

S'il manque des pages, veuillez communiquer avec l'université qui a conféré le grade.

La qualité d'impression de certaines pages peut laisser à désirer, surtout si les pages originales ont été dactylographiées à l'aide d'un ruban usé ou si l'université nous a fait parvenir une photocopie de qualité inférieure.

La reproduction, même partielle, de cette microforme est soumise à la Loi canadienne sur le droit d'auteur, SRC 1970, c. C-30, et ses amendements subséquents.



National Library
of Canada

Bibliothèque nationale
du Canada

Canadian Theses Service

Service des thèses canadiennes

Ottawa, Canada
K1A 0N4

The author has granted an irrevocable non-exclusive licence allowing the National Library of Canada to reproduce, loan, distribute or sell copies of his/her thesis by any means and in any form or format, making this thesis available to interested persons.

The author retains ownership of the copyright in his/her thesis. Neither the thesis nor substantial extracts from it may be printed or otherwise reproduced without his/her permission.

L'auteur a accordé une licence irrévocable et non exclusive permettant à la Bibliothèque nationale du Canada de reproduire, prêter, distribuer ou vendre des copies de sa thèse de quelque manière et sous quelque forme que ce soit pour mettre des exemplaires de cette thèse à la disposition des personnes intéressées.

L'auteur conserve la propriété du droit d'auteur qui protège sa thèse. Ni la thèse ni des extraits substantiels de celle-ci ne doivent être imprimés ou autrement reproduits sans son autorisation.

ISBN 0-315-56339-7

Canada

Stochastic Model for Flame Propagation
at Lean Ignition Limit and Partial Burn Limit
of Spark Ignition Engines

by

In-Heng Martin Lei

A Thesis presented to
the School of Graduate Studies at the University of Ottawa
in partial fulfillment of the requirements for the degree
of
Master of Applied Science
in
Mechanical Engineering



In-Heng Martin, Ottawa, Canada, 1989



UNIVERSITÉ D'OTTAWA
UNIVERSITY OF OTTAWA

**Stochastic Model for Flame Propagation
at Lean Ignition Limit and Partial Burn Limit
of Spark Ignition Engines**

**Dr. Roger Milane
Supervisor**

**In-Heng Martin Lei
Candidate**

ABSTRACT

A phenomenological model with stratification of temperature and species concentration was developed to simulate engine misfire. The fuel mixture in the combustion chamber is divided into equal mass particles, each of which has its own temperature and species concentration. The model incorporates the coalescence dispersion model for finite rate mixing and the mass entrainment model for flame propagation. The chemical rate of the first order reaction for the combustion of propane in air is used to formulate a set of ordinary differential equations for the evolution of temperature and species concentration. An ODE solver of the predictor corrector method was developed to solve the equations.

Two types of engine misfire limits were simulated : the ignition limit and partial burn limit. The model was tested extensively for the ignition limit, including the effect of turbulence intensity, intake temperature and pressure, equivalence ratio, ignition energy, spark gap distance, and engine RPM. The turbulence intensity, intake temperature and equivalence ratio were observed to have the strongest effect on ignition limit. Examples of partial burn cycles were also obtained. The concept of age mixing was implemented as an attempt to simulate partial burn more adequately, but more studies are required for the age mixing model to predict partial burn. Computation of a complete cycle has not been performed in any of the tests due to limited computing time. However, conclusion can still be reached with about 20 degree crank angles of result after ignition for the case of ignition limited misfire, and about 40 degree crank angles of result after ignition for the case of partial burn. The model in its present form has not been calibrated with actual engine experiments due to the lack of complete engine specifications in available literature. Such calibration has to be performed for model applications on any specific engine.

ACKNOWLEDGEMENT

The author would like to express his deepest appreciation and gratitude to Professor Roger Milane of the Department of Mechanical Engineering at the University of Ottawa, for his help and support throughout the project and the preparation of this thesis.

NOMENCLATURE

A	Pre-exponential constant
A_c	Flame front area
a	Exponent of fuel
b	Exponent of oxygen
C	Constant of mixing frequency
C_m	Mean molecular speed of chain carriers
C_v	Specific heat at constant volume
D	Velocity divergence
d	Electrode diameter
E	Activation energy
E_b	Internal energy of the burned gas
E_{ign}	Ignition energy
E_T	Dissipation of turbulent kinetic energy
E_u	Internal energy of the unburned gas
F_1, F_2, F_3	Fuel fraction of a particle
$F(r_c)$	Function of iteration for the flame radius
$g_i(t)$	Derivative of the dependent variable
H_{last}	Last time step
H_{new}	Current time step
h	Chamber height
K	Dimensionless parameter of pressure
K_T	Turbulent kinetic energy
L	Integral length scale
l	Spark gap distance
M_r	Mean molecular weight

M_x	Molecular weight of species x
m	Mass of a particle
m_e	Entrained mass
N	Number of particles in the chamber
N_i	Number of moles per gram of mixture in particle i
N_m	Number of mixing pairs
N_t	Number of particles in the reactor
n	Number of moles of mixture
P	Pressure
P_{in}	Pressure at the closing of the intake valve
P_r	Reference pressure
Q	Heat transfer to the system
q	Specific heat transfer to the system
R	Universal gas constant
R_b	Gas constant of the burned gas
R_c	Bore radius of the chamber
R_u	Gas constant of the unburned gas
r_e	Entrainment radius
r_s	Spark location offset
S	Error to tolerance ratio
S_l	Laminar flame speed
T_b	Burned gas temperature
T_i	Temperature of particle i
T_{in}	Temperature at the closing of the intake valve
T_m	Mean temperature of the reaction zone
T_u	Unburned gas temperature
Δt	Time interval
U	Internal energy

U_1, U_2, U_3	Internal energy of a particle
U_{mi}	Internal energy per mole of mixture for particle i
u	Specific internal energy
u_e	Entrainment velocity
u'	Turbulence intensity
V	Chamber volume
V_b	Burned gas volume
V_c	Entrained volume
V_{in}	Chamber volume at the closing of the intake valve
Vol_1, Vol_2, Vol_3	Volume of a particle
V_p	Total volume of the particles
V_T	Actual chamber volume
v	Specific volume of a particle
W	Work done by the system
w	Moles of water per gram of mixture
X	Moles of fuel per cc of mixture
x	Moles of fuel per gram of mixture
$x_i(t)$	Dependent variable of an ordinary differential equation
Y	Moles of oxygen per cc of mixture
Y_f	Mole fraction of fuel
Y_{O_2}	Mole fraction of oxygen
y	Moles of oxygen per gram of mixture
z	Moles of carbon dioxide per gram of mixture
α	Exponent of pressure ratio
ϵ	Error bound
γ	Ratio of specific heats
ν	Moles of nitrogen per gram of mixture
ρ	Density

τ_i

Equilibration time

ω

Mixing frequency

TABLE OF CONTENTS

Abstract	i
Acknowledgements	ii
Nomenclature	iii
Table of Contents	vii
List of Tables	x
List of Figures	xi
Chapter 1 Introduction	1
1.1 General Overview	1
1.2 Literature Survey	2
1.3 Objective	5
1.4 Model Approach	6
Chapter 2 Supporting Models	9
2.1 Ignition	9
2.2 Turbulent Entrainment	12
2.3 Turbulent Mixing	14
2.3.1 Mixing Frequency	15
2.3.2 Random Selection of Mixing Pairs	15
2.3.3 Binary Mixing	16
2.4 Governing Equations for Thermodynamic States	17
2.4.1 Chemical Rate Equations	17

2.4.2 Rate of Temperature Rise of a Burning/Particle	19
2.4.3 Rate of Pressure Rise of the System	22
Chapter 3 Method of Solution	27
3.1 Ignition	27
3.2 Turbulent Entrainment	30
3.3 Binary Mixing	31
3.4 Governing Equations for Thermodynamic States	33
3.4.1 Ordinary Differential Equation Solvers	34
3.4.2 The Adopted Method	36
3.5 Overall Solution Procedure	39
3.6 Approximation of Pressure Derivative	41
3.7 Selection of Time Interval	43
Chapter 4 Results and Discussion	45
4.1 Empirical Constants in Model	45
4.2 Turbulence Intensity	47
4.3 Intake Pressure	49
4.4 Intake Temperature	50
4.5 Fuel Equivalence Ratio	52
4.6 Spark Advance	53
4.7 Ignition Energy	54
4.8 Spark Gap Distance	55
4.9 Engine Speed	55
4.10 Number of Ignited Particles	56
4.11 Partial Burn Limit	57
4.12 Age Mixing	59
Chapter 5 Conclusion and Recommendation	61

5.1 Conclusion	61
5.1.1 Ignition Limit	61
5.1.2 Partial Burn and Age Mixing	62
5.2 Recommendation	63
References	65
Appendix A Main Program Listing	106
Appendix B Thermodynamic Properties of Particles	113
Appendix C Subroutine SPEED	115
Appendix D Subroutine MIXFRO	120
Appendix E Subroutine RANMIX	123
Appendix F Subroutine KINET	124
Appendix G Function VTO	131
Appendix H Subroutine <u>CLDPRD</u> and UPROP	132
Appendix I Subroutine SHAPE	138
Appendix J Subroutine ISCOMP	140
Appendix K Subroutine CODE	142
Appendix L Subroutine AGEMIX	144

LIST OF TABLES

Table 1. Engine Specifications	70
Table 2. Testing Conditions : Variations of Empirical Constants	71
Table 3. Testing Conditions : Variation of Turbulence Intensity	72
Table 4. Testing Conditions : Variation of Pressure	73
Table 5. Testing Conditions : Variation of Pressure and Turbulence Intensity	74
Table 6. Testing Conditions : Variation of Intake Temperature	75
Table 7. Testing Conditions : Variation of Equivalence Ratio	76
Table 8. Testing Conditions : Variation of Spark Advance	77
Table 9. Testing Conditions : Variation of Ignition Energy	78
Table 10. Testing Conditions : Variation of Spark Gap	79
Table 11. Testing Conditions : Variation of Engine Speed	80
Table 12. Testing Conditions : Variation of Number of Ignited Particles	81
Table 13. Testing Conditions : Partial Burn	82
Table 14. Coefficients of Polynomial Fit of Thermodynamic Properties	83

LIST OF FIGURES

Figure 1. Flame Geometry in the Combustion Chamber	84
Figure 2. Mass Burn Fraction versus Crank Angle for different Mixing Frequency Constant	85
Figure 3. Mass Burn Fraction versus Crank Angle for different Activation Energy	86
Figure 4. Mass Burn Fraction versus Crank Angle for different Pre-exponential Constant	87
Figure 5. Mass Burn Fraction versus Crank Angle for different level of Turbulence Intensity.	88
Figure 6. Pressure versus Crank Angle for different Turbulence Intensity	89
Figure 7. Mass Burn Fraction versus Crank Angle for different Intake Pressure	90
Figure 8. Mass Burn Fraction versus Crank Angle for different Intake Pressure and Turbulence Intensity	91
Figure 9. Mass Burn Fraction Versus Crank Angle for different Intake Temperature	92
Figure 10. Pressure versus Crank Angle for different Intake Temperature	93
Figure 11. Mass Burn Fraction versus Crank Angle for different Equivalence Ratio	94
Figure 12. Pressure Versus Crank Angle for different Equivalence Ratio	95
Figure 13. Mass Burn Fraction versus Crank Angle for different Spark Advance	96
Figure 14. Mass Burn Fraction versus Crank Angle for different Ignition Energy	97
Figure 15. Mass Burn Fraction versus Crank Angle for different Gap Size	98
Figure 16. Mass Burn Fraction versus Crank Angle for different Engine Speed	99
Figure 17. Mass Fraction versus Crank Angle for different Number of Ignited Particles	100

Figure 18. Mass Burn Fraction versus Crank Angle for a Partial Burn Cycle : Spark Advance at 10° BTDC	101
Figure 19. Mass Burn Fraction versus Crank Angle for a Partial Burn Cycle : Spark Advance at 30° BTDC	102
Figure 20. Mass Burn Fraction versus Crank Angle for the inclusion of Age Mixing at Early Spark Advance (60° BTDC)	103
Figure 21. Mass Burn Fraction versus Crank Angle for the inclusion of Age Mixing at Late Spark Advance (10° BTDC)	104
Figure 22. Mass Burn Fraction versus Crank Angle for the inclusion of Age Mixing at late Spark Advance (30° BTDC)	105

CHAPTER 1 INTRODUCTION

1.1 GENERAL OVERVIEW

Lean combustion improves specific fuel consumption and reduces emissions of carbon monoxide (CO) and oxides of nitrogen (NO_x) in spark ignition engines (Shiomoto et al, 1978). However, misfire and cycle to cycle variation in lean burning engines cause rough operation and higher hydrocarbon (HC) emissions. Misfire limit is usually defined as the equivalence ratio at which a small percentage of cycles fail to ignite or burn completely for given operating conditions, namely, temperature, turbulence, spark advance etc.. A percentage of cycles is used because cyclic variation causes some cycles to misfire, and the others to burn completely. Different experimental methods have been used to determine if a cycle misfires. There is no agreement among researchers as to what percentage of cycles per minute misfires in the limit or on the specific method used to identify these cycles. Quader (1974) assumed that at the misfire limit, 0.5 to 0.8 % of the cycles misfired. He identified them by observing the pressure curve, the flame front position using an ionization probe and the exhaust HC level. Anderson and Lim (1985) used 0.4 to 2% of the cycles misfiring as the limit. They identified them by observing that the pressures at 40 degrees before and after top dead center in the same cycle are equal. Quader (1976) described two misfire limits: the ignition limit and the partial-burn limit. The ignition limit is reached if the spark fails to ignite a sufficiently large flame kernel to sustain flame propagation by the heat release of combustion. On the other hand, the partial burn limit is reached when the flame has not traversed the entire combustion chamber when the exhaust valve opens.

1.2 LITERATURE SURVEY

Germane et al (1983) provided an extensive review on the research works of lean mixture in spark ignition engines. They included over one hundred references dated from 1908 to 1983. The following literature survey does not intend to cover all available literature. Instead, the literature relevant to the present study will be reviewed.

As early as 1971, Tanuma et al (1971) investigated ways to improve lean combustion in spark ignition engines. They performed engine experiments with a modified ignition system, intake valve seat and combustion chamber geometry. The results showed that the lean limit can be extended using a larger spark gap, longer spark gap projection, higher ignition energy, and by using a valve seat with six inclined vanes. It was found that a compact combustion chamber and heated intake mixture improved fuel consumption and smoothness of operation. The engine speed was set at 1600 RPM for the testing of the lean limit. The authors defined the lean limit as the largest air to fuel ratio without misfire in 300 cycles. This definition was considered to be ambiguous by later researchers (Germane et al, 1983). The lean limit defined this way depended on the number of cycles observed. Tanuma et al (1971) were one of the earliest to investigate the lean limit of spark ignition engines. Their work did not provide insight in understanding the mechanism of lean misfire. Quader (1974) has done extensive experimental studies on lean misfire limit with propane and air and isooctane and air mixtures. The effects of varying different engine operating variables were investigated. His results indicated that the lean misfire limit was extended by increasing compression ratio and temperature, improving mixture homogeneity, decreasing charge dilution and engine speed. Quader (1976) also studied two types of misfire : misfire at ignition and partial burn. He investigated whether the lean limit occurred at ignition or during flame propagation. His study showed that at early spark timing, misfire occurred at ignition and that misfire at ignition can be avoided by retarding the spark advance. However, at

late spark timing, misfire occurred during flame propagation and the partial burn limit was reached. The two papers by Quader (1974, 1976) have stimulated great interest in understanding misfire. The author defined misfire using experimental measurements. The combined effects of engine operating variables on misfire were presented. Several questions concerning misfire remained unanswered. In fact, the measurement technique to distinguish ignition misfire from partial burn did not suggest that they were two different phenomena.

Smith et al (1977) analyzed the bulk quenching of flame in an expanding chamber using schlieren photographs. Their study showed that bulk quenching depended on the amount of volume expansion rather than the rate of volume expansion. Therefore, the unburned gas density was critical when bulk quenching occurred. The authors also correlated the lean limit with the Karlovitz number for different ignition timing. They concluded that bulk quenching contributed to flame extinguishment when ignition timing was retarded. Their results were in agreement with the results of Quader (1976) that partial burn occurred at late ignition timing. On the other hand, Peters (1979) investigated some cases of partial burn. He obtained pressure traces for a large ensemble of partially burned cycles, and deduced the mass burn fraction using the two zone heat release model of Krieger and Borman (1967). Their results showed few cases of flame quenching before the exhaust valve opened. The majority of the partial burn cycles were still burning when the exhaust valve opened due to slow burning rate. Peters also observed that the calculated flame temperature at quenching was between 1650 to 1880⁰K, but the slow burning cycles had a flame temperature above this range. The works of Smith et al (1977) and Peters (1979) have contributed to the understanding of partial burn. However, the question left open by Quader's studies remained unanswered.

The limitation of experimental works in understanding the physical mechanism behind misfire is mainly due to nature of engine experiments. All engines operate at a set of inter-related operating variables. For instance, if the speed of

the engine is changed, the turbulence intensity, residual fraction and other variables will also be affected. The effect of varying one operating parameter alone is very difficult to obtain. Engine experiments can only yield results of combined effects. Numerical models, on the other hand, can demonstrate the effect of varying any selected engine operating parameter, while perfectly isolating all other variables. Therefore, modelling provides information that is not available from experiments.

To date, attempts to model ignition limits have been made. Arici et al (1983) postulated that at the ignition limit, the energy production from combustion in the flame kernel was equal to the amount of heat dissipated to the unburned surrounding by turbulence. The burned mass was obtained using a mass entrainment model following the work of Tabaczynski et al (1977). The entrainment velocity was the sum of laminar flame speed and turbulence intensity. The effects of varying compression ratio, engine speed, intake temperature and exhaust gas recirculation were investigated. Comparison of model results with experimental results showed good agreement. Anderson and Lim (1985) determined experimentally the critical spark gap distance at which the leanest mixture could be ignited for a given spark advance. They called it the minimum energy condition. The critical spark gap distance was called the quench distance. At the minimum energy condition, reducing the spark gap would increase heat loss through the spark plug electrode and the flame would be quenched. On the other hand, increasing the spark gap would increase heat loss to the unburned gas and the flame would be quenched. The authors used a model by Ballal and Lefebvre (1977) to relate the quench distance to the effective (turbulent) flame thickness. The model failed to predict the effect of engine speed changes.

These two models for ignition limit provided some insights into the physics behind misfire at ignition. However, complete understanding of ignition misfire and partial burn is not obtained yet. As Quader(1976) stated in his paper in studying the constraint limits of lean operation, that 'this would require modelling the

thermochemical interactions near the spark gap to establish flame initiation during compression, and modelling the flame quenching process during expansion.' Since the thermochemical interaction at the spark and the flame quenching (partial burn) process are strongly influenced by local temperature and species concentration, a model incorporating temperature and species stratification coupled with finite rate chemistry and finite rate turbulent mixing is essential to predict the ignition limit and partial burn limit.

1.3 OBJECTIVE

The objective of this study is to formulate a model for flame propagation in a lean mixture to predict both ignition limit and at partial burn limit. At the present time, models for partial burn are not available in the literature. Both the misfire at ignition and partial burn are affected by the same type of engine operating variables, namely inlet flow condition, inlet condition of fuel mixture, ignition system, ignition timing, engine speed, and compression ratio. Therefore a model predicting both the ignition limit and partial burn limit will be useful in understanding the mechanism of engine misfire.

The model should be sensitive to the variation of all parameters that are believed to affect the misfire limits. These parameters have been used by Quader (1974) and Anderson and Lim (1985) in their extensive experimental works. They included the equivalence ratio, intake temperature, pressure, turbulence, engine speed, spark advance, spark gap and ignition energy. The model is expected to predict experimental trends when the parameters are varied. It should also predict the exact ignition limit and partial burn limit if complete engine data are available for precise model validation. However, this cannot be accomplished at the present stage due to the lack of complete engine data.

It should be noted that the model does not replace any engine experiments. The purpose is to assist researchers in understanding the results of engine experiments, and to direct future experiments. At the lean limit, misfire and cycle to cycle variation are coupled. Due to cyclic variation, the misfire limit predicted by the model represents some cycles of an engine operating at the lean limit. The percentage of misfiring cycles is an important consideration from the practical point of view. It cannot be obtained without knowing the cyclic distribution of mixture conditions from experiment. Therefore, experiment and modelling should always complement one another.

1.4 MODEL APPROACH

Combustion models for spark ignition engines are classified as either multi-dimensional or phenomenological. In multi-dimensional models, the conservation of mass, momentum, species and energy are solved numerically, and spatial variations of velocity, temperature and species concentration are calculated. These models require fine grids and excessive computing time. They are still in the development phase, and have not been used to calculate lean misfire limit. Phenomenological models assume a spatial average for the thermodynamic state of the mixture. They require less computing time, and can be used with engine development. A detailed classification is discussed by Heywood (1978).

In this study, a phenomenological model employing the coalescence dispersion approach by Curl (1963) is developed. The fuel mixture in the combustion chamber is divided into a number of equal mass particles, each having a homogeneous species concentration and temperature. Initially, a number of particles having a volume equal to the volume of the spark plug gap are selected and ignited to a fully burned state. The ignition energy released by the spark is equally distributed to those few particles. Then the thermodynamic state of the burned and unburned par-

ticles is calculated using the first law of thermodynamics and the volume constraint of the combustion chamber.

After ignition, the burned particles constitute the flame kernel. The flame front propagates by entraining unburned particles in the burned volume behind the flame front. This volume is assumed to be a partially stirred reactor. A turbulent entrainment model similar to Blizard and Keck (1974) is used to describe the rate of entrainment. The entrainment speed is a function of turbulence intensity (Tabaczynski et al, 1977). The particles in the partially stirred reactor mix in a binary fashion at a frequency determined by the turbulence intensity. The turbulence intensity is calculated assuming the rapid distortion theory for a spherical eddy in a homogeneous turbulent field (Morel and Mansour, 1982). The turbulence intensity in this simplified model depends on the unburned density. The binary mixing of particles are assumed to occur instantaneously, and separation occurs immediately after mixing. The resulting two particles have identical species concentration, temperature and volume. The burning of particles will take place when a burned particle is mixed with an unburned, or a burning with other particles. All three types of particles: unburned, burned, and burning particles can co-exist in the partially stirred reactor. This is consistent with the experimental observation by Namazian et al (1980).

The evolution of species and temperature of the burning particles is described by a set of chemical rate equations for all species applied to each burning particle. Using the first law and assuming a perfect gas, an expression for the rate of temperature rise is derived. An expression describing the rate of pressure rise is also obtained by applying the perfect gas law to the ensemble of particles and using the chamber volume constraint. These equations are solved simultaneously. The results give the species concentration and temperature of each burning particle, and the pressure of the system at each instant of time.

This model incorporates a turbulent flame front, finite rate turbulent mixing

and finite rate chemistry. It differs from other phenomenological models by incorporating temperature and species stratification. It is more accurate than using an average value of temperature, since the specific reaction rate given by Arrhenius is extremely sensitive to temperature, as demonstrated by Pratt (1976). The inclusion of the chemical rate in the model is an important feature. As shown in the literature survey, other models studying misfire do not include chemical rate explicitly; they use the laminar flame speed correlation. However, the comparison of chemical time with turbulent mixing (diffusion) time is important in the study of lean misfire. Peters (1979) stated that 'if the time required to complete the chemical reactions is longer than the time it takes for chemical species and energy to be transported away from the reaction zone, the flame will go out.' Explicit chemical rate in the model facilitates such a comparison.

CHAPTER 2 SUPPORTING MODELS

2.1 IGNITION

The ignition is modeled by burning completely the mixture within the spark gap during the specified ignition duration. The ignition energy is equally distributed among the burned particles. The thermodynamic states of the burned and unburned gases are calculated using the first law. The first law applied to the unburned gas outside the spark gap is expressed as,

$$E_u - E_{u,o} = Q - W_u \quad (1a)$$

where $E_{u,o}$ and E_u are respectively the internal energy of unburned gas before and after ignition, Q is the heat transferred to the unburned gas and W_u is the work done by the unburned gas. Assuming that the process is adiabatic, and that the ignition energy is delivered to the burned gas only, then the heat transfer term Q is zero and the first law applied to the unburned is rewritten as

$$E_u = E_{u,o} - W_u \quad (1b)$$

The first law applied to the burned gas is

$$E_b - E_{b,o} = Q - W_b \quad (2a)$$

where $E_{b,o}$ and E_b are respectively the internal energy of the burned gas before and after ignition, Q is the heat transferred to the burned gas, and W_b is the work done by the burned gas. Here, the heat transfer is equal to the ignition energy. Therefore the first law becomes

$$E_b = E_{b,o} + E_{ign} - W_b \quad (2b)$$

where E_{ign} is the ignition energy transferred to the burned gas. It is to be noted that E_{ign} represents the amount of energy transferred to the ignited gas rather than the total amount that the spark plug produces. In reality the energy supplied by ignition system is partially lost by heat transfer through the spark plug electrodes. This treatment is beyond the scope of the present study.

The work terms W_u and W_b in equations (1b) and (2b) are determined by the change in pressure and volume of the unburned and burned gases during the spark duration; they are

$$W_u = - \int P dV_u \quad (3a)$$

$$W_b = - \int P dV_b \quad (4a)$$

Since the spark duration is short, the variation of pressure can be assumed linear. The integrals are approximated using the trapezoidal rule, and equation (3a) and (4a) become,

$$W_u = \frac{P+P_o}{2} (V_u - V_{u,o}) \quad (3b)$$

$$W_b = \frac{P+P_o}{2} (V_b - V_{b,o}) \quad (4b)$$

where subscript o denotes properties before ignition, and P is the pressure after ignition. The unburned gas undergoes an isentropic compression from its initial pressure P_o to the pressure P . Therefore the unburned volume is given by

$$V_u = V_{u,o} \left(\frac{P_o}{P} \right)^{1/\gamma} \quad (5)$$

where γ is the ratio of specific heat. The volume of the burned gas is expressed using the perfect gas law,

$$V_b = \frac{N_b R_b T_b}{P} \quad (6)$$

where T_b is the burned temperature.

Substituting the unburned volume V_u in equation (3b) using equation (5) and replacing the work term in equation (1b), the first law applied to the unburned gas is rewritten as

$$E_u = E_{u,o} - \frac{P+P_a}{2} (V_{u,o} (\frac{P_a}{P})^{1/\gamma} - V_{u,o}) \quad (7)$$

Substituting the burned gas volume V_b in equation (4b) using equation (6) and replacing the work term in equation (2b), the first law applied to the burned gas is expressed as

$$E_b = E_{b,o} + E_{ign} - \frac{P+P_a}{2} (\frac{N_b R_b T_b}{P} - V_{b,o}) \quad (8)$$

The volume of the combustion chamber can be expressed as,

$$V = V_u + V_b \quad (9a)$$

Replacing the unburned and burned gas volumes (V_u and V_b) in equation (9a) using equation (5) and (6),

$$V = V_{u,o} (\frac{P_a}{P})^{1/\gamma} + \frac{N_b R_b T_b}{P} \quad (9)$$

The three unknowns in equations (7), (8), (9) are the temperatures of the burned and unburned gases, and the pressure. The system of equations is closed since there are three unknowns in three equations.

The input variables to the ignition model are the initial temperature and pressure and equivalence ratio, spark timing, spark duration, spark gap distance, ignition energy, and the number of equal mass particles corresponding to the volume of the ignited gas. The volume of the ignited gas is assumed to be equal to the spark gap volume. This volume is estimated to be either a cylindrical volume $\frac{1}{4} \pi d^2 l$ or a spherical volume $\frac{1}{6} \pi l^3$, where d , the electrode diameter, is equal to 2.5 mm, and l is the spark gap distance. The total number of particles in the chamber is calculated as

$$N = \frac{N_b}{V_b} V \quad (10)$$

where N is the calculated number of particles in the combustion chamber, V is the volume of the combustion chamber and N_b is the number of particles ignited. The computer program for the ignition model is included in the main program listed in appendix (A). The solution requires calculation of the internal energies of burned (E_b) and unburned (E_u). The calculations of the internal energies are discussed in appendix (B).

2.2 TURBULENT ENTRAINMENT

After ignition, the unburned mass will be entrained into the flame zone at a rate determined by (Blizard and Keck, 1974)

$$\frac{dm_e}{dt} = \rho_u A_e u_e \quad (11)$$

where m_e is the entrained mass, ρ_u is the unburned density, A_e is the flame front area, u_e is the entrainment velocity. Models for the flame front area and entrainment velocity are required. The flame front is assumed to grow spherically from the spark plug located at the top of the disk shape combustion chamber (Figure 1). The model for entrainment velocity is taken from Tabaczynski et al (1977). The authors extended the model for entrainment velocity given by Blizard and Keck (1974) by assuming that the entrainment velocity u_e is equal to the sum of the turbulence intensity u' (root mean square of the velocity fluctuation component) and the laminar flame speed S_l .

$$u_e = u' + S_l \quad (12a)$$

However, Daneshyar and Hill (1988) estimated the entrainment velocity using the following relation,

$$u_e = \sqrt{\frac{2\rho_u}{3\rho_b}} u' + S_l \quad (12b)$$

where ρ_u is the unburned density and ρ_b is the burned density. Milane and Hill (1988) confirmed the validity of this relationship with extensive experimental work, and suggested that equation (12b) is a better model than equation(12a). Therefore, the present study uses equation(12b) for the entrainment velocity. The laminar flame speed model of van Tiggelen (1957) is used,

$$S_l = K C_m [Y_f^a Y_{O_2}^b \exp(-\frac{E}{RT_m})]^{1/2} \quad (13)$$

$$C_m = \sqrt{\frac{8RT_m}{\pi M_r}}$$

$$K = \frac{2T_u}{\sqrt{3\pi T_m}} \left(\frac{P}{P_r}\right)^\alpha$$

$$T_m = T_u + 0.74(T_b^o - T_u)$$

where C_m is the mean molecular speed of chain carriers whose mean molecular weight is M_r . Y_f is the mole fraction of fuel molecules in the unburned mixture, Y_{O_2} is the mole fraction of oxygen molecules in unburned mixture, a and b are reaction orders with respect to fuel and oxygen respectively, and E is the activation energy. T_m is the mean temperature of the reaction zone as proposed by van Tiggelen and Duval (1967). K is a dimensionless parameter dependent on pressure P and P_r is equal to 1 atm. The kinetic parameters for propane proposed by van Tiggelen (1957) are

$$M_r = 31 \text{ g/mole} \quad \alpha = -0.06$$

$$a = -0.46 \quad b = 1.46$$

$$E = 37.7 \text{ Kcal/mole}$$

The turbulence intensity in equation (12b) is described by the rapid distur-

tion theory for compression of spherical eddies as discussed in Morel and Mansour (1982),

$$\frac{1}{K} \frac{dK}{dt} = -\frac{2}{3} D \quad (14)$$

where the turbulent kinetic energy K is $\frac{3}{2} u'^2$ and D is the velocity divergence. The conservation of mass is

$$\frac{1}{\rho} \frac{d\rho}{dt} = -D \quad (15)$$

where ρ is the density. Replacing D in equation (14) by equation (15),

$$\frac{1}{K} \frac{dK}{dt} = \frac{2}{3} \frac{1}{\rho} \frac{d\rho}{dt} \quad (16)$$

Here the turbulence is assumed homogeneous in the combustion chamber. At any time after intake valve closing, the turbulence intensity is calculated by integrating equation (16),

$$u' = u'_o \left(\frac{\rho_{u,o}}{\rho_u} \right)^{1/3} \quad (17)$$

where u'_o is the turbulence intensity at intake valve closing, $\rho_{u,o}$ is the unburned density at intake valve closing, and ρ_u is the instantaneous unburned density.

At any instant of time, the turbulence intensity, the laminar flame speed and entrainment velocity are calculated by subroutine SPEED listed in appendix (C).

2.3 TURBULENT MIXING

The entrained volume behind the flame front is considered to be a partially stirred reactor, where binary mixing of particles is assumed (Pratt, 1976). The number of mixing pairs in a given period of time Δt is determined by the mixing frequency and the total number of particles in the reactor,

$$N_m = \omega N_t \Delta t \quad (18)$$

where N_m is the number of mixing pairs, N_t is the total number of particles in reactor, and ω is the mixing frequency.

2.3.1 MIXING FREQUENCY

The mixing frequency is related to the turbulent kinetic energy K_T , and dissipation of the turbulent kinetic energy E_T (see Milane et al, 1983) as,

$$\omega \sim \frac{E_T}{K_T} \quad (19)$$

The dissipation is expressed as,

$$E_T \sim \frac{K_T^{3/2}}{L} \quad (20a)$$

where L is the integral length scale.

The conservation of angular momentum of large eddies gives;

$$K_T^{1/2} L \sim \text{constant} \quad (21)$$

Substituting for L in equation (20a) using equation (21), the dissipation is expressed as,

$$E_T \sim K_T^2 \quad (20b)$$

Replacing for E_T in equation (19) using equation (20b),

$$\omega = C u'^2 \quad (22)$$

where C is an empirical constant to be determined using experimental data.

2.3.2 RANDOM SELECTION OF MIXING PAIRS

Each particle in the partially stirred reactor is assigned a number according to the order in which it enters the reactor. A random number generator is used to select the N_m pairs which will mix. The random number generator is described in subroutine GGUD, whose listing is in the IMSL library of the main frame computer of University of Ottawa. Subroutine GGUD selects a desired number of integers between one and the total number of particles (N_t) in the entrained volume. Subroutine GGUD is called N_m times. Two integers representing the mixing pair are selected each time. If any one of the two particles has already been selected in the same period of time, subroutine GGUD is called again until a new pair of particles is selected.

2.3.3 BINARY MIXING

The mixing process assumes that two particles mix and separate instantaneously. They become identical after mixing. During the mixing process, the composition is assumed 'frozen'. Therefore, the conservation of species applied to the system of two particles yields that the fuel fraction (ratio of mass of fuel to total mass) after mixing is the arithmetic average fuel fraction of the two particles before mixing,

$$F_3 = \frac{F_1 + F_2}{2} \quad (23)$$

where F_1 and F_2 are the fuel fraction of the two particles before mixing and F_3 is their fuel fraction after mixing. The total volume does not change during mixing because the composition is frozen and mixing takes place instantaneously,

$$Vol_3 = \frac{Vol_1 + Vol_2}{2} \quad (24)$$

where Vol_1, Vol_2 are the volume of the two particles before mixing and Vol_3 is the volume of each particle after mixing.

The temperature after mixing is calculated using the first law written for the pair of mixing particles,

$$dU = dQ - PdV$$

Since frozen composition is assumed, heat release by combustion and heat transfer to neighbouring particles is nil ($dQ = 0$), and the total volume does not change, ($dV = 0$). The first law becomes

$$dU = 0$$

therefore,

$$U_1 + U_2 = 2U_3 \quad (25)$$

where U_1 and U_2 are the internal energies of two particles before mixing and U_3 is the internal energy of each particle after mixing.

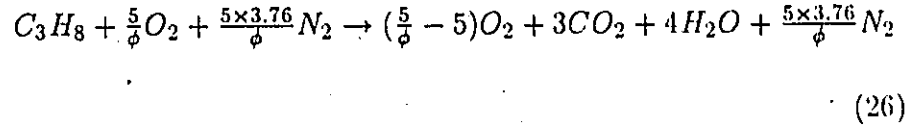
The internal energies are calculated as a function of temperature and species composition (see appendix (B)). Equation (25) is solved by iterating on the temperature after mixing until the calculated internal energy converges to $2U_3$. These calculations are performed by subroutine MIXFRO listed in appendix (D).

The turbulent mixing is performed by subroutine RANMIX listed in appendix (E). The subroutine RANMIX calls subroutines GGUD and MIXFRO. The results of MIXFRO are the initial conditions of the thermodynamic states of particles for the time interval.

2.4 GOVERNING EQUATIONS FOR THERMODYNAMIC STATES

2.4.1 CHEMICAL RATE EQUATIONS

The global reaction equation for the combustion of propane and air is assumed for each burning particle,



where ϕ is the equivalence ratio defined as

$$\phi = \frac{\text{actual air fuel ratio}}{\text{stoichiometric air fuel ratio}}$$

The reaction rate is described by the single step reaction mechanism of Westbrook and Dryer (1981),

$$\frac{dX_i}{dt} = -A \exp(-E/RT_i) X_i^a Y_i^b \quad (27)$$

where X_i is the concentration of propane in moles/cc and subscript i denotes the i th burning particle, T_i is the temperature of the mixture, Y_i is the concentration of oxygen in moles/cc, A is the pre-exponential constant, E is the activation energy, and a, b are empirical constants. The authors suggested the following values of the constants for a single step propane in air reaction.

$$E = 30.0 \text{ Kcal/mole} \quad A = 8.6 \times 10^{11} \text{ Kcal/mole}$$
$$a = 0.1 \quad b = 1.65$$

(27) can be rewritten as

$$\frac{dx_i}{dt} = -Av_i \exp(-E/RT_i) x_i^a y_i^b \quad (28)$$

where x_i, y_i are respectively the moles of fuel and oxygen per gram of mixture, and v_i is the specific volume of mixture. The rates of change of the number of moles of species per gram of mixture for oxygen y_i , carbon dioxide z_i , water w_i and nitrogen v_i are related to that of propane x_i by the stoichiometric coefficients of the reaction equation (26),



$$\frac{dy_i}{dt} = 5 \frac{dx_i}{dt} \quad (29)$$

$$\frac{dx_i}{dt} = 3 \frac{dx_i}{dt} \quad (30)$$

$$\frac{dw_i}{dt} = -4 \frac{dx_i}{dt} \quad (31)$$

$$\frac{dv_i}{dt} = 0 \quad (32)$$

2.4.2-RATE OF TEMPERATURE RISE OF A BURNING PARTICLE

The temperature of a burning particle which is required in (28) is calculated using the first law of thermodynamics applied to the individual particle i ,

$$\frac{du_i}{dt} = q_i - P \frac{dv_i}{dt} \quad (33)$$

where u_i , q_i and v_i are specific quantities. In an adiabatic process the heat transfer is zero ($q = 0$). The specific internal energy is,

$$u_i = M_x x_i u_x + M_y y_i u_y + M_\nu \nu_i u_\nu + M_z z_i u_z + M_w w_i u_w \quad (34)$$

where $x_i, y_i, \nu_i, z_i, w_i$ are respectively the moles of species per gram of mixture for C_3H_8, O_2, N_2, CO_2 and H_2O for particle i , $M_x, M_y, M_\nu, M_z, M_w$ are molecular weight of species, in gram/mole of species and $u_x, u_y, u_\nu, u_z, u_w$ are specific internal energies of species in cal/gram of species. The derivative of equation (34) is

$$\begin{aligned} du_i = & M_x x_i du_x + M_y y_i du_y + M_\nu \nu_i du_\nu + M_w w_i du_w \\ & + M_x u_x dx_i + M_y u_y dy_i + M_\nu u_\nu d\nu_i + M_z u_z dz_i + M_w u_w dw_i \end{aligned} \quad (35)$$

The change of internal energy of each species is expressed in terms of the specific heat at constant volume C_v .

$$du_x = C_{v_x} dT_i$$

$$du_y = C_{v_y} dT_i$$

$$du_v = C_{v_v} dT_i$$

$$du_z = C_{v_z} dT_i$$

$$du_w = C_{v_w} dT_i$$

Replacing the above terms as well as dy_i , $d\nu_i$, dz_i , dw_i in equations (35) using equations (29), (30), (31), (32), and rearranging,

$$\begin{aligned} \frac{du_i}{dt} = & (M_x x_i C_{v_x} + M_y y_i C_{v_y} + M_\nu \nu_i C_{v_\nu} + M_z z_i C_{v_z} + M_w w_i C_{v_w}) \frac{dT_i}{dt} \\ & + (M_x u_x + 5M_y u_y - 3M_z u_z - 4M_w u_w) \frac{dx_i}{dt} \end{aligned} \quad (36)$$

Eliminating the derivative of internal energy by equating equation (33) and equation (36) and rearranging,

$$\frac{dT_i}{dt} = \frac{-\frac{dx_i}{dt} (M_x u_x + 5M_y u_y - 3M_z u_z - 4M_w u_w) - P \frac{dv_i}{dt}}{M_x x_i C_{v_x} + M_y y_i C_{v_y} + M_\nu \nu_i C_{v_\nu} + M_z z_i C_{v_z} + M_w w_i C_{v_w}} \quad (37)$$

The derivative of specific volume ($\frac{dv_i}{dt}$) is required in equation (37). The perfect gas law applied to particle i ,

$$Pv_i = \frac{n_i}{m} RT_i$$

where m is the mass of the particle, R is the universal gas constant and n_i is the

$$n_i = m(x_i + y_i + \nu_i + z_i + w_i)$$

Therefore, the specific volume v_i is expressed as,

$$v_i = \frac{(x_i + y_i + \nu_i + z_i + w_i)RT_i}{P}$$

The derivative of specific volume is

$$\begin{aligned} \frac{dv_i}{dt} = & \left(\frac{dx_i}{dt} + \frac{dy_i}{dt} + \frac{d\nu_i}{dt} + \frac{dz_i}{dt} + \frac{dw_i}{dt} \right) \frac{RT_i}{P} + (x_i + y_i + \nu_i + z_i + w_i) \frac{R}{P} \frac{dT_i}{dt} \\ & - (x_i + y_i + \nu_i + z_i + w_i) \frac{RT_i}{P^2} \frac{dP}{dt} \end{aligned} \quad (38)$$

Substituting $\frac{dv_i}{dt}$ (equation (38)) in equation (37), and simplifying using equations (29) to (32),

$$\frac{dT_i}{dt} = \frac{\frac{dx_i}{dt} [RT_i - (M_x u_x + 5M_y u_y - 3M_z u_z - 4M_w u_w)] + (x_i + y_i + \nu_i + z_i + w_i) \frac{RT_i}{P} \frac{dP}{dt}}{(M_x x_i C_{v_x} + M_y y_i C_{v_y} + M_\nu \nu_i C_{v_\nu} + M_z z_i C_{v_z} + M_w w_i C_{v_w}) + (x_i + y_i + \nu_i + z_i + w_i) R} \quad (39a)$$

Equation (39a) is composed of several terms. The internal energy per mole of mixture for particle i is,

$$Um_i = M_x x_i u_x + 5M_y y_i u_y - 3M_z z_i u_z - 4M_w w_i u_w$$

The specific heat at constant volume of particle i is,

$$C_{v_i} = M_x x_i C_{v_x} + M_y y_i C_{v_y} + M_\nu \nu_i C_{v_\nu} + M_z z_i C_{v_z} + M_w w_i C_{v_w}$$

The number of moles per gram of mixture in particle i is,

$$N_i = x_i + y_i + \nu_i + z_i + w_i$$

Equation (39a) is rewritten as

$$\frac{dT_i}{dt} = \frac{\frac{dz_i}{dt}(RT_i - Um_i) + N_i \left(\frac{RT_i}{P} \right) \frac{dP}{dt}}{C_{v_i} + (N_i)(R)} \quad (39b)$$

2.4.3 RATE OF PRESSURE RISE OF THE SYSTEM

The rate of change of temperature of a burning particle depends on the value of pressure, the rate of change of pressure, and the concentrations of different species. The rate of change of pressure in the system is derived using the perfect gas law applied to the ensemble of particles in the chamber, composed of N_1 burning, N_2 unburned and N_3 burned particles. The perfect gas law applied to each burning particle is⁶

$$PV_i = n_i RT_i \quad (40a)$$

where R is the universal gas constant. The perfect gas law applied to N_1 burning particles is

$$P \sum_{i=1}^{N_1} V_i = R \sum_{i=1}^{N_1} n_i T_i \quad (40b)$$

The perfect gas law applied to each unburned particle is

$$PV_u = n_u RT_u \quad (41a)$$

where

$$n_u = m(X_u + Y_u + \nu_u)$$

The perfect gas law applied to N_2 identical unburned particles is

$$N_2 PV_u = N_2 n_u RT_u \quad (41b)$$

The perfect gas law applied to each burned particle is

$$PV_j = n_j RT_j \quad (42a)$$

where

$$n_j = m(Y_j + Z_j + \nu_j + W_j)$$

The perfect gas law applied to N_3 burned particles is

$$P \sum_{j=1}^{N_3} V_j = R \sum_{j=1}^{N_3} n_j T_j \quad (42b)$$

Therefore, the perfect gas law applied to the ensemble of particles is obtained by summing equations (40b), (41b), (42b),

$$P \left(\sum_{i=1}^{N_1} V_i + N_2 V_u + \sum_{j=1}^{N_3} V_j \right) = R \left(\sum_{i=1}^{N_1} n_i T_i + N_2 n_u T_u + \sum_{j=1}^{N_3} n_j T_j \right) \quad (43a)$$

The volume of the chamber V is expressed as,

$$V = \left(\sum_{i=1}^{N_1} V_i + N_2 V_u + \sum_{j=1}^{N_3} V_j \right)$$

Therefore, equation (43a) is written as,

$$PV = R \left(\sum_{i=1}^{N_1} n_i T_i + N_2 n_u T_u + \sum_{j=1}^{N_3} n_j T_j \right) \quad (43b)$$

The expression for the rate of pressure rise is calculated by taking the derivative of equation (43b),

$$\begin{aligned} V \frac{dP}{dt} + P \frac{dV}{dt} &= R \left[\sum_{i=1}^{N_1} \left(T_i \frac{dn_i}{dt} + n_i \frac{dT_i}{dt} \right) + N_2 \left(T_u \frac{dn_u}{dt} + n_u \frac{dT_u}{dt} \right) \right. \\ &\quad \left. + \sum_{j=1}^{N_3} \left(T_j \frac{dn_j}{dt} + n_j \frac{dT_j}{dt} \right) \right] \end{aligned} \quad (44)$$

The composition of the unburned and burned particles does not change, therefore the number of moles remains constant,

$$\frac{dn_u}{dt} = \frac{dn_j}{dt} = 0 \quad (45)$$

Also, the rate of change of the number of moles for each burning particle is

$$\frac{dn_i}{dt} = m \left(\frac{dx_i}{dt} + \frac{dy_i}{dt} + \frac{dv_i}{dt} + \frac{dz_i}{dt} + \frac{dw_i}{dt} \right)$$

Replacing $\frac{dy_i}{dt}$, $\frac{dv_i}{dt}$, $\frac{dz_i}{dt}$ and $\frac{dw_i}{dt}$ using equations (29) to (32),

$$\frac{dn_i}{dt} = -m \frac{dx_i}{dt} \quad (46)$$

Therefore equation (44) is rewritten as,

$$V \frac{dP}{dt} + P \frac{dV}{dt} = R \left[\sum_{i=1}^{N_1} \left(-m T_i \frac{dx_i}{dt} + n_i \frac{dT_i}{dt} \right) + N_2 n_u \frac{dT_u}{dt} + \sum_{j=1}^{N_3} n_j \frac{dT_j}{dt} \right] \quad (47)$$

The derivatives of the temperature of burned and unburned are calculated assuming isentropic relations. The temperature of the unburned particle is,

$$T_u = T_{u,o} \left(\frac{P}{P_o} \right)^{\frac{\gamma_u-1}{\gamma_u}} \quad (48)$$

where $T_{u,o}$ and P_o are initial unburned temperature and pressure, and γ_u is the ratio of specific heat for unburned gas at T_u and P . The temperature of a burned particle is,

$$T_j = T_{j,o} \left(\frac{P}{P_o} \right)^{\frac{\gamma_j-1}{\gamma_j}} \quad (49)$$

where $T_{j,o}$ is the initial temperature of burned particle j and γ_j is the ratio of specific heat of particle j at T_j and P .

Therefore, the rates of change of unburned and burned temperatures are respectively,

$$\frac{dT_u}{dt} = T_{u,o} \left(\frac{1}{P_o} \right)^{\frac{\gamma_u-1}{\gamma_u}} \left(\frac{\gamma_u-1}{\gamma_u} \right) P^{-\frac{1}{\gamma_u}} \frac{dP}{dt} \quad (50)$$

and

$$\frac{dT_j}{dt} = T_{j,o} \left(\frac{1}{P_o} \right)^{\frac{\gamma_j-1}{\gamma_j}} \left(\frac{\gamma_j-1}{\gamma_j} \right) P^{-\frac{1}{\gamma_j}} \frac{dP}{dt} \quad (51)$$

Replacing $\frac{dT_i}{dt}$ and $\frac{dT_j}{dt}$ in equation (44) by equation (50) and (51),

$$\begin{aligned}
 V \frac{dP}{dt} + P \frac{dV}{dt} = R \left\{ \sum_{i=1}^{N_1} (-mT_i \frac{dx_i}{dt} + n_i \frac{dT_i}{dt}) \right. \\
 + N_2 n_u T_{u,o} \left(\frac{1}{P_o} \right)^{\frac{\gamma_u-1}{\gamma_u}} \left(\frac{\gamma_u-1}{\gamma_u} \right) P^{-\frac{1}{\gamma_u}} \frac{dP}{dt} \\
 \left. + \sum_{j=1}^{N_3} [n_j T_{j,o} \left(\frac{1}{P_o} \right)^{\frac{\gamma_j-1}{\gamma_j}} \left(\frac{\gamma_j-1}{\gamma_j} \right) P^{-\frac{1}{\gamma_j}} \frac{dP}{dt}] \right\}
 \end{aligned}
 \tag{52}$$

Now, the term $\frac{dT_i}{dt}$ is eliminated from equation (52) using equation (39b),

$$\begin{aligned}
 V \frac{dP}{dt} + P \frac{dV}{dt} = R \left\{ \sum_{i=1}^{N_1} \left(-mT_i \frac{dx_i}{dt} + n_i \frac{\frac{dx_i}{dt} (RT_i - Um_i) + N_i \left(\frac{RT_i}{P} \right) \frac{dP}{dt}}{C_{v_i} + (N_i)(R)} \right) \right. \\
 + N_2 n_u T_{u,o} \left(\frac{1}{P_o} \right)^{\frac{\gamma_u-1}{\gamma_u}} \left(\frac{\gamma_u-1}{\gamma_u} \right) P^{-\frac{1}{\gamma_u}} \frac{dP}{dt} \\
 \left. + \sum_{j=1}^{N_3} [n_j T_{j,o} \left(\frac{1}{P_o} \right)^{\frac{\gamma_j-1}{\gamma_j}} \left(\frac{\gamma_j-1}{\gamma_j} \right) P^{-\frac{1}{\gamma_j}} \frac{dP}{dt}] \right\}
 \end{aligned}$$

Rearranging,

$$\begin{aligned}
 \frac{dP}{dt} = \frac{R \sum_{i=1}^{N_1} \left\{ \frac{dx_i}{dt} [-mT_i + \frac{n_i (RT_i - Um_i)}{C_{v_i} + N_i(R)}] \right\} - P \frac{dV}{dt}}{\left\{ V - \sum_{i=1}^{N_1} \left[\frac{n_i N_i RT_i}{C_{v_i} + N_i(R)} \right] - N_2 n_u T_{u,o} \left(\frac{1}{P_o} \right)^{\frac{\gamma_u-1}{\gamma_u}} \left(\frac{\gamma_u-1}{\gamma_u} \right) P^{-\frac{1}{\gamma_u}} - \sum_{j=1}^{N_3} [n_j T_{j,o} \left(\frac{1}{P_o} \right)^{\frac{\gamma_j-1}{\gamma_j}} \left(\frac{\gamma_j-1}{\gamma_j} \right) P^{-\frac{1}{\gamma_j}}] \right\}}
 \end{aligned}
 \tag{53}$$

The set of ordinary differential equations describing the evolution of thermodynamic properties during a time interval is equation (28), (29), (30), (31), (32), (39b) for each burning particle and equation (53) for the entire ensemble of particles. Therefore, the number of equations is $6N_1 + 1$, for N_1 burning particles. The unknowns are the number of moles of the five species (C_3H_8 , O_2 , N_2 , CO_2 , H_2O) per gram of mixture in each burning particle ($5N_1$ unknowns), the temperature of each burning particle (another N_1 unknowns), and the pressure in the chamber. Therefore, a total of $6N_1 + 1$ unknowns are to be solved. This set of equations is

handled by subroutine KINET in appendix (F).

CHAPTER 3 METHODS OF SOLUTION

After ignition, the flame propagation, turbulent mixing and chemical reaction take place simultaneously. The governing equations are solved numerically by discretizing the continuous phenomena of flame propagation and turbulent mixing. The solution procedure of ignition, turbulent entrainment, binary mixing, and the thermodynamic states of particles are discussed in the following sections.

3.1 IGNITION

As discussed in section 2.1, ignition is described by three equations, equations (7), (8), and (9). The three unknowns are the temperatures of the burned particles T_b and unburned particles T_u , and the pressure of the system P . The mixture conditions before ignition are calculated assuming isentropic compression from the closing of the intake valve to the time of ignition,

$$P_o = P_{in} \left(\frac{V_o}{V_{in}} \right)^\gamma \quad (54)$$

$$T_o = T_{in} \left(\frac{P_o}{P_{in}} \right)^{\frac{\gamma-1}{\gamma}} \quad (55)$$

where P_{in} and T_{in} are pressure and temperature at the closing of the intake valve, V_{in} is the chamber volume at closing of the intake valve, P_o and T_o are respectively the pressure and temperature after the spark event when the chamber volume is V_o , and γ is the specific heat ratio of the unburned mixture.

The volumes V_{in} and V_o corresponding to given crank angles are calculated by function subroutine VTO(CA). This function calculates the volume of the com-

bustion chamber as a function of crank angle, given the cylinder dimensions (see Table 1). The listing of VTO(CA) is in appendix (G)

The ratio of specific heat γ is obtained from subroutine UPROP in appendix (II). Since γ is dependent on temperature, its value is updated for new temperature every 0.5 crank angle using equations (54) and (55).

Now that the mixture conditions before ignition are obtained, the governing equations of ignition, equations (7),(8) and (9), can be solved,

$$E_u = E_{u,o} - \frac{P+P_o}{2} (V_{u,o} (\frac{P_o}{P})^{1/\gamma} - V_{u,o}) \quad (7)$$

$$E_b = E_{b,o} + E_{ign} - \frac{P+P_o}{2} (\frac{N_b R_b T_b}{P} - V_{b,o}) \quad (8)$$

$$V = V_u + V_b \quad (9)$$

An iteration method is used :

1. The initial guess of pressure P is taken as the pressure before ignition.
2. This pressure is used to calculate the volume and temperature of unburned gas assuming isentropic relations,

$$V_u = V_{u,o} (\frac{P_o}{P})^{1/\gamma} \quad (56)$$

$$T_u = T_o (\frac{P_o}{P})^{\frac{\gamma-1}{\gamma}} \quad (57)$$

3. The volume of burned gas is calculated using (9),

$$V_b = V - V_u$$

4. The temperature of burned gas is given by the perfect gas law,

$$T_b = \frac{V_b P}{n_b R_u}$$

5. The internal energies of burned and unburned after ignition, E_b and E_u , are obtained by subroutines CLDPRD and UPROP in appendix (H). The method of calculation is explained in appendix (B).
6. The internal energies before ignition for the unburned gas within the spark gap $E'_{b,o}$ and the rest of the chamber $E'_{u,o}$ are calculated by equations (7) and (8).
7. If the calculated values of $E'_{u,o}$ and $E'_{b,o}$ are close to the actual values $E_{u,o}$ and $E_{b,o}$ corresponding to the temperatures before ignition, the solution has converged.

$$\frac{|E'_{u,o} - E_{u,o}|}{E_{u,o}} < \epsilon$$

and

$$\frac{|E'_{b,o} - E_{b,o}|}{E_{b,o}} < \epsilon$$

where ϵ is a small positive number.

8. If their calculated values are either greater or smaller than the actual values,

$$\frac{|E'_{u,o} - E_{u,o}|}{E_{u,o}} > \epsilon$$

or

$$\frac{|E'_{b,o} - E_{b,o}|}{E_{b,o}} > \epsilon$$

then the pressure is guessed using the Half Interval Method (Carnahan et al, 1969), and the solution is iterated again from step (2).

3.2 TURBULENT ENTRAINMENT

Mass entrainment is calculated by integrating equation (11) using Euler's rule

$$m_e(t + \Delta t) - m_e(t) = \rho_u A_e u_e \Delta t \quad (58)$$

where $m_e(t + \Delta t) - m_e(t)$ is the mass to be entrained in the time interval Δt . This mass $m_e(t + \Delta t) - m_e(t)$ may not correspond to an integer number of particles. Any fraction in excess of the integer is counted in the next time interval. Now, the flame front area A_e is calculated assuming that the flame propagates hemispherically from the spark plug (see Figure 1). In general, the volume of this hemisphere can be written as

$$V_e = \int_0^h (\alpha r^2 + \beta R_c^2 - r_s R \sin \beta) dz \quad (59a)$$

where;

$$\cos \alpha = (r_s^2 + r^2 - R_c^2) / 2r_s r \quad (59b)$$

$$\cos \beta = (r_s^2 + R_c^2 - r^2) / 2r_s R_c \quad (59c)$$

$$r^2 = r_e^2 - z^2 \quad (59d)$$

α, β, r and z are shown in Figure 1, R_c is half the bore of the cylinder, h is the chamber height, and r_e is the entrainment radius. Before the flame reaches the piston and the side wall, α is equal to π and β is equal to 0. Therefore, (59a) is simplified to

$$V_e = \frac{2}{3} \pi r_e^3 \quad (60)$$

and the flame front area is

$$A_e = 2\pi r_e^2 \quad (61)$$

After the flame reaches the piston or the side wall, a Newton Raphson iteration

method is required to calculate the flame front area. (59a) is rewritten as

$$F(r_e) = \int_0^h (\alpha r^2 + \beta R_c^2 - r_s R \sin \beta) dz - V_e \quad (62)$$

The derivative of $F(r_e)$ with respect to the entrained radius r_e is also required in the Newton Raphson method,

$$\frac{dF(r_e)}{dr_e} = A_e(r_e) = 2r_e \int_0^h \alpha dz \quad (63)$$

An initial guess of r_e is needed to start the iteration. The $(K + 1)_{th}$ iterated value of r_e in terms of its K_{th} iterated value, according to the Newton Raphson method, is

$$r_{e,k+1} = r_{e,k} - \frac{F(r_{e,k})}{A(r_{e,k})} \quad (64)$$

The solution converges when the following is satisfied,

$$|r_{e,k+1} - r_{e,k}| < \varepsilon$$

where ε is a small positive number. This method essentially iterates on $F(r_e)$ until it is equal to a small number. Once the solution for r_e is calculated, the flame front area $A_e(r_e)$ is obtained from equation (63). The above calculation of the flame front area is performed by the subroutine SHAPE; the listing is found in appendix (I).

3.3 BINARY MIXING

The thermodynamic states of the mixing pairs are calculated for burning and burned particles. In order to recognize whether a particle is unburned, burning or burned, an index is assigned to each of them according to the fuel fraction. If a particle's fuel fraction is equal to that of an unburned particle, the index is assigned to be 2. If the fuel fraction is zero, it is fully burned, and the index is 3. Otherwise, the index is 1, indicating a burning particle. The mass of fuel is related to the

concentration. The fuel fraction of an unburned particle can be determined by the stoichiometric coefficients of the chemical reaction equation.

The thermodynamic state of a particle is determined by its composition, volume and temperature. The composition and volume of particles after mixing are their average values before mixing. The temperature after mixing is given by the first law (equation (25)),

$$U_1 + U_2 = 2U_3$$

An iteration procedure is used to obtain the final temperature corresponding to the internal energy U_3 .

1. The initial guessed temperature T_{guess} is the average temperature of the pair before mixing.
2. The total internal energy U_{guess} is calculated from T_{guess} using polynomial curve fitting of thermodynamic properties in the JANAF Tables (1971). The method of calculation is described in appendix (B).
3. If the calculated internal energy U_{guess} is close to the actual value $2U_3$, the solution of the temperature is adequate.

$$\frac{|2U_3 - U_{guess}|}{2U_3} < \epsilon$$

4. Otherwise, the temperature is adjusted to T_{next} as follows, and iteration repeated from step (2).

$$2U_3 - U_{guess} = mC_v(T_{next} - T_{guess}) \quad (65)$$

C_v is the heat capacity at constant volume. Rearranging equation (65),

$$T_{next} = \frac{U_{exact} - U_{guess}}{mC_v} + T_{guess} \quad (66)$$

3.4 GOVERNING EQUATIONS FOR THERMODYNAMIC STATES

The thermodynamic state of a burning particle is determined by the species concentrations, temperature and volume. These properties are calculated using the chemical rate equations for propane, oxygen, carbon dioxide, water, nitrogen and the equation for the rate of temperature rise of a burning particle.

$$\frac{dx_i}{dt} = -Av_i \exp(-E/RT_i) x_i^a y_i^b \quad (28)$$

$$\frac{dy_i}{dt} = 5 \frac{dx_i}{dt} \quad (29)$$

$$\frac{dz_i}{dt} = -3 \frac{dx_i}{dt} \quad (30)$$

$$\frac{dw_i}{dt} = -4 \frac{dx_i}{dt} \quad (31)$$

$$\frac{d\nu_i}{dt} = 0 \quad (32)$$

$$\frac{dT_i}{dt} = \frac{\frac{dx_i}{dt}(RT_i - Um_i) + N_i \left(\frac{RT_i}{P}\right) \frac{dP}{dt}}{C_v + (N_i)(R)} \quad (39b)$$

Equations (29) to (32) can be replaced by algebraic relationships,

$$y_i = y_{i,o} + 5(x_i - x_{i,o}) \quad (67)$$

$$z_i = z_{i,o} - 3(x_i - x_{i,o}) \quad (68)$$

$$w_i = w_{i,o} - 4(x_i - x_{i,o}) \quad (69)$$

$$\nu_i = \nu_{i,o} \quad (70)$$

where the initial moles of species per grams of mixture are $y_{i,o}$, $z_{i,o}$, $w_{i,o}$, $\nu_{i,o}$ respectively.

The thermodynamic properties of burned and unburned particles are calcu-

lated using the isentropic relations provided by the equation for the rate of pressures rise,

$$\frac{dP}{dt} = \frac{R \sum_{i=1}^{N_1} \left\{ \frac{dx_i}{dt} \left[-mT_i + \frac{n_i(RT_i - U_{m,i})}{C_{v,i} + N_i(R)} \right] \right\} - P \frac{dV}{dt}}{\left\{ V - \sum_{i=1}^{N_1} \left[\frac{n_i N_i R T_i}{C_{v,i} + N_i(R)} \right] - N_2 n_u T_{u,o} \left(\frac{1}{P_o} \right)^{\frac{\gamma_u-1}{\gamma_u}} \left(\frac{\gamma_u-1}{\gamma_u} \right) P^{-\frac{1}{\gamma_u}} - \sum_{j=1}^{N_3} \left[n_j T_{j,o} \left(\frac{1}{P_o} \right)^{\frac{\gamma_j-1}{\gamma_j}} \left(\frac{\gamma_j-1}{\gamma_j} \right) P^{-\frac{1}{\gamma_j}} \right] \right\}} \quad (53)$$

where the following terms in equation (53) calculate the rate of temperature rise for the unburned and burned particles respectively.

$$T_{u,o} \left(\frac{1}{P_o} \right)^{\frac{\gamma_u-1}{\gamma_u}} \left(\frac{\gamma_u-1}{\gamma_u} \right) P^{-\frac{1}{\gamma_u}} \frac{dP}{dt} = \frac{dT_u}{dt}$$

$$T_{j,o} \left(\frac{1}{P_o} \right)^{\frac{\gamma_j-1}{\gamma_j}} \left(\frac{\gamma_j-1}{\gamma_j} \right) P^{-\frac{1}{\gamma_j}} \frac{dP}{dt} = \frac{dT_j}{dt}$$

The ordinary differential equations (ODE), to be solved are the rate equation of propane (equation (28)), temperature of each burning particle (equation (39b)) given by the first law, and the pressure derivative (equation (53)). If the number of burning particles in a time step is N_1 , then the ODE system consists of N_1 rate equations, N_1 temperature equations and one pressure equation, a total of $2N_1 + 1$ equations.

Several methods to solve the set of (ODE) are attempted, and the one with least computing time and moderate accuracy is selected. If no burning particles are present in the time interval, subroutine ISCOMP in appendix (J) is used to perform isentropic compression calculations.

3.4.1 ORDINARY DIFFERENTIAL EQUATION SOLVERS

The first method considered was DGEAR. This subroutine is in the IMSL.

library of the main frame computer at the University of Ottawa. DGEAR is capable of dealing with a wide variety of ODE's. It uses the variable order Adams predictor corrector method if the user specifies that the ODE system is non-stiff, or the Gears backward differential formula if a stiff system is specified. The method of DGEAR was appealing because of its capability to solve a stiff system, which is typically the case for chemical rate equations. The program is accessible and ready to be used. The user specifies either one of the two basic methods (Adams or Gears), and the desired tolerance for error, the initial step size, and one of six methods of corrector iteration. DGEAR automatically selects the step size to minimize computing time. The algorithm is adapted from a package designed by Hindmarsh (1974) based on Gear's subroutine DIFSUB (1971). A similar method by Hindmarsh called LSODE (1980) was evaluated by Radhakrishnan (1985) for a batch reactor, and it was found to be very efficient for the test problem. However, upon testing DGEAR with the present model, DGEAR was found to be very sensitive to the specified tolerance, initial step size and corrector iteration method used, but relatively insensitive to whether the stiff method of Gear or the non-stiff method of Adams is used. Most importantly, the computing time was excessively long. The results constantly indicated that a large number of steps were taken. If the tolerance and initial step size is increased in order to reduce the number of steps, warning and error messages indicate that the step size was reduced more than once and the error bound was exceeded. After experimenting with different values of tolerance, initial step size and different corrector iteration methods, it was found that small tolerance and initial step size yielded most stable computation at the expense of longer computing time. The user attempted to obtain the listing of DGEAR in order to understand its detail algorithm, but did not succeed due to the copyright protection policy of IMSL. Both the Adams predictor corrector method and Gear backward differentiation formula are implicit linear multistep methods. Since DGEAR did not yield satisfactory results, an explicit one step method was considered.

The Runge-Kutta fourth order method is often used among explicit one step methods. Among the different Runge-Kutta methods, the one derived by England (1969) is a fourth order six stage method having an error estimate valid for a system of non-linear equations. The error estimate at each step is used to control step size and minimize the number of steps required, hence minimizing computing time. The initial step size and tolerance are required in this method. It was found that the solution is sensitive to the values of initial step size and tolerance. The iteration in each step requires excessive computing time, and the method was not as efficient as DGEAR. If the initial step size and tolerance are very small, England's method is even slower than DGEAR. However this method accepts large values of initial step size and tolerance but DGEAR does not. This study shows that DGEAR is more efficient than England for the same level of accuracy.

Since DGEAR and Runge-Kutta methods are designed for general systems of ODE, it was then decided to test a method specifically designed for chemical rate equations. A method developed by Young and Boris (1977) (called CHEMEQ) uses a second order predictor-corrector method. It determines the stiff equations among the system equations, and applies an asymptotic integration method. The other normal equations (non-stiff) are treated using Euler's predictor and the trapezoidal rule as the corrector. The user specifies the error tolerance. The initial step is automatically determined. The step size control is based on the number of iterations required to achieve convergence. If the step converges in a small number of iterations, the step size is increased. If the step does not converge within a specified number of iterations, the step size is reduced and the calculation of the step is repeated. The algorithm is simpler than the Runge-Kutta method, and most importantly, requires fewer iterations at each step.

3.4.2 THE ADOPTED METHOD

The method by Young and Boris (1977) is designed to solve chemical rate equation in the form of,

$$\frac{dx_i}{dt} = Q_i - \frac{x_i}{\tau_i} \quad (71)$$

where Q is the production rate and τ_i is the equilibration time. Rewriting equation (71),

$$\frac{dx_i(t)}{dt} = g_i(t) \quad (72)$$

where

$$g_i(t) = Q_i(t) - \frac{x_i(t)}{\tau_i(t)} \quad (73)$$

The initial step size is taken as proportional to the minimum of the characteristic time $\frac{x_i(0)}{g_i(0)}$ among all the equations,

$$\delta t = \epsilon \min \left\{ \frac{x_i(0)}{g_i(0)} \right\} \quad (74)$$

where ϵ is a scale factor typically of order 10^{-3} . An equation is considered stiff if the production term Q_i and the dissipation term x_i/τ_i are large and nearly equal.

This is determined by,

$$\frac{\delta t}{\tau_i(0)} > 1 \quad (75)$$

For normal equations, Euler's method is used as predictor,

$$x_i(1) = x_i(0) + \delta t g_i(0) \text{ for normal equations.} \quad (76)$$

and the trapezoidal rule is used as the corrector,

$$x_i(m+1) = x_i(0) + \frac{\delta t}{2} [g_i(m) + g_i(0)] \quad (77)$$

For stiff equations, an asymptotic integration method is used. The predictor is,

$$x_i(1) = \frac{x_i(0)[2\tau_i(0) - \delta t] + 2\delta t \tau_i(0) Q_i(0)}{2\tau_i(0) + \delta t} \quad (78)$$

and the corrector is,

$$x_i(m+1) = \frac{\left\{ \frac{\delta t}{2} [\tau_i(m) + \tau_i(0)] [Q_i(m) + Q_i(0)] + x_i(0) [\tau_i(m) + \tau_i(0) - \delta t] \right\}}{[\tau_i(m) + \tau_i(0) + \delta t]} \quad (79)$$

A step converges when consecutive corrector iterations yield nearly equal results, indicated by the local error being smaller than the specified tolerance,

$$\frac{|x_i(m+1) - x_i(m)|}{\min[x_i(m+1), x_i(m)]} < \epsilon_3 \quad (80)$$

where ϵ_3 is of order 10^{-3} . If convergence is not achieved in two to four iterations, the step size is reduced by a factor of two to three and the calculation of the step is repeated. This was found to be more efficient than reducing the step size by a factor of less than two. If convergence is achieved in one or two iterations, the step size is increased by 5-10% for the next step. It was found that increasing the step size by more than 10% would be less efficient due to the need to reduce the step size again in the next step.

Upon applying this method to the present problem, it was found that none of the equations met the criterion for stiffness. Therefore, only the predictor and corrector for normal equations are used. The fact that the chemical rate equations in this model are non-stiff may be explained by Radhakrishnan (1985), who stated that 'The problem of stiffness in chemical kinetics is the result of widely varying rates of change in different species'. Since there is only one rate equation for propane in the model, widely varying rates of change in different species are not present in the model. Also the initial step size is determined by equation (74) can sometimes be an order of magnitude smaller than the last step size used in the previous time interval. In order to prevent an excessively small initial step size, equation (74) is extended as,

$$\delta t = \max[\epsilon \min\left\{\frac{n_i(0)}{y_i(0)}\right\}, H_{last}, \Delta t/10] \quad (81)$$

where H_{last} is the last step size used in the previous time interval and Δt is the length of the present time interval.

It was found that five corrector iterations should be allowed before reducing step size and repeating the step in order to minimize the required number of steps

and avoid an excessive reduction of step size. If more than five corrector iterations are required, step size is reduced by a factor of two to five.

$$H_{new} = \max\{\min(\delta t/2, \delta t/S), \delta t/5\} \quad (82)$$

where H_{new} is the new step size, δt is the step size to be reduced, and

$$S = \frac{|x_i(m+1) - x_i(m)|}{\min\{x_i(m+1), x_i(m)\} \epsilon_3}$$

S is the ratio of local error to the specified tolerance ϵ_3 . It is greater than one when convergence has not been achieved. S measures the difference between the actual error and its desired value (ϵ_3). If this ratio S is less than two, the step size is reduced by a factor of two. If S is between two and five, the step size is reduced by a factor of S . If S is greater than five, the step size is reduced by a factor of five. Reducing the step size by a factor of two to five is more efficient than reducing it by a factor of two to three as used by Young and Boris (1977). The step size is allowed to be reduced up to three times, after which computation is stopped. If a step converges within two corrector iterations, the next step size is increased by 50% to minimize the number of steps. The total number of steps allowed is one hundred; however, warning messages are issued when the number of steps exceeds fifty. Computation is stopped when the number of steps exceeds one hundred. The method being adopted is more efficient than DGEAR and Runge-Kutta when moderate accuracy is required. The listing of this ODE solver subroutine CODE is in appendix (K).

3.5 OVERALL SOLUTION PROCEDURE

The solutions for ignition, entrainment, mixing and thermodynamic states of particles are calculated using the following procedure.

1. Specify the input parameters at the closing of the intake valve, namely

the crank angle at which the intake valve closes, the turbulence intensity, mixture temperature, pressure, equivalence ratio, spark advance, spark duration, ignition energy, spark gap, number of particles to be ignited, engine RPM, time interval (see section 3.6), and the timing for the opening of the exhaust valve.

2. Calculate temperature and pressure before ignition, using the isentropic relations as discussed in the solution procedure for ignition (section 3.1).
3. Calculate temperature and pressure of burned and unburned gases after ignition, using the first law and volume constraint as discussed in the solution procedure for ignition (section 3.1).
4. The volume of the burned particles after ignition is considered to be the partially stirred reactor.
5. The surface area of the reactor is calculated using subroutine SHAPE. The entrainment velocity is calculated using subroutine SPEED. The number of unburned particles entering the reactor is calculated using the entrainment model as discussed in the solution procedure for turbulent entrainment (section 3.2).
6. The mixing frequency is calculated as a function of turbulence intensity. The number of mixing pairs is calculated as a function of the mixing frequency and the number of particles in the reactor.
7. The random number generator GGUD is called to select pairs of particles to be mixed. The results of each binary mixing is calculated using subroutine MIXFRO, as discussed in the solution procedure for binary mixing (section 3.3). The results of binary mixings are the initial thermodynamic states of particles at the beginning of the time interval.

8. The thermodynamic states of particles are calculated using the chemical rate equations, rate equations of temperature rise for each burning particle, and the rate equation of pressure rise for the system, which includes the isentropic relations for the compression of burned and unburned particles. The solution procedure for these equations is discussed in section 3.4.
9. The thermodynamic states of particles at the end of the time interval are used to calculate the volume and surface area of the partially stirred reactor for the next time interval.
10. Step (5) to (9) are repeated for the calculations of the next time interval, until misfire occurs or the exhaust valve opens.

3.6 APPROXIMATION OF PRESSURE DERIVATIVE

The computing time spent on the iteration of the rate of pressure rise (equation (53)) was found excessive regardless of the method used. The thermodynamic state of each particle, including the unburned particle outside the partially stirred reactor is updated in each iteration, consuming a large amount of computing time. The result showed that the pressure rise is smooth and increases slightly in for the time interval used in the study. Therefore, a linear pressure rise approximation in the time interval is adequate, and significant computing time is saved. The pressure rise is estimated using an iteration procedure.

1. The initial guessed pressure derivative is assumed to be the same as in the previous time interval.

$$\frac{dP}{dt} = \frac{P(t) - P(t - \Delta t)}{\Delta t}$$

2. The pressure during the time interval Δt is calculated using the guessed

pressure derivative,

$$P(t + \Delta t) = P(t) + \frac{dP}{dt} \Delta t$$

3. The system of ODE without the pressure equation is solved in the time interval.
4. Thermodynamic states of all particles are updated at the end of the time interval.
5. The volume constraint is used as the criterion of convergence. If the total volume is close to the chamber volume, then the solution is converged.

$$|V_p - V_t| < \epsilon$$

where ϵ is a small positive number.

6. Otherwise, the pressure derivative is adjusted using the perfect gas law applied to the chamber volume,

$$P_{next} = P \left(\frac{V_p}{V_t} \right) \quad (83)$$

$$\frac{dP}{dt} = \frac{(P_{next} - P_o)}{\Delta t} \quad (84)$$

where P_{next} is the next guessed pressure at the end of time interval, P is the pressure at the end of the time interval obtained from the present guessed pressure rise, V_p is the total volume of particles with the present guessed pressure rise, V_t is the chamber volume at the end of time interval, $\frac{dP}{dt}$ is the next guessed pressure rise, P_o is the pressure at the beginning of the time interval. The iteration is repeated from step (2).

A maximum of three iterations is allowed, after which computation is stopped.

This procedure eliminates the need of the rate of pressure rise equation, so that the number of equations to be solved by CODE is $2N_1$ where N_1 is the number of burning particles. This procedure is performed by subroutine KINET listed in appendix (F).

3.7 SELECTION OF TIME INTERVAL

As discussed in section 3.1, the flame propagation, turbulent mixing and chemical reaction take place simultaneously. Therefore, the time interval should be as short as possible for accurate simulation. However, computing time generally increases as the number of time intervals increases. On the other hand, if the time interval is long, all the burning particles will have sufficient time to become fully burned before being mixed with other particles, since all mixing occurs only at the beginning of each time interval. The quenching of the burning particles is not realistically modeled in this case, no matter how high the mixing frequency is. The balance between realistic simulation and computational efficiency should be considered.

In the early stage of the development of the model, a time interval corresponding to one crank angle degree at 1500 RPM was used. It was observed from the result that some of the burning particles remain burning if the pre-exponential constant in the rate equation is taken as 4.3×10^{11} , which is half of the value given in Westbrook and Dryer (1981). This constant is empirical and can be adjusted as suggested by Westbrook and Dryer. It affects the time scale in which a burning becomes a fully burned. The sensitivity to the selection of time interval was studied using one degree crank angle, one half degree crank angle and one quarter degree crank angle. The study showed that the use of different time intervals yielded the same solution. The use of a half degree crank angle resulted in less computing time than using one degree. This is due to the nature of the rate equations being

solved and the method of solution. When one crank angle interval was selected, the adopted method determined an initial step size, and proceeded with calculation until the portion of the solution where the rate of change was high, then the step size was reduced to follow the solution. In the case of half a degree crank angle interval, the slope of the solution did not vary as much, and computing time was saved since there was no need to reduce the step size. One quarter of a degree crank angle was also attempted, but no improvement was found. Therefore, one half crank angle degree was used for an engine speed of 1500 RPM. When engine speed is increased to 3000 RPM, one crank angle degree is selected.

CHAPTER 4

RESULTS AND DISCUSSION

The model was tested for the ignition limit and partial burn limit. The sensitivity of the model to turbulence, intake pressure and temperature, fuel equivalence ratio, spark advance, ignition energy, spark gap and engine speed were investigated for the ignition limit. Furthermore, the sensitivity of the model to the number of particles ignited and to the activation energy was also studied. For the partial burned limit, two cases of flame quenching at the expansion stroke were obtained. To determine if the cycle misfires, the mass burn fraction is calculated against the engine crank angle. The mass burn fraction is defined as the ratio of the mass of combustion product to the total mass of mixture in the combustion chamber. Misfire occurs when the mass burn fraction does not increase with respect to crank angle.

4.1 EMPIRICAL CONSTANTS IN MODEL

The empirical constants of the model should be adjusted using experimental data from an actual engine. However, since experimental investigation is beyond the scope of this study, typical values are used. Experimental results from other researchers have been considered. However, incomplete engine specifications prohibited precise comparison of data. The empirical constants are the constants in the mixing frequency expression and chemical rate equations.

The constant C (ω/u') in the mixing frequency expression was selected such that when the turbulent intensity u' is about 200 cm/sec, the mixing frequency ω will be about 700 Hz. The value of C is 0.017 sec/cm^2 . Figure 2 shows the sensitivity of the model to constant C for the engine operating conditions shown in Table 2. (

All results shown in graphs have a resolution of one crank angle degree.)

There are four constants in the chemical rate equation,

$$\frac{dX_i}{dt} = -AT_i \exp\left(\frac{-E}{RT}\right) X_i^a Y_i^b \quad (27)$$

Westbrook and Dryer (1981) proposed that the pre-exponential A was 8.6×10^{11} *Kcal/mole*, the activation energy E was 30.0 *Kcal/mole*, the concentration exponents for fuel and oxygen, a and b , were respectively 0.1 and 1.65. In their study, the authors adjusted the pre-exponential and activation energy to predict the laminar flame speed. However, the values of these constants are not certain due to the absence of experimental data for the laminar flame thickness. In their work, the authors adjusted the value of the pre-exponential while keeping the activation energy at 30.0 *Kcal/mole*. In the present study, when the pre-exponential was 8.6×10^{11} and activation energy was 30.0 *Kcal/mole*, all the burning particles become fully burned in half a degree crank angle even at the equivalence ratio of 0.5. The pre-exponential constant was lowered to 50% of the suggested value. The result shows some burning particles remained burning in the same condition. Radhakrishnan and Pratt (1984) adjusted this constant to 60% of the value proposed by Westbrook and Dryer (1981). The activation energy E may also have to be adjusted (Hallett, 1988). The sensitivity of the present model to the pre-exponential and activation energy was investigated. The value for the activation energy E was varied from 25.0 to 40.0 *Kcal/mole* and the pre-exponential constant was 8.3×10^{11} . Testing conditions are shown in Table 2. The results are shown in Figure 3. The burning rate is sensitive to the activation energy. It decreases with increasing activation energy, and misfire occurred when the activation energy was equal to 40.0 *Kcal/mole*. The activation energy represents the energy required to initiate chemical reaction. Therefore, it is reasonable to assume that burning rate decreases with increasing activation energy. The prediction of the model (Figure 3) confirms this trend.

The pre-exponential A was varied from 2.0×10^{11} to 8.6×10^{11} *Kcal/mole*.

The activation energy was kept at 30.0 *Kcal/mole*. The model is sensitive to the variation of the pre-exponential (Figure 4). However, the burning rate is more sensitive to the variation of activation energy than the pre-exponential. It varies exponentially with activation energy and linearly with the pre-exponential. Radhakrishnan and Pratt (1984) followed Westbrook and Dryer (1981), keeping the activation energy constant, and adjusting the pre-exponential. This approach is adopted in the present study. The following constants are used for chemical kinetics in the the present study.

$$\begin{aligned} E &= 30.0 \text{ Kcal/mole} & A &= 4.6 \times 10^{11} \text{ Kcal/mole} \\ a &= 0.1 & b &= 1.65 \end{aligned}$$

4.2 TURBULENCE INTENSITY

The sensitivity to turbulence intensity of the model was investigated. In these tests, the intake temperature and pressure respectively were 300°K and 0.5 atm. The mass per cycle was about 0.24 grams. The engine speed was set at 1500 RPM, and ignition at 60 degrees before top dead center. The ignition energy was 6 mJ and deposited to 10 particles in 2 crank angle degrees, corresponding to the ignition duration of 0.2 msec. The fuel equivalence ratio was 0.5. The turbulence intensity at the closing of the intake valve was varied from 1 m/sec to 2 m/sec, then varied again to 3 m/sec. The engine specification for all tests is shown in Table 1. The complete testing conditions are listed in Table 3. Each computer experiment took about 30 minutes of CPU time, which yielded about 20 crank angle degrees of results.

A comparison of the mass burned fraction of the three cases is shown in Figure 5. The model is sensitive to the changes in turbulence intensity. As turbulence intensity was increased from 1 m/sec to 2 m/sec, the mass burned fraction rate increased. This was due to the higher rate of mass entrainment and mixing frequency

when turbulence intensity was increased. When the turbulence intensity was further increased to 3 m/sec, the mass burn fraction increased even faster initially, but became constant after about 10 degrees. The flat portion of the curve shows that no burning took place after about 10 degrees after ignition. In other words, misfire occurred. At a high turbulence intensity, the rate of mixing was high. The burning particles were quenched by being mixed with unburned before having enough time to become fully burned. A mixing time can be defined as a characteristic time inversely proportional to the mixing frequency. It measures the duration between consecutive mixing events. When turbulence intensity is increased, the mixing frequency increases. As a result, the mixing time decreases. Therefore, the time available for undisturbed chemical reaction, which is the duration between consecutive mixings, is shorter at higher turbulence intensity.

At low turbulence intensity (1 m/sec), the mixing time is longer, and the mass burning rate is controlled by flame propagation and mixing rate. Therefore, higher turbulence intensity increases mass burning rate. At higher turbulence intensity (3 m/sec), the mixing time is shorter, and the mass burning rate is controlled by the chemical rate. Consequently, higher mixing frequency decreases mass burning rate. There is an optimum level of turbulence intensity at which the mass burning rate is highest. The result shows that 2 m/sec can be the optimum turbulence level for the given operating condition. The existence of an optimum turbulence intensity is consistent with the finding of Ho and Santavicca (1987) : the authors stated that wrinkling of the flame front by turbulence increases burning rate, while a very high level of turbulence extinguishes the flame.

The pressure traces for different turbulence intensities are essentially identical (see Figure 6). This is due to the small fraction of the mixture being burned. The pressure rise was mostly due to the compression by the piston, since the burned mass was less than 0.05 % . Such results were also observed in other tests in this study, except when mentioned otherwise.

Turbulence intensity in engines is a function of the design of the intake system. The level of turbulence at the closing of intake valve is a fraction of the volumetric flow velocity passing through the intake valve (see for example R.E. Milane et al, 1983). Therefore the turbulence intensity can be increased by reducing the valve lift and increasing the flow velocity. However, this will also affect the intake pressure and mass flow. On the other hand, increasing throttle or load to the engine also increases turbulence intensity due to the increased mass flow, but this will also increase the pressure. The previous results on the variation in turbulence intensity while keeping other variables constant are not applicable. The effect of pressure variation will be discussed in the following section, and the combined effect of turbulence intensity and pressure variation will also be investigated.

4.3 INTAKE PRESSURE

The change of pressure leads to a change in mass flow if temperature stays constant. Any change in mass flow rate affects the flow velocity across the intake valve, and in turn affect the turbulence intensity of the flow field. If the change of pressure is the result of changing the throttle position, the variation in turbulence intensity is linearly proportional to that of the pressure in the combustion chamber. The turbulence intensity, pressure and mass flow are functions of the valve geometry. The change of pressure can result from changing the valve lift. But the valve geometry is not known in this study, therefore only the case of constant intake valve area will be used in the testing.

The model was first tested for the variation of pressure while the turbulence intensity was kept constant. Complete testing conditions are listed in Table 4. The result shows that the mass burning rate decreased with increasing pressure, when the pressure was varied from 0.2 atm to 0.8 atm. (see Figure 7). This is the result of (39b) describing the temperature rate of the combustion of propane and

air mixture. This equation shows that temperature rate increases with decreasing pressure. The increase of temperature rate then causes an increase in mass burning rate. It is to be noticed that such an effect of variation of pressure alone does not usually occur in real engines, because any variation of pressure will also affect other variable such as the turbulence intensity as discussed above.

The model was tested for the effect of variation of pressure and turbulence intensity. The turbulence intensity is assumed to be linearly proportional to the intake pressure. Four different sets of pressure and turbulence intensity combinations were used. They were 0.4 atm with 1.6 m/s, 0.5 atm with 2.0 m/s, 0.65 atm with 2.6 m/s and 0.8 atm with 3.2 m/s, all taken at the closing of the intake valve. Spark advance was set at 60 degrees before top dead center, and intake temperature at 300 degrees Kelvin. Table 5 lists the complete testing conditions. The mass flow rates under these conditions varied from about 0.2 grams/cycle to 0.4 grams/cycle at an engine speed of 1500 RPM. The results show that the mass burning rates were higher for the case of higher pressure and turbulence intensity for the first 10 degrees crank angle after ignition (see Figure 8), but the trend was reversed afterwards. The mass burning rate stayed at a constant level in the case of 0.8 atm with 3.2 m/s of turbulence, indicating that misfire has occurred. This is the result of flame quenching caused by high turbulence intensity and high rate of mixing between the burning and unburned particles. The overall effect of variation of pressure and turbulence intensity is very similar to that of the variation of turbulence intensity alone. In other words, turbulence intensity has a stronger influence on mass burning rate than the pressure has.

4.4 INTAKE TEMPERATURE

The model was tested for the sensitivity to the variation of intake temperature. The intake temperature is the temperature of fuel mixture in the combustion

chamber at the closing of the intake valve. This temperature is not necessarily the same as the temperature of the flow in the intake manifold or the ambient temperature. The relationship of these different temperatures are functions of the design of the particular intake system, which is beyond the scope of the present study. The model was tested with intake temperatures of $200^{\circ}K$, $250^{\circ}K$, $300^{\circ}K$, $350^{\circ}K$, and $400^{\circ}K$. The intake pressure was 0.5 atm with the turbulence intensity at 2 m/s. The engine ran at 1500 RPM with the spark advance at 60 degrees before top dead center. Complete testing conditions are shown in Table 6. The mass flow rates of the three temperature settings ranged from 0.18 grams/cycle to 0.24 grams/cycle. The result of the variation of temperature indicates that the mass burning rate increases with increasing temperature (see Figure 9): Misfire occurs at $200^{\circ}K$.

The pressure traces of the three cases are shown in Figure 10. The three pressure traces are very close to each other, and approximately parallel to one another. As expected in the ignition period, the mass burned fractions are small. However, we observe that at the lower intake temperature, the pressure was higher. The pressure rise at the initial period of combustion was not due to combustion itself, since the mass burned fraction was very small. Therefore, the pressure rise in this regime was the result of compression. The fuel mixture went through the same amount of change in volume for the three cases of different temperatures, but the ratio of specific heat for the mixture is a function of temperature. Its value decreases with increasing temperature for any given composition of the mixture. Therefore, the mixture at lower temperature will have a higher ratio of specific heat and a higher final pressure after compression. The resulted pressure traces show that the model is sensitive to the variation of the ratio of specific heat. A similar conclusion was also reached in the following section on the variation of the fuel equivalence ratio.

4.5 FUEL EQUIVALENCE RATIO

The model's sensitivity to the variation of equivalence ratio was one of the most important tests, since the most accepted definition of misfire limit is defined as the equivalence ratio at which combustion fails. The test was conducted with four different values of equivalence ratio, 0.3, 0.5, 0.7 and 0.9. The intake conditions were set at $300^{\circ}K$, 0.5 atm and a turbulence intensity of 2 m/s. The engine ran at 1500 RPM and the spark advance was set at 60 degrees before top dead center. Complete testing conditions are shown in Table 7. Results of Figure 11 indicate that burning rate increased with equivalence ratio. For an equivalence ratio of 0.3, misfire occurred after about 12 degrees from ignition. Although the result shows no misfire for the case of 0.5 equivalence ratio, it does not contradict with the result of other researches which suggested that the lean misfire limit was generally in the range of 0.6, because the testing result does not correspond to any actual engines. The model needs to be calibrated in order to generate more solid data instead of showing general trends.

The pressure traces in Figure 12 for the different fuel-air ratios also show trends similar to that of the variation of intake temperature. Again, the pressure traces are close together and approximately parallel because of the very small mass burned and heat release, but the one with the lower equivalence ratio is always higher than that with the higher equivalence ratio. The pressure rise was the result of compression since burned mass is small. The ratio of specific heat of the fuel mixture is now a function of composition. Its value increases with decreasing equivalence ratio. Therefore, the leaner mixture has a higher final pressure than the richer mixture for the same amount of change in volume due to compression.

4.6 SPARK ADVANCE

The spark advance was varied from 90 degrees before top dead center to 60 and 30 degrees before top dead center. The model was tested at 1500 RPM, with the fuel equivalence ratio of 0.5, and intake temperature and pressure as 300°K and 0.5 atm respectively. The turbulence intensity was 2 m/s at the closing of the intake valve. Table 8 shows the complete testing conditions. The variation of spark advance affects the temperature, pressure and turbulence intensity at ignition, whose values increase when spark timing is retarded. The results show that the mass burning rate increased when spark advance was retarded (see Figure 13). For the earliest spark advance (90 degrees BTDC), the burning was slow just after ignition, and misfire occurred after about 17 degrees. The volume in the spark gap which was ignited was the same for the three cases, but the mass was slightly higher when the spark timing was retarded (to 30 degrees before top dead center) because of higher density. This effect combined with the higher temperature and turbulence intensity at ignition resulted in an increase in the burning rate when spark timing was retarded to 30 degrees BTDC. The higher pressure at ignition, at 30 degrees BTDC, did not slow down the chemical reaction enough to affect the burning rate. Furthermore, the high turbulence intensity did not produce a quenching effect on the burning particles at high temperature, because the chemical time at high temperature was relatively short. Therefore the combined effect of higher temperature, pressure and turbulence intensity increases the mass burning rate.

The trend of misfiring when spark timing is advanced also agrees with the experiments of Anderson and Lim (1985). The ignition energy and spark gap used in this study were respectively 6 mJ and 1 mm. The spark duration during which the selected 10 particles became fully burned was 2 degrees, or about 0.2 msec at 1500 RPM. The influence of these ignition variables will be discussed in the following sections.

4.7 IGNITION ENERGY

Ignition energy refers to the energy deposited in the ignited particles from the spark, as described in Chapter 2. The amount of energy required to initiate combustion is not investigated in this study. The objective of this study is to investigate flame propagation after ignition. The influence of the ignition energy on the flame propagation was investigated using several ignition energies : 3 mJ, 6 mJ and 9 mJ. The engine speed was 1500 RPM and spark advance was 60 degrees before top dead center. The fuel equivalence ratio was 0.5, and the intake temperature and pressure were respectively $350^{\circ}K$ and 0.5 atm. The turbulence intensity was 2 m/s at the closing of intake valve, and the spark gap was 1 mm. Table 9 lists the complete testing conditions. The result shows that the mass burning rate increased with increasing ignition energy (see Figure 14). The higher ignition energy caused the temperature of the ignited particles to increase, which in turn yielded a higher burning temperature when they mixed with other unburned particles. The adiabatic flame temperature increased from $2000^{\circ}K$ to $2700^{\circ}K$ as the ignition energy was increased from 3 mJ to 9 mJ. No misfire was observed even when the ignition energy was 3 mJ. This is not surprising. The model for ignition assumes that the mass within the spark gap is ignited, and initial flame propagation is supported by the heat release from the burned mass. In reality, heat is lost to the electrode, and a fraction of the mass within the spark may be ignited. Anderson and Lim (1985) related the minimum ignition energy to a quench distance, and stated that if the flame kernel grows to the size of the quench distance, propagation can be supported by the chemical heat release alone. Therefore, if the cases tested in the model had their initial flame kernel size at least as large as a theoretical quench distance, misfire due to insufficient ignition energy will not occur. The variation of spark gap size simulated by igniting a different initial volume represents another aspect of the effect of spark ignition on misfire.

4.8 SPARK GAP DISTANCE

The spark gap distances used were 0.5 mm, 1 mm and 2 mm. The ignition energy was held constant. In reality, heat loss to the spark plug electrode decreases when the gap distance is increased. However, the amount of energy being transferred to the ignited gas as a function of the gap distance is not established in this study. This energy depends on the specific design of the ignition system, which is beyond the scope of this study. The present tests were conducted with an ignition energy of 6 mJ and 2 degree spark duration. The engine ran at 1500 RPM and spark advance was set at 60 degrees before top dead center. Intake temperature and pressure were 350°K and 0.5 atm respectively, while the turbulence intensity at the closing of the intake valve was 2 m/s. Complete testing conditions are listed in Table 10. For the fuel equivalence ratio of 0.5, the result shows that the mass burning rate was not a strong function of spark gap. (see Figure 15). The burned particles of the smaller spark gap had a higher temperature (3000°K for 0.5 mm), because the same amount of ignition energy was deposited to all three cases. However, the higher temperature at 3000°K was offset by the small burned volume of 0.5 mm spark gap. The present ignition model is not able to predict the effect of spark gap distance due to the lack of a model for the heat losses through electrode and the unburned surrounding. If the heat loss through the electrode is taken into account, the burned temperature at small spark gap of 0.5 mm will be lower than 3000°K. If heat loss to the unburned surrounding is taken into account, the spark will not be able to ignite all the mass within the spark gap when the gap distance is large (2 mm). Therefore, a more realistic model should include the relationship between the spark gap, ignition energy and amount of mixture to be ignited.

4.9 ENGINE SPEED

The sensitivity of the model to the variation of engine speed was tested.

The change of engine speed alters the turbulence intensity at the closing of the intake valve. It is assumed that turbulence intensity varies linearly with RPM (Tabaczynski, 1976). The model was tested with 2 m/s of turbulence intensity at 1500 RPM and 4 m/s at 3000 RPM. Spark advance was set at 60 degrees before top dead center. The fuel equivalence ratio was 0.5, with the intake temperature and pressure of $350^{\circ}K$ and 0.5 atm respectively. Table 11 lists the complete testing conditions. The results shown in Figure 16 indicated that the engine misfired right after ignition at 3000 RPM, while a fast burning rate was obtained at 1500 RPM. The large difference between the two cases was the result of the very high turbulence intensity generated at 3000 RPM. The turbulence intensity at the closing of the intake valve at 3000 RPM was assumed to be double that at 1500 RPM at the same intake temperature and pressure. In reality, the intake temperature and pressure is not necessarily the same as the engine speed increases from 1500 to 3000 RPM. Therefore the turbulence intensity will also be affected by the intake pressure. Nevertheless, the present result shows the trend toward misfire as engine speed and turbulence intensity increase.

4.10 NUMBER OF IGNITED PARTICLES

The number of particles to be ignited is an input variable in the model. The selection of its value is independent on the spark gap size, which determines the volume to be ignited. Therefore, it does not influence the amount of fuel mixture being burned initially, but it determines the size of each particle. One expects that the size of particle should be very small to closely simulate the actual phenomena, but an excessively small particle size and a large number of particles require longer computing time. The objective is to select a number of particles yielding reasonably accurate results with the least computing time. The model was tested by igniting 10, 25 and 50 particles, with the fuel equivalence ratio of 0.5. The intake temperature

and pressure were respectively $350^{\circ}K$ and 0.5 atm. The turbulence intensity of 2 m/s was used, and the engine ran at 1500 RPM, with the spark advance set at 60 degrees before top dead center. Complete testing conditions are shown in Table 12. All three cases were computed using 5 minutes of CPU time. When 10 particles were ignited, 13 crank angle degrees of results were obtained, for 25 ignited particles, 11 degrees, and for 50 ignited particles, 8 degrees (see Figure 17). It is obvious that the smaller number of particles reduces computing time significantly. A comparison of the mass burning rate of the three cases shows that the case with larger number of particles burned slightly faster at the beginning, but the difference was reduced after a few crank angles. These results also reveal that the initial burning rate when 50 particles was used is smoother than the others. This is due to the more accurate modelling of the mass entrainment at the initial stage when the number of particles in the partially stirred reactor is large. However, after several particles are entrained into the reactor, the cases of 25 and 10 ignited particles also yield good accuracy. The slight difference in the results does not justify using a large number of particles because it uses a longer computing time. Therefore, all model testing was done using 10 ignited particles. The minimum number of ignited particles also depends on the turbulence intensity which controls both the entrainment and mixing of particles. A smaller number of ignited particles can be used for higher turbulence intensity since more particles will be entrained and mixed in a shorter period of time, eliminating the initial inaccuracy due to the small number of particles.

4.11 PARTIAL BURN LIMIT

The above model tests have demonstrated several cases of misfire at the ignition limit. Arici et al (1983) believed that the ignition limit occurred more often than the partial burn limit for actual engine conditions. Peters (1979) observed that partial burn corresponded to slow burning cycles still burning at the opening

of the exhaust valve, rather than being quenched before the exhaust valve opened. However, quenching during the expansion stroke still occurs. This has led to the experimental study of Smith et al (1977) in an expanding chamber. It was the purpose of this present model to simulate both the ignition and partial burn limited misfire. Therefore, the model will be tested for partial burn. Various attempts were made to create a partial burn cycle, but few were successful. This agrees with the observations of Peter (1979). The case of expansion stroke quenching is rare. However, two combinations of operating conditions shown in Table 13 were observed to create quenching during the expansion stroke. The engine displacement in these two cases was taken as about half the size of other tests, because much computing time can be saved with a smaller cylinder since it contains fewer particles. The specification of the engine is listed in Table 1. More efficient computation is necessary for partial burn cycles because more crank angles of results are required for a conclusion. The two cases observed had the same inlet conditions, at $290^{\circ}K$ and 0.5 atm, as well as a turbulence intensity of 3 m/s at 3000 RPM when the intake valve was closed. The first case deposited 1 mJ of energy to the ignited gas at the spark advance of 10 degrees before the top dead center, while the second case deposited 3 mJ of ignition energy at 30 degrees before top dead center. The flame was quenched at 25 degrees after top dead center in the first case (Figure 18), which was 35 degrees after ignition, while the quenching occurred at 15 degrees after top dead center in the second case, (Figure 19), about 45 degrees after ignition. The mass burned fractions in both cases were less than one percent, but the flame had entrained respectively 40 and 50 percent of the volume in the two cases. The results of ignition misfire indicate that about one percent of volume was entrained by the flame. The partial burned cycles are distinguished from the ignition misfire by the following conditions. Firstly, the volume entrained at partial burned limit is near 50%, while the ignition misfiring cycles entrained about 1% of the volume. Secondly, partial burn occurs in the expansion stroke, but the ignition misfire occurs in the

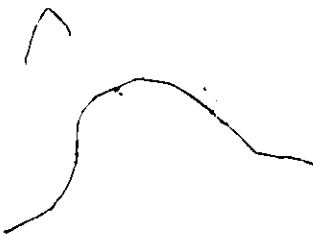
compression stroke. In the present study, the model could not reproduce the same data reported by Peters (1979). The two examples of partial burn in the present study have a mass burn fraction of less than 1%, but Peters (1979) reported that 20% of mass had burned in some cycles which were quenched during the expansion stroke. The small percentage of mass burn fraction predicted by the present model is possibly due to the lack of age mixing in the flame zone. In reality, only particles near each other can mix. However, the present model allows particles anywhere in the flame zone to mix. The lack of age mixing in the model affects the result of partial burn more severely than the ignition misfire, because the flame zone volume is large in the partially burned cycles. Therefore, introducing age mixing may prove to predict partial burn more adequately.

4.12 AGE MIXING

Age mixing allows only the neighbouring particles to mix. A particle close to the spark location cannot mix with one that is entrained later in time and therefore far away from the spark. The mixing of particles that are entrained at different time is controlled using the following procedure :

1. The burned particles from ignition are assigned to be at age 1.
2. For each time interval, unburned particles are entrained behind the flame front, creating a new age of particles. The ages of particles are assigned according to the order in which they are entrained. For example, the particles entrained one time interval after ignition are assigned to be at age 2, and those entrained in the next time interval are at age 3.
3. Particles with an age difference of one are allowed to mix. The mixing starts between age 1 and 2, followed by age 2 and 3 and so on. Mixing procedure is completed when all ages of particles have participated.

The procedure for age mixing is performed by subroutine AGEMIX (appendix L). Subroutine RANMIX is used when the volume behind the flame front is treated as a partially stirred reactor, without using the age mixing procedure. Tests for the ignition misfire regime and partial burn regime were performed. Results of the age mixing model are shown in Figures 20 to 22. Figure 20 shows that at early spark advance (60° BTDC), the burning rate predicted by the age mixing model is slower than that without age mixing. Age mixing allows fewer unburned particles to mix with burned ones, reducing the probability of creating burning particles. The result is a reduction in burning rate. This result is not expected to change the trend of the ignition limit although it predicts a higher equivalence ratio at the ignition limit. Figures 21 and 22 show that at late spark timings (at 10° and 30° BTDC), the age mixing model did not predict partial burn while the model without age mixing did. The burning rates predicted by the age mixing model are faster. At late spark timing, the turbulence intensity is high, and more unburned particles are entrained. The large number of unburned particles compared to burning and burned ones reduces the probability of mixing between unburned and burned or between unburned and burning particles (The highest probability of mixing two types of particles occurs when their numbers are about the same). Restricting mixing between neighbouring reaction zones by age mixing reduces the number of unburned allowed to mix with burned and burning. Therefore, age mixing increases burning rate. It is concluded that for the ignition limit, age mixing is not expected to alter the trend predicted by the model without age mixing. However, the age mixing model did not predict partial burn while the model without age mixing did. Further studies on the partial burn limit are required.



CHAPTER 5 CONCLUSION AND RECOMMENDATION

5.1 CONCLUSION

The model was developed to study misfire in lean combustion in spark ignition engines. It has the capability to simulate both the ignition limit and the partial burn limit. Tests have been performed extensively for the ignition limited cases. It usually requires no more than 20 degrees of crank angles after ignition to observe whether the ignition limit is reached, but the result after TDC is usually required to determine if the partial burn limit is reached. The results of partial burn cycles suggest that the concept of age mixing should be investigated. It was also observed that there was only a narrow range of combination of variables for which partial burn would occur when age mixing was not used.

5.1.1 IGNITION LIMIT

The testing on the effect of mixture, engine and ignition system variables on the ignition limit led to the following conclusions.

1. Turbulence intensity is a critical parameter for ignition limit.
2. Pressure does not have very strong effect on ignition limit, but it affects the flow rate into the cylinder, and the turbulence intensity is affected accordingly.
3. Temperature is another important parameter affecting the ignition limit.
4. Fuel equivalence ratio, the parameter often used to measure ignition limit, has great influence on ignition misfire.

5. Spark advance combines the effect of temperature, pressure and turbulence intensity. It shows the dominant effect of temperature, while turbulence intensity enhances flame propagation at higher temperature.
6. Ignition energy has an effect on the early burning rate, but does not influence the ignition limit as much as temperature and turbulence intensity.
7. Spark gap does not have direct influence on ignition limit, but the present ignition model lacks the detailed relations between ignition energy, gap distance and mass burned.
8. The model is not sensitive to the number of particles to be ignited initially, provided the number is sufficiently large, depending on the turbulence intensity.
9. Engine speed does not affect the ignition limit directly, but it changes turbulence intensity, and that has a strong effect on ignition limit.

The parameters affecting the ignition limit are the turbulence intensity, temperature and fuel equivalence ratio. The turbulence intensity controls flame propagation and particle mixing, while the temperature and fuel equivalence ratio control the chemical rate. Therefore, one can conclude that the balance of mixing and chemical rate is of great importance in engine misfire. High frequency of mixing enhances burning rate at high temperature and equivalence ratio. If the mixing frequency is further increased, it will adversely affect the burning rate, particularly at low temperature and equivalence ratio. In other words, the comparison of chemical time to mixing time determines the occurrence of misfire.

5.1.2 PARTIAL BURN AND AGE MIXING

Extensive parametric study on the partial burn limit was not performed due to the narrow range of combination of variables for which partial burn would

occur, and the longer computing time for the study. Therefore, it is not known how different parameters will influence the partial burn limit. However, cases of partial burn limited misfire have been obtained. The flame had propagated to 50 percent of the volume when it was quenched, but the mass burned fraction remained very small (less than 1 percent). The concept of age mixing was introduced in an attempt to improve the result of partial burn cycles. It was found that in the ignition misfire regime (early spark advance), the model of age mixing predicts a slower burning rate than that without age mixing. In the partial burn regime (late spark advance), the burning rate predicted by the age mixing model is faster than that without age mixing. The age mixing model did not predict partial burn when the model without age mixing did. More studies on partial burn cases are required. The difference in burning rate prediction between the model with age mixing and without age mixing is due to the probability of mixing between unburned and other particles.

5.2 RECOMMENDATION

The major difficulty encountered in the development of the model is the computing time required to yield a reasonable amount of results. There has not been a single run of the Fortran program giving results of a complete cycle. Only about 20 to 40 crank angle degrees of results has been obtained in most tests. Therefore, a more efficient algorithm should be included in the future development of this model, particularly for the method of solving the ODE system of the chemical kinetics.

A more efficient computation will make possible a more extensive study of the partial burn limit. A parametric study similar to the one performed on the ignition limit described in the previous chapter will help to understand the behavior of partial burn in engines. The age mixing model was implemented and initial tests were performed. However, ignition limit and partial burn limit have not been studied using the age mixing model as extensively as the model without age mixing. In the

partial burn regime, the age mixing model has not shown any occurrence of partial burn. Therefore, it is recommended that more studies on age mixing, particularly for partial burn cases, are required.

The model presently assumes that ignition always takes place regardless of the amount of ignition energy supplied to the unburned gas surrounding the spark plug. Therefore, it showed that the occurrence of misfire is not greatly influenced by the ignition energy. This is not true in reality. A more detailed ignition model including the relationship between the spark gap distance, ignition energy and the mass or volume ignited by the given energy should be considered in future development.

The rapid distortion theory without dissipation of kinetic energy is presently used to calculate turbulence intensity. A more accurate model should include the dissipation. The lean misfire limit is strongly influenced by the turbulence intensity; therefore, a turbulence model including dissipation may prove to be important, especially in the expansion stroke. The present model does not take into account the residual fraction or exhaust gas recirculation. If such parameters are of interest, they should also be incorporated into the model. Heat transfer is another aspect the present model does not include, and it is a possible future development.

The model constants have not been adjusted with any actual engine experiment due to the unavailability of complete data and engine specification. Therefore any future application of the model has to include constants validation with actual engine experiments.

REFERENCES

- R.G. Abdel-Gayed and D. Bradley (1985) Criteria for Turbulence Propagation Limits of Premixed Flames, *Combustion and Flame*, 62 : 61 - 68, 1985.
- R.W. Anderson, M.T. Lim (1985), Investigation of Misfire in a Fast Burn Spark Ignition Engine, *Combustion Science and Technology*, 1985, Vol 43, pp. 183 - 196.
- O. Arici, R.J. Tabaczynski, V.S. Arpaci (1983), A Model for the Lean Misfire Limit in Spark Ignition Engines, *Combustion Science and Technology*, 1983, Vol 30, pp. 31 - 45.
- D.K. Ballal, A.H. Lefebvre (1977), Ignition and Flame-Quenching Flowing Gaseous Mixtures, *Proc. Roy. Soc. London, Ser A* 357, 163.
- N.C. Blizard and J.C. Keck (1974), Experimental and Theoretical Investigation of Turbulent Burning Model for Internal Combustion Engines, SAE paper 740191.
- B. Carnhan, H.A. Luther, J.Q. Wilkes (1969), 'Applied Numerical Methods', Wiley and Son, P.178
- J. Chomiak and J. Jarosinski (1982), Flame Quenching by Turbulence, *Combustion and Flame*, 48 : 241 - 249, 1982.
- R.L. Curl (1963), Dispersed Mixing : Theory and Effects in Simple Reactions, *A.I. Ch. E. journal* 9, no. 2.
- H. Daneshyar, P.G. Hill (1988), The Structure of Small Scale Turbulence and Its Effect on Combustion in Spark Ignition Engines. To appear in *Progress in Energy and Combustion Science*.
- R. England (1969), Error Estimates for Runge - Kutta Type Solutions to Systems of Ordinary Differential Equations, *Comput. J.*, 12, pp. 166 - 170.

C.W. Gear (1971), Algorithm 407, DIFSUB for Solution of Ordinary Differential Equations. *Comm ACM*, 14, pp. 185 - 190.

G.J. Germane, C.G. Wood, C.C. Hess (1983), Lean Combustion in Spark Ignited Internal Combustion Engines - A Review, SAE paper 831694.

W.L.H. Hallett (1988), private communication.

J.B. Heywood (1978), Symposium on Combustion Modeling in Reciprocating Engines, General Motor Research Laboratories, 1978, New York, Plenum Press, 1980.

A.C. Hindmarsh (1974), GEAR : Ordinary Differential Equation System Solver, Lawrence Livermore Laboratory, Report UCID - 30091, Revision 3, December, 1974.

A.C. Hindmarsh (1980), LSOD and LSODI, Two New Initial Value Ordinary Differential Equation Solvers, *SIGNUM* newsletter 15,10.

S.D. Hire, A. Ekchian, J.B. Heywood, R.J. Tabaczynski, J.C. Wall (1976), Performance and NOx Emission Modeling of a Jet Ignition Prechamber Stratified Charged Engine, SAE paper 760161.

C.M. Ho, D.A. Santavicca (1987), Turbulence Effect on Early Flame Kernel Growth, SAE paper 872100.

Janaf Thermo - Chemical Tables (1971), National Bureau of Standards Publications, NSRDS - NBS 37.

R.B. Kriegen, G.L. Borman (1967), The Computation of Apparent Heat Release for Internal Combustion Engines, ASME Diesel and Gas Power Div., 39th Conference Proceedings, 1967.

Lewis and von Elbe (1961), *Combustion, Flame and Explosions of Gases*, Academic Press Inc., New York, 1961.

R.H. Merson (1957), An Operational Method for the Study of Integration Processes, Proc. Symp. Data Processing, Weapons Research Establishment, Salisbury, S. Australia, 1957.

R.E. Milane, P.G. Hill (1988), Turbulent Characteristics of Premixed Fuel and Air, Combustion Science and Technology, Vol 59, 4 - 6, p.275.

R.E. Milane, R.J. Tabaczynski, V.S. Arpaci (1983), A Stochastic Model of Turbulent Mixing for the Prediction of Burn Rate in a Spark Ignition Engine, Combustion Science and Technology, 1983, Vol 32, pp. 211 - 235.

T. Morel, N.N. Mansour (1982), Modeling of Turbulence in Internal Combustion Engines, SAE paper 820040.

M. Namazián, S. Hansen, E. Lyford-Pike, J. Sanchez-Barsse, J. Heywood, J. Rife (1980), Schlieren Visualization of the Flow and Density Fields in the Cylinder of a Spark Ignition Engine, SAE paper 800044.

B.D. Peters, A.A. Quader (1978), 'Wetting' the Appetite of Spark Ignition Engines for Lean Combustion, SAE paper 780234.

B.D. Peters (1979), Mass Burning Rate in a Spark Ignition Engine Operating in the Partial Burn Regime, I. Mech. E. Conference Publication, 1979.

D.T. Pratt (1976), Mixing and Chemical Reaction in Continuous Combustion, Prog. Energy Combust. Sci. 1, 73.

A.A. Quader (1974), Lean Combustion and the Misfire Limit in Spark Ignition Engines, SAE paper 741055.

A.A. Quader (1976), What Limits Lean Operation in Spark Ignition Engines - Flame Initiation or Propagation ? SAE paper 760760.

K. Radhakrishnan, D.T. Pratt (1984), A Coalescence/Dispersion Model for Turbu-

- lent Flame Stability, AIAA Journal, Vol 22, No 3, pp. 338 - 393, March 1984.
- K. Radhakrishnan (1985), New Integration Techniques for Chemical Kinetic Rate Equations. I. Efficiency Comparison. Combustion Science and Technology, 1986, 46, (1-2), pp. 59 - 81.
- S.B. Reed (1967), Flame Stretch - A Connecting Principle for Blow - Off Data, Combustion and Flame, 1967, 11(3), pp. 177 - 189.
- R.E. Scraton (1964), Estimation of the Truncation Error in Runge - Kutta Method and Allied Processes, Comput. J., 7, pp. 246 - 248.
- G.H. Shiomoto, R.F. Sawyer and B.P. Kelly (1978), Characterization of the Lean Misfire Limit, SAE paper 780234, 1978.
- O.I. Smith, C.K. Westbrook, R.F. Sawyer (1977), Lean Limit Combustion in an Expanding Chamber, International Symposium on Combustion, 1977.
- R.J. Tabaczynski (1976), Turbulence and Turbulent Combustion in Spark Ignition Engines, Prog. Energy Combustion Sci, Vol 2, pp. 143 - 165, 1976.
- R.J. Tabaczynski, C.R. Ferguson, K. Radhakrishnan (1977), A Turbulent Entrainment Model for Spark Ignition Engine Combustion, SAE paper 770647.
- A. van Tiggelen, J. Deckers (1957), Sixth Symposium (International) on Combustion, Reinhold, New York, 1957, p.61.
- T. Tanuma, K. Sasaki, T. Kaneneko, H. Kawasaki (1971), Ignition, Combustion and Exhaust Emissions of Lean Mixtures in Automotive Spark Ignition Engines, SAE paper 710159.
- P.J. van Tiggelen, A. Duval (1967), Bulletins de L'Academie Royal de Belgique Classes des Sciences 8, 1967, pp. 326 - 365.

C.K. Westbrook, F.L. Dryer (1981), Simplified Reaction Mechanisms for the Oxidation of Hydrocarbon Fuels in Flames, Combustion Science and Technology, 1981, Vol 27, pp. 31 - 43.

T.R. Young, J.P. Boris (1977), A Numerical Technique for Solving Stiff Ordinary Differential Equations Associated with Chemical Kinetics of Reactive Flow Problem, J. Phys. Chem. 81, 2424.

TABLE 1
ENGINE SPECIFICATIONS

(For Testings of Ignition Limit)

Bore	=	8.0 cm
Stroke	=	8.0 cm
Length of Connecting Rod	=	15.0 cm
Spark Plug Offset from Center	=	1.5 cm
Compression Ratio	=	9.9

(For Testings of Partial Burn,
Age Mixing, and Empirical Constants)

Bore	=	4.0 cm
Stroke	=	4.0 cm
Length of Connecting Rod	=	7.5 cm
Spark Plug Offset from Center	=	0.75 cm
Compression Ratio	=	8.0

TABLE 2
TESTING CONDITIONS : VARIATIONS OF EMPIRICAL CONSTANTS

Constants	A	B	C
Engine Speed (RPM)	1500.	1500.	3000.
Closing of Intake Valve (BTDC)	140.	140.	140.
Opening of Exhaust Valve (ATDC)	120.	120.	120.
Equivalence Ratio	0.5	0.5	0.5
Turbulence Intensity at Closing of Intake Valve (m/sec)	2.0	2.0	3.0
Intake Pressure (atm)	0.5	0.5	0.7
Intake Temperature (K)	300.	300.	270.
Spark Advance (BTDC)	60.	60.	10.
Spark Duration (Crank Angles)	2.	2.	2.
Ignition Energy (mJ)	6.0	6.0	1.0
Spark Gap (mm)	1.0	1.0	1.0
Number of Particles Ignited	10.	10.	5.

Constants : A = Pre-exponential constant
 B = Activation Energy
 C = Constant for Mixing Frequency

TABLE 3
TESTING CONDITIONS : VARIATION OF TURBULENCE INTENSITY

Engine Speed (RPM)	1500.	1500.	1500.
Closing of Intake Valve (BTDC)	140.	140.	140.
Opening of Exhaust Valve (ATDC)	120.	120.	120.
Equivalence Ratio	0.5	0.5	0.5
Turbulence Intensity at Closing of Intake Valve (m/sec)	1.0	2.0	3.0
Intake Pressure (atm)	0.5	0.5	0.5
Intake Temperature (K)	300.	300.	300.
Spark Advance (BTDC)	60.	60.	60.
Spark Duration (Crank Angles)	2.	2.	2.
Ignition Energy (mJ)	6.0	6.0	6.0
Spark Gap (mm)	1.0	1.0	1.0
Number of Particles Ignited	10.	10.	10.
Result	Slower burning.	Fastest burning.	Misfire.

TABLE 4
TESTING CONDITIONS : VARIATION OF PRESSURE

Engine Speed (RPM)	1500.	1500.	1500.
Closing of Intake Valve (BTDC)	140.	140.	140.
Opening of Exhaust Valve (ATDC)	120.	120.	120.
Equivalence Ratio	0.5	0.5	0.5
Turbulence Intensity at Closing of Intake Valve (m/sec)	2.0	2.0	2.0
Intake Pressure (atm)	0.2	0.5	0.8
Intake Temperature (K)	350.	350.	350.
Spark Advance (BTDC)	60.	60.	60.
Spark Duration (Crank Angles)	2.	2.	2.
Ignition Energy (mJ)	6.0	6.0	6.0
Spark Gap (mm)	1.0	1.0	1.0
Number of Particles Ignited	10.	10.	10.
Result	Burning rate decreased with increasing pressure.		

TABLE 5

TESTING CONDITIONS : VARIATION OF PRESSURE & TURBULENCE INTENSITY

Engine Speed (RPM)	1500.	1500.	1500.	1500.
Closing of Intake Valve (BTDC)	140.	140.	140.	140.
Opening of Exhaust Valve (ATDC)	120.	120.	120.	120.
Equivalence Ratio	0.5	0.5	0.5	0.5
Turbulence Intensity at Closing of Intake Valve (m/sec)	1.6	2.0	2.6	3.2
Intake Pressure (atm)	0.4	0.5	0.65	0.8
Intake Temperature (K)	300.	300.	300.	300.
Spark Advance (BTDC)	60.	60.	60.	60.
Spark Duration (Crank Angles)	2.	2.	2.	2.
Ignition Energy (mJ)	6.0	6.0	6.0	6.0
Spark Gap (mm)	1.0	1.0	1.0	1.0
Number of Particles Ignited	10.	10.	10.	10.
Result	Burning rate decreased with increasing turbulence intensity.			Misfire.

TABLE 6

TESTING CONDITIONS : VARIATION OF INTAKE TEMPERATURE

Engine Speed (RPM)	1500.	1500.	1500.
Closing of Intake Valve (BTDC)	140.	140.	140.
Opening of Exhaust Valve (ATDC)	120.	120.	120.
Equivalence Ratio	0.5	0.5	0.5
Turbulence Intensity at Closing of Intake Valve (m/sec)	2.0	2.0	2.0
Intake Pressure (atm)	0.5	0.5	0.5
Intake Temperature (K)	250.	300.	350.
Spark Advance (BTDC)	60.	60.	60.
Spark Duration (Crank Angles)	2.	2.	2.
Ignition Energy (mJ)	6.0	6.0	6.0
Spark Gap (mm)	1.0	1.0	1.0
Number of Particles Ignited	10.	10.	10.
Result	Burning rate increased with increasing temperature.		

TABLE 7

TESTING CONDITIONS: VARIATION OF EQUIVALENCE RATIO

Engine Speed (RPM)	1500.	1500.	1500.	1500.
Closing of Intake Valve (BTDC)	140.	140.	140.	140.
Opening of Exhaust Valve (ATDC)	120.	120.	120.	120.
Equivalence Ratio	0.3	0.5	0.7	0.9
Turbulence Intensity at Closing of Intake Valve (m/sec)	2.0	2.0	2.0	2.0
Intake Pressure (atm)	0.5	0.5	0.5	0.5
Intake Temperature (K)	350.	350.	350.	350.
Spark Advance (BTDC)	60.	60.	60.	60.
Spark Duration (Crank Angles)	2.	2.	2.	2.
Ignition Energy (mJ)	6.0	6.0	6.0	6.0
Spark Gap (mm)	1.0	1.0	1.0	1.0
Number of Particles Ignited	10.	10.	10.	10.
Result	Misfire.	Burning rate increased with increasing equivalence ratio.		

TABLE 8

TESTING CONDITIONS : VARIATION OF SPARK ADVANCE

Engine Speed (RPM)	1500.	1500.	1500.
Closing of Intake Valve (BTDC)	140.	140.	140.
Opening of Exhaust Valve (ATDC)	120.	120.	120.
Equivalence Ratio	0.5	0.5	0.5
Turbulence Intensity at Closing of Intake Valve (m/sec)	2.0	2.0	2.0
Intake Pressure (atm)	0.5	0.5	0.5
Intake Temperature (K)	350.	350.	350.
Spark Advance (BTDC)	90.	60.	30.
Spark Duration (Crank Angles)	2.	2.	2.
Ignition Energy (mJ)	6.0	6.0	6.0
Spark Gap (mm)	1.0	1.0	1.0
Number of Particles Ignited	10.	10.	10.

Result

Misfire.

Burning rate increased with decreasing spark advance.

TABLE 9
TESTING CONDITIONS.: VARIATION OF IGNITION ENERGY

Engine Speed (RPM)	1500.	1500.	1500.
Closing of Intake Valve (BTDC)	140.	140.	140.
Opening of Exhaust Valve (ATDC)	120.	120.	120.
Equivalence Ratio	0.5	0.5	0.5
Turbulence Intensity at Closing of Intake Valve (m/sec)	2.0	2.0	2.0
Intake Pressure (atm)	0.5	0.5	0.5
Intake Temperature (K)	350.	350.	350.
Spark Advance (BTDC)	60.	60.	60.
Spark Duration (Crank Angles)	2.	2.	2.
Ignition Energy (mJ)	3.0	6.0	9.0
Spark Gap (mm)	1.0	1.0	1.0
Number of Particles Ignited	10.	10.	10.
Result	Burning rate increased with increasing ignition energy.		

TABLE 10
TESTING CONDITIONS : VARIATION OF SPARK GAP

Engine Speed (RPM)	1500.	1500.	1500.
Closing of Intake Valve (BTDC)	140.	140.	140.
Opening of Exhaust Valve (ATDC)	120.	120.	120.
Equivalence Ratio	0.5	0.5	0.5
Turbulence Intensity at Closing of Intake Valve (m/sec)	2.0	2.0	2.0
Intake Pressure (atm)	0.5	0.5	0.5
Intake Temperature (K)	350.	350.	350.
Spark Advance (BTDC)	60.	60.	60.
Spark Duration (Crank Angles)	2.	2.	2.
Ignition Energy (mJ)	6.0	6.0	6.0
Spark Gap (mm)	0.5	1.0	2.0
Number of Particles Ignited	10.	10.	10.
Result	Burning rate is not a strong function of spark gap.		

TABLE 11

TESTING CONDITIONS : VARIATION OF ENGINE SPEED

Engine Speed (RPM)	1500.	3000.
Closing of Intake Valve (BTDC)	140.	140.
Opening of Exhaust Valve (ATDC)	120.	120.
Equivalence Ratio	0.5	0.5
Turbulence Intensity at Closing of Intake Valve (m/sec)	2.0	4.0
Intake Pressure (atm)	0.5	0.5
Intake Temperature (K)	350.	350.
Spark Advance (BTDC)	60.	60.
Spark Duration (Crank Angles)	2.	2.
Ignition Energy (mJ)	6.0	6.0
Spark Gap (mm)	1.0	1.0
Number of Particles Ignited	10.	10.
Result	Normal combustion.	Misfire.

TABLE 12

TESTING CONDITIONS : VARIATION OF NO. OF IGNITED PARTICLES

Engine Speed (RPM)	1500.	1500.	1500.
Closing of Intake Valve (BTDC)	140.	140.	140.
Opening of Exhaust Valve (ATDC)	120.	120.	120.
Equivalence Ratio	0.5	0.5	0.5
Turbulence Intensity at Closing of Intake Valve (m/sec)	2.0	2.0	2.0
Intake Pressure (atm)	0.5	0.5	0.5
Intake Temperature (K)	350.	350.	350.
Spark Advance (BTDC)	60.	60.	60.
Spark Duration (Crank Angles)	2.	2.	2.
Ignition Energy (mj)	6.0	6.0	6.0
Spark Gap (mm)	1.0	1.0	1.0
Number of Particles Ignited	10.	25.	50.

Result

Burning rate increased slightly with increasing no. of ignited particles just after ignition. Difference decreased afterward.

TABLE 13
TESTING CONDITIONS : PARTIAL BURN

Engine Speed (RPM)	3000.	3000.
Closing of Intake Valve (BTDC)	140.	140.
Opening of Exhaust Valve (ATDC)	120.	120.
Equivalence Ratio	0.5	0.5
Turbulence Intensity at Closing of Intake Valve (m/sec)	3.0	3.0
Intake Pressure (atm)	0.5	0.5
Intake Temperature (K)	290.	290.
Spark Advance (BTDC)	10.	30.
Spark Duration (Crank Angles)	2.	2.
Ignition Energy (mJ)	1.0	3.0
Spark Gap (mm)	1.0	1.0
Number of Particles Ignited	10.	10.
Result	Partial burn : Flame was quenched after travelling over 50 % of volume.	

Table 14

Coefficients for Polynomial Fit to Thermodynamic Properties

Coefficients for temperature between $100^{\circ}K$ to $500^{\circ}K$:

<i>i</i>	Species	a_{i1}	a_{i2}	a_{i3}	a_{i4}	a_{i5}	a_{i6}
1	CO_2	11.94033	2.088581	-0.17029	0.037363	-0.589447	-97.1418
2	H_2O	6.139094	4.60783	-0.9356009	0.06669498	0.0335801	-56.62588
3	CO	7.099556	1.275957	-0.2877457	0.022356	-0.1598696	-27.73464
4	H_2	5.555680	1.787191	-0.2881342	0.01951547	0.1611828	0.76498
5	O_2	7.865847	0.6883719	-0.031944	-0.00268708	-0.2013873	-0.893455
6	N_2	6.807771	1.453404	-0.328985	0.02561035	-0.1189462	-0.331835

Coefficients for temperature between $500^{\circ}K$ to $6000^{\circ}K$:

<i>i</i>	Species	a_{i1}	a_{i2}	a_{i3}	a_{i4}	a_{i5}	a_{i6}
1	CO_2	4.737305	16.65283	-11.23249	2.828001	0.00676702	-93.75793
2	H_2O	7.809672	-0.2023519	3.418708	-1.179013	0.00143629	-57.08004
3	CO_2	6.97393	-0.8238319	2.942042	-1.176239	0.0004132409	-27.19597
4	H_2	6.991878	0.1617044	-0.2182071	0.2968197	-0.01625234	-0.118189
5	O_2	6.295715	2.388387	-0.0314788	-0.3267433	0.00435925	0.103637
6	N_2	7.0922	-1.2958	3.2069	-1.2022	-0.0003458	-0.013967

Figure 2. Mass Burn Fraction versus Crank Angle for different Mixing Frequency constant (C)

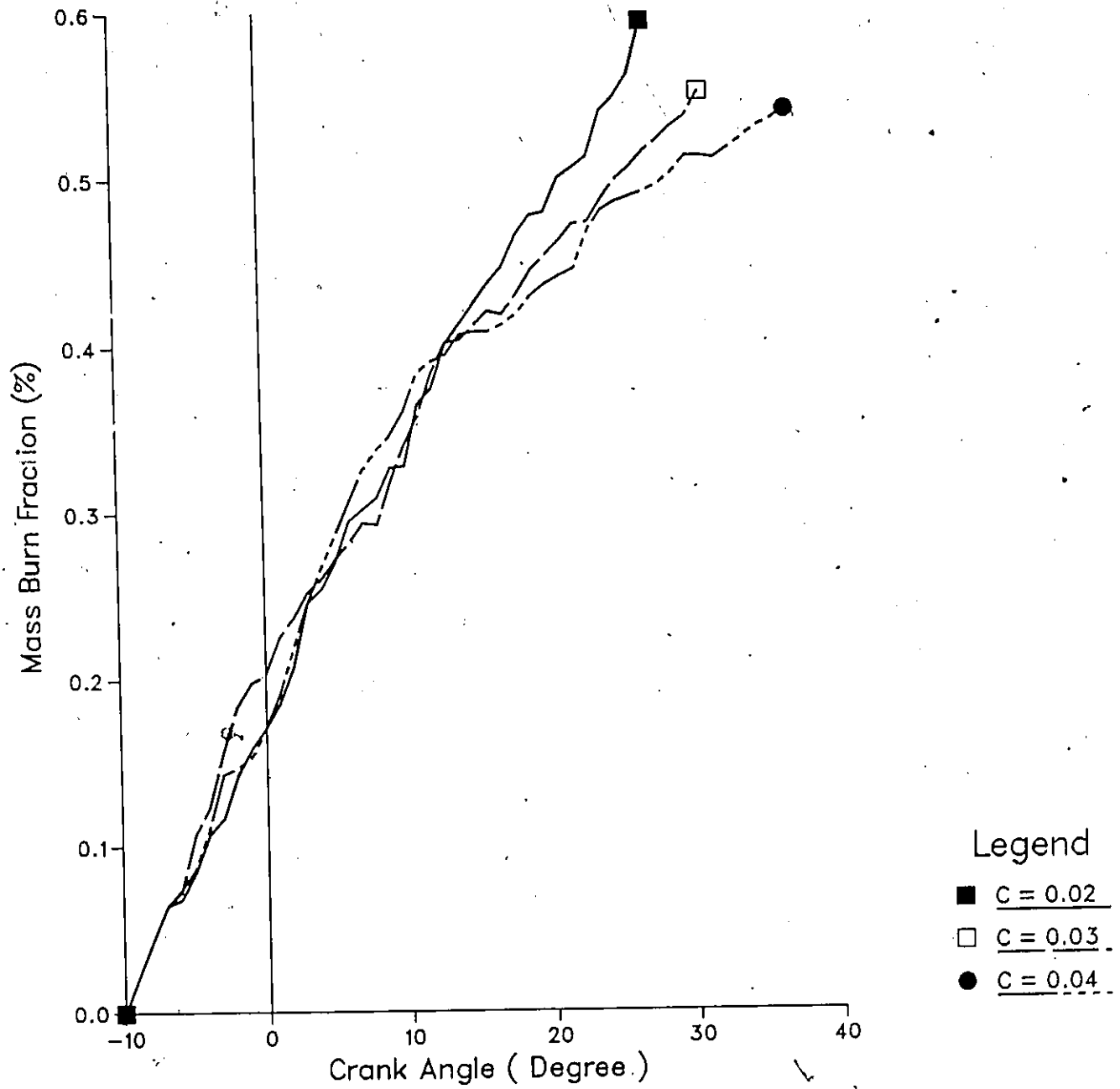


Figure 3. Mass Burn Fraction versus Crank Angle for different Activation Energy (B)

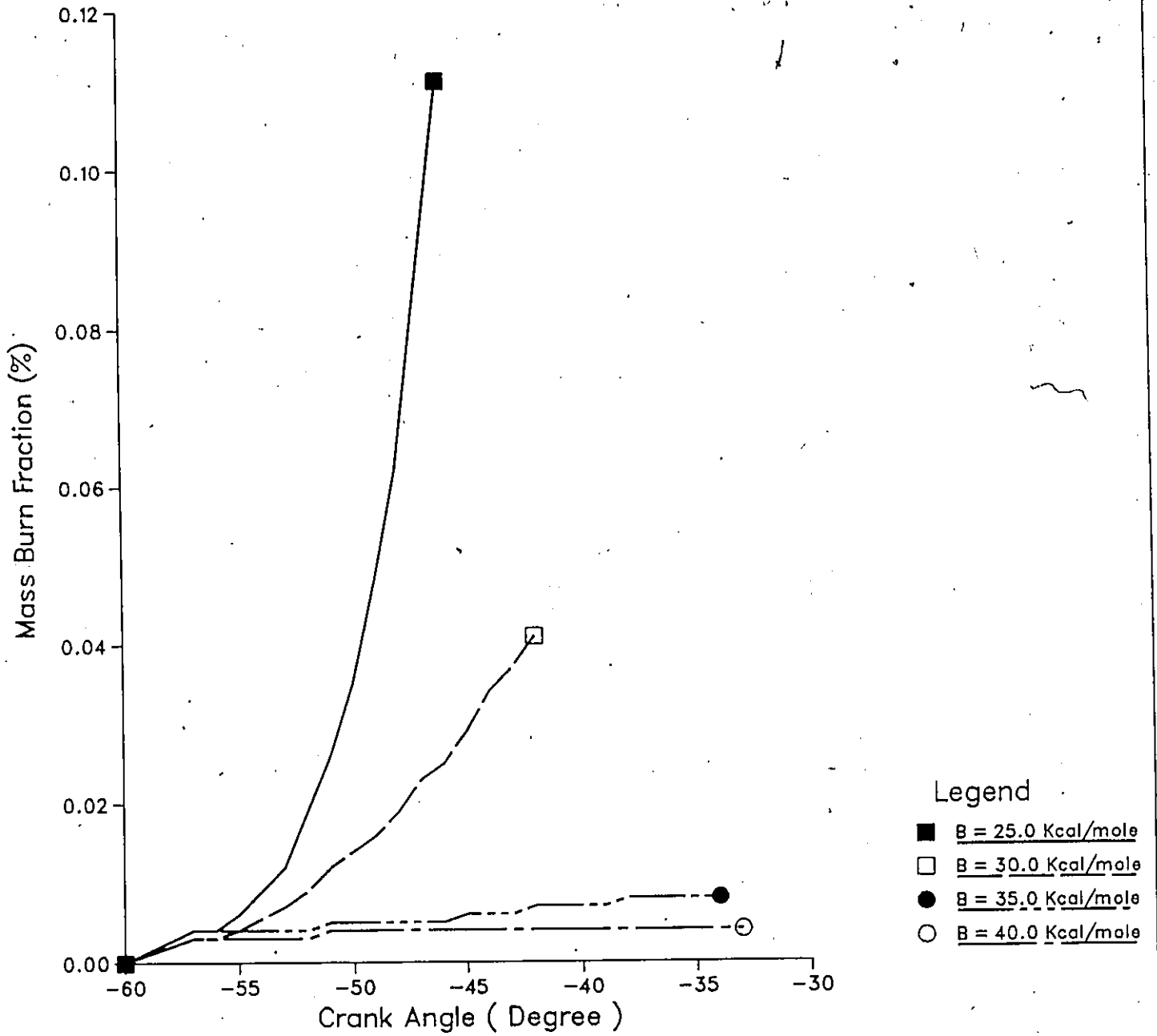


Figure 4. Mass Burn Fraction versus Crank Angle for different Pre-exponential Constant (A)

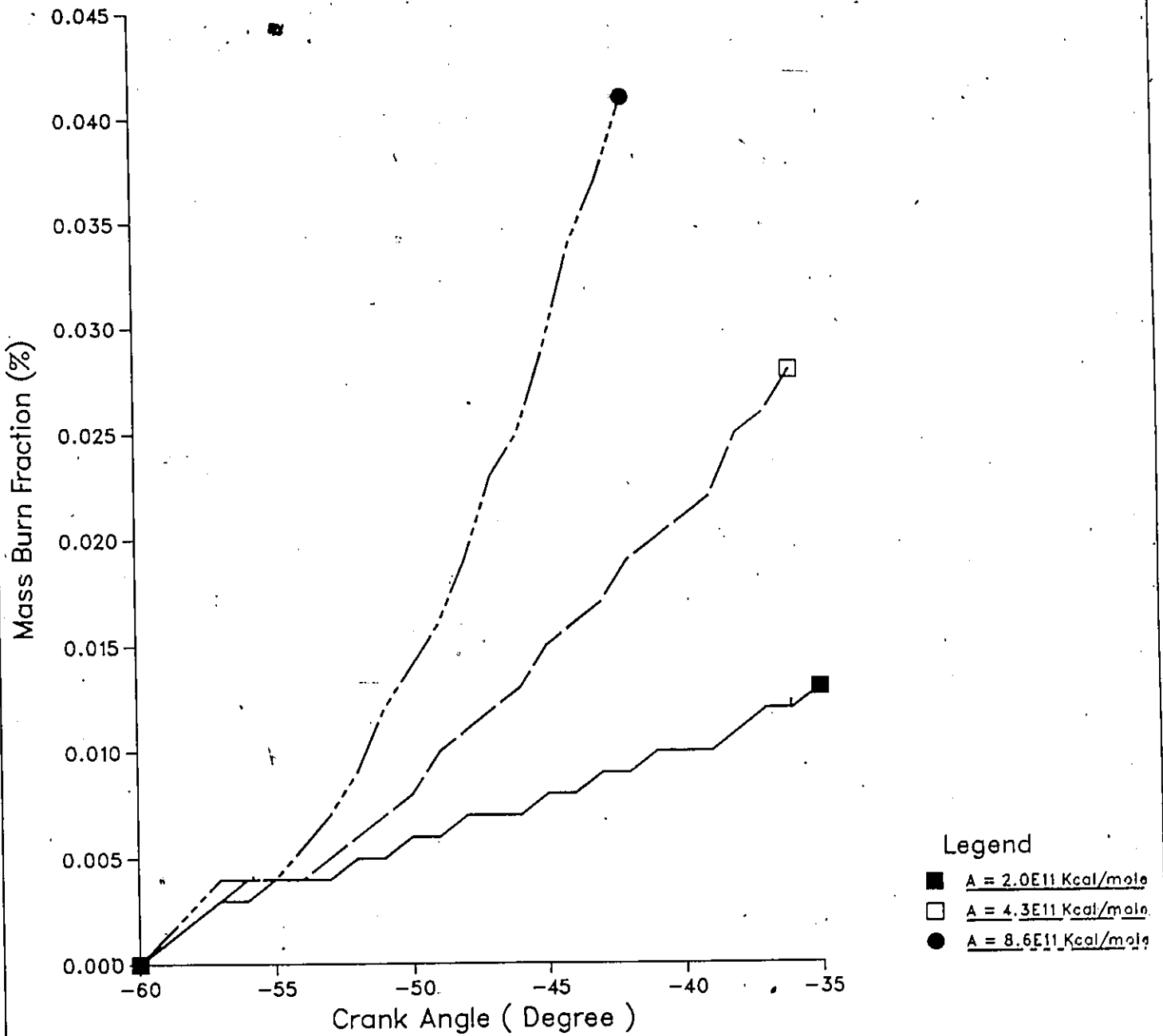


Figure 5. Mass Burn Fraction versus Crank Angle for different level of Turbulence Intensity

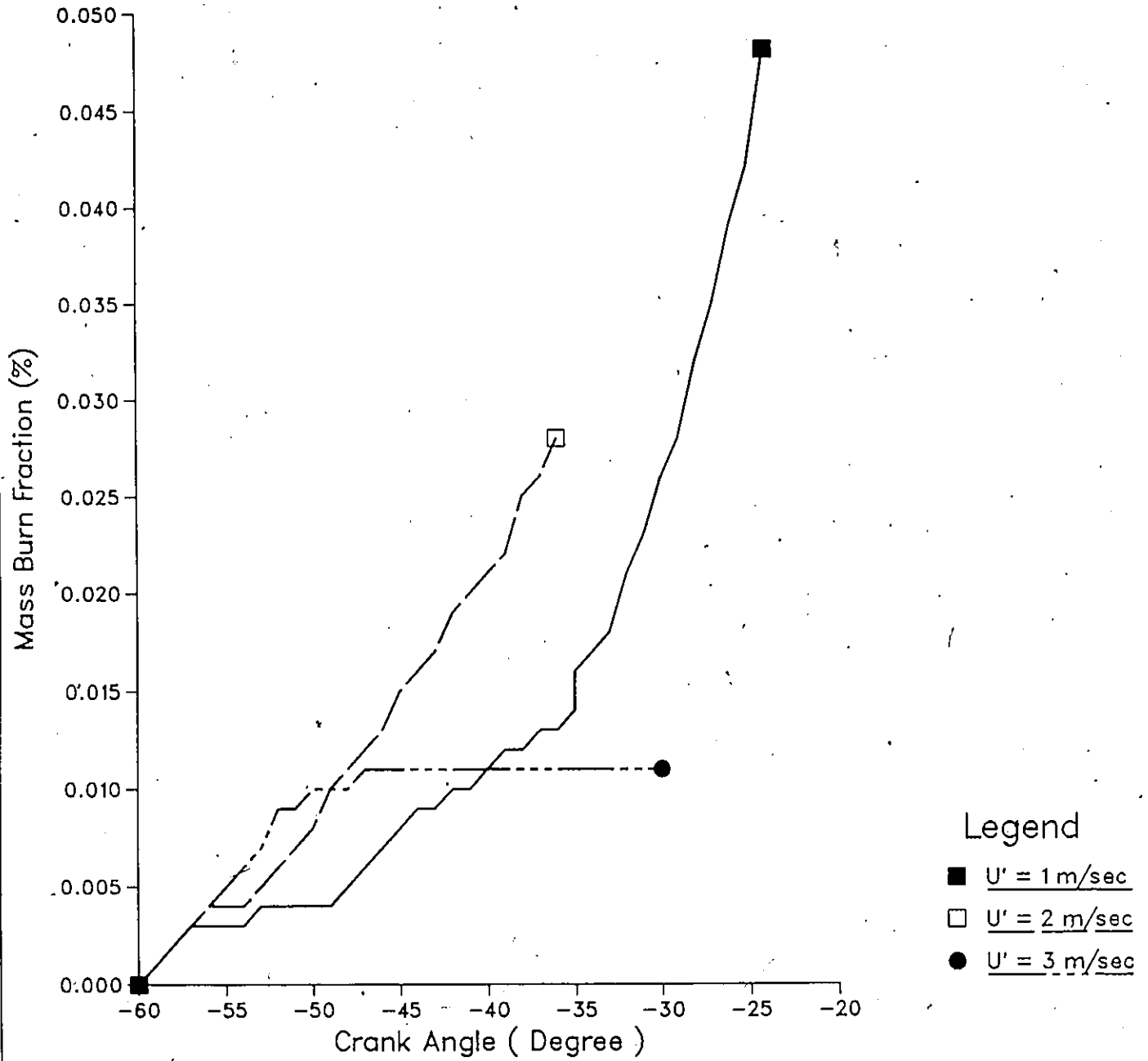


Figure 6. Pressure versus Crank Angle for different level of Turbulence Intensity

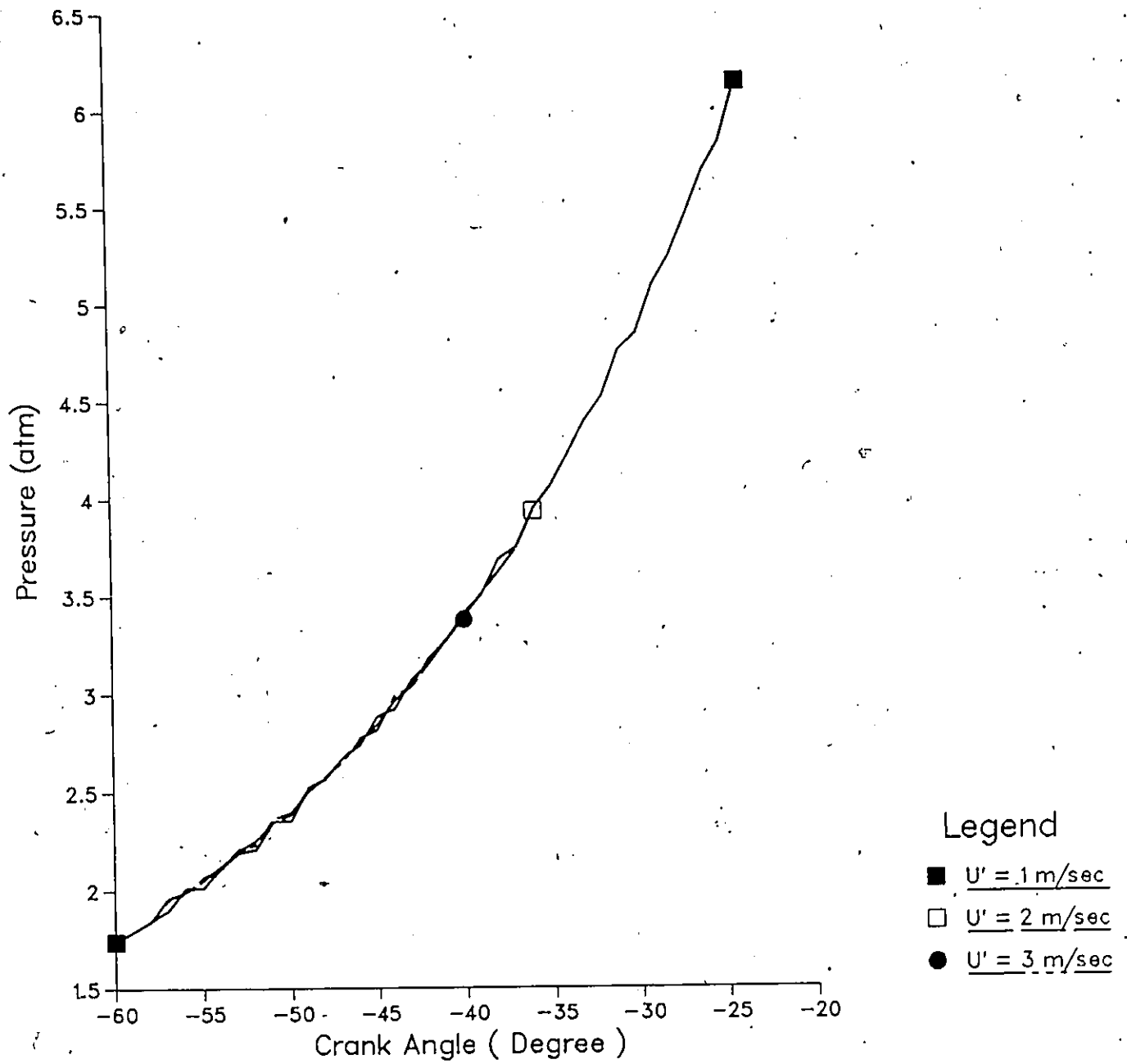


Figure 7. Mass Burn Fraction versus Crank Angle for different Intake Pressure.

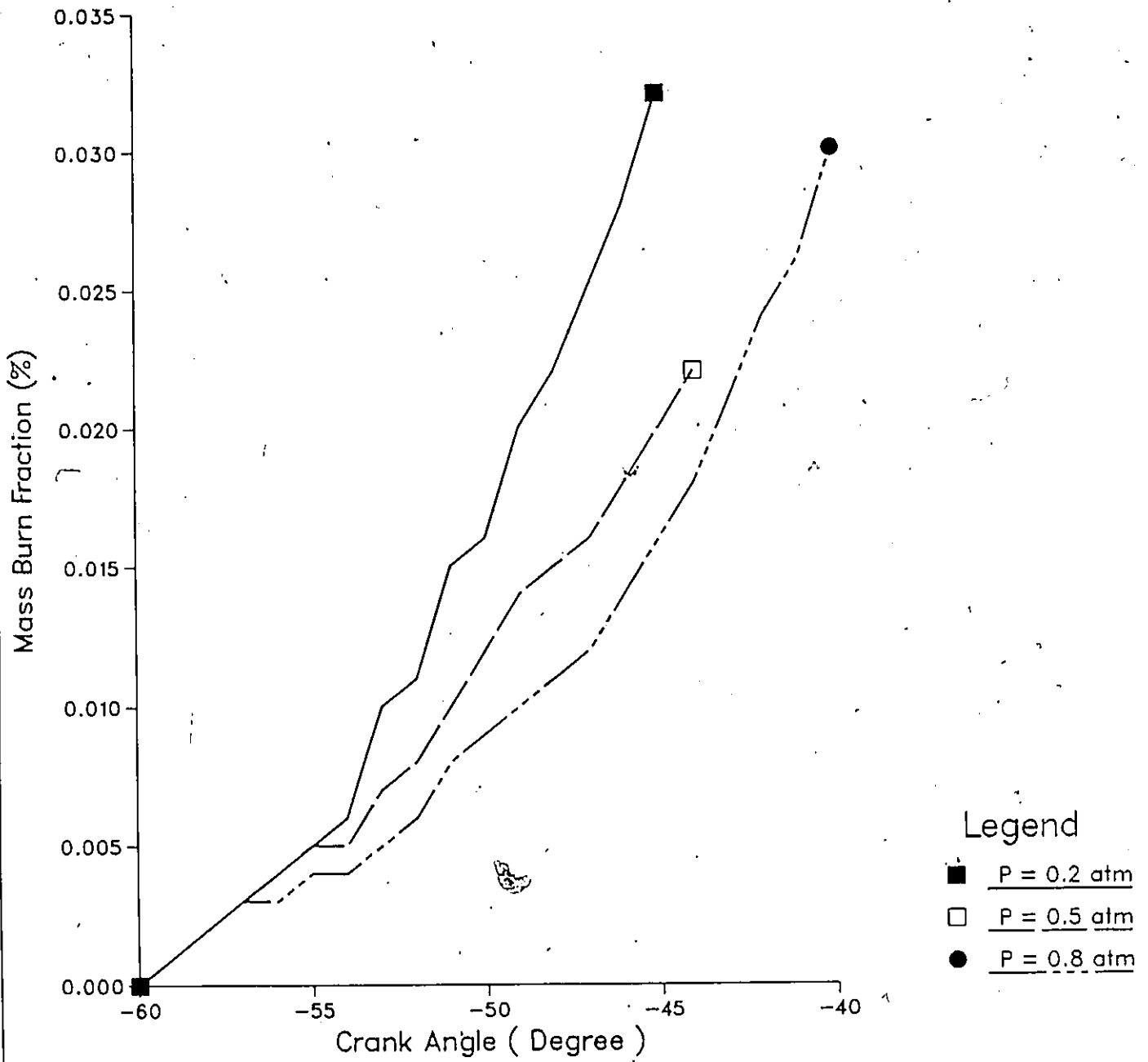


Figure 8. Mass Burn Fraction versus Crank Angle for different Intake Pressure and Turbulence Intensity

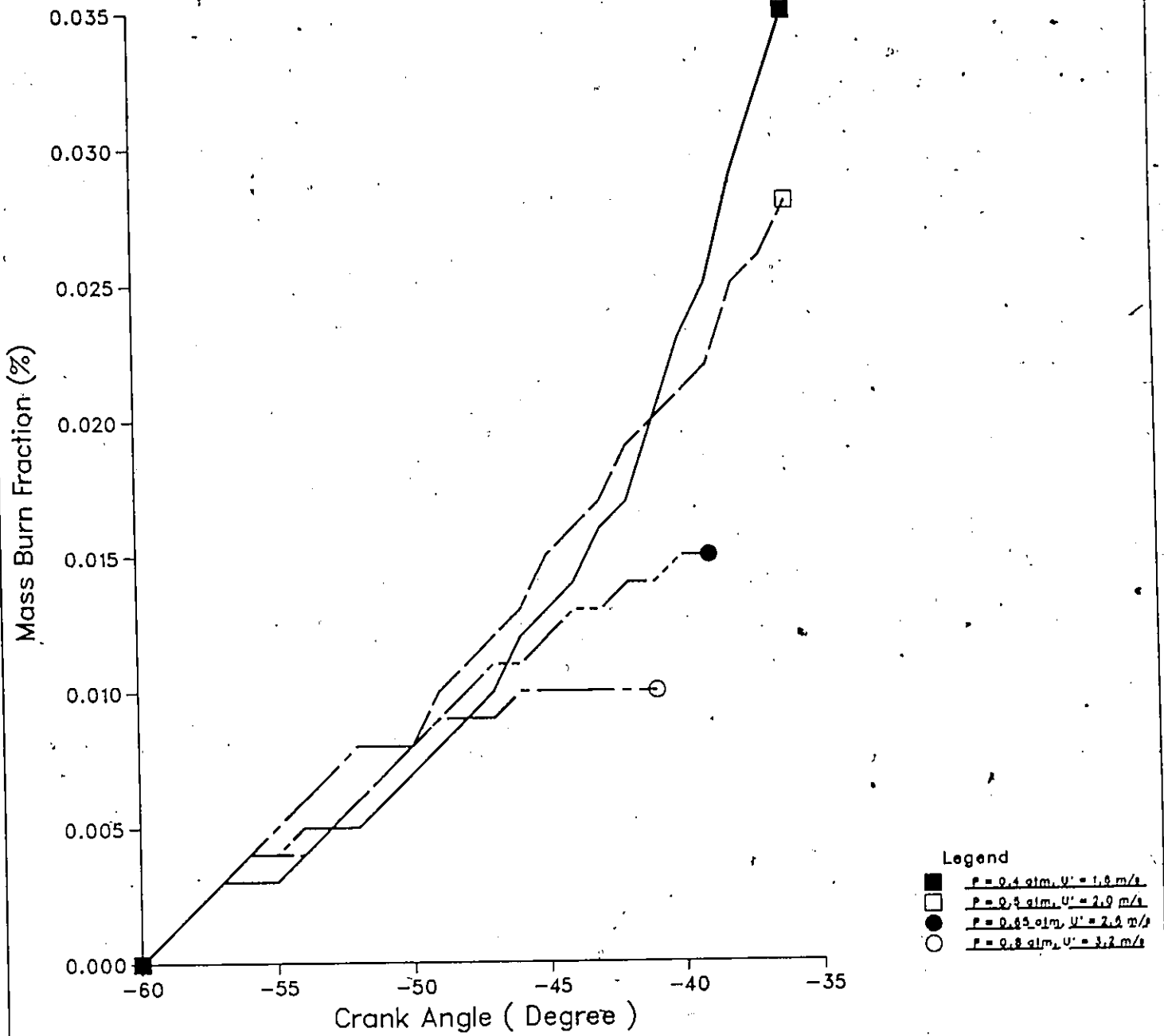


Figure 9. Mass Burn Fraction versus Crank Angle for different Intake Temperature

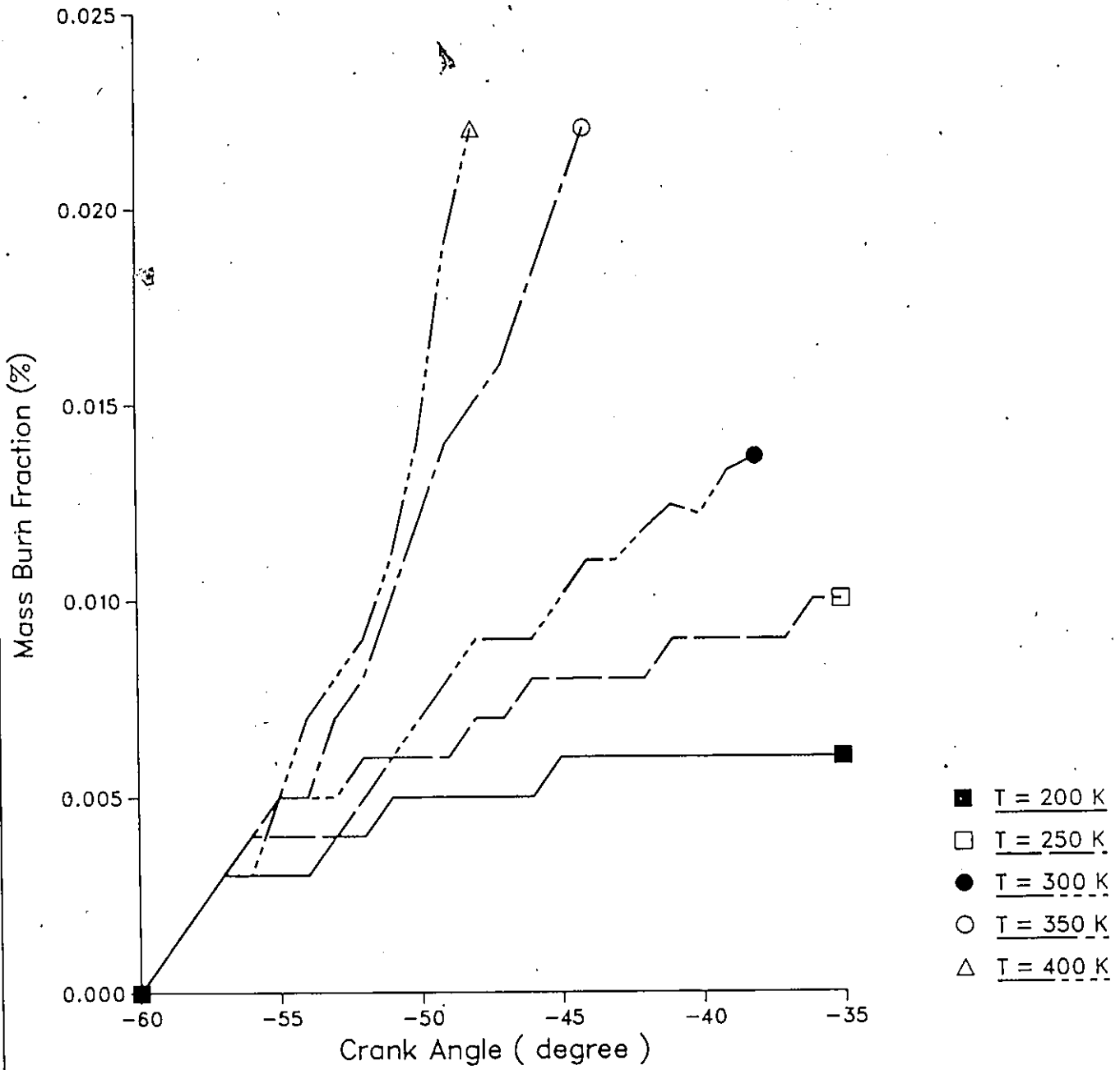


Figure 10. Pressure versus Crank Angle for different Intake Temperature

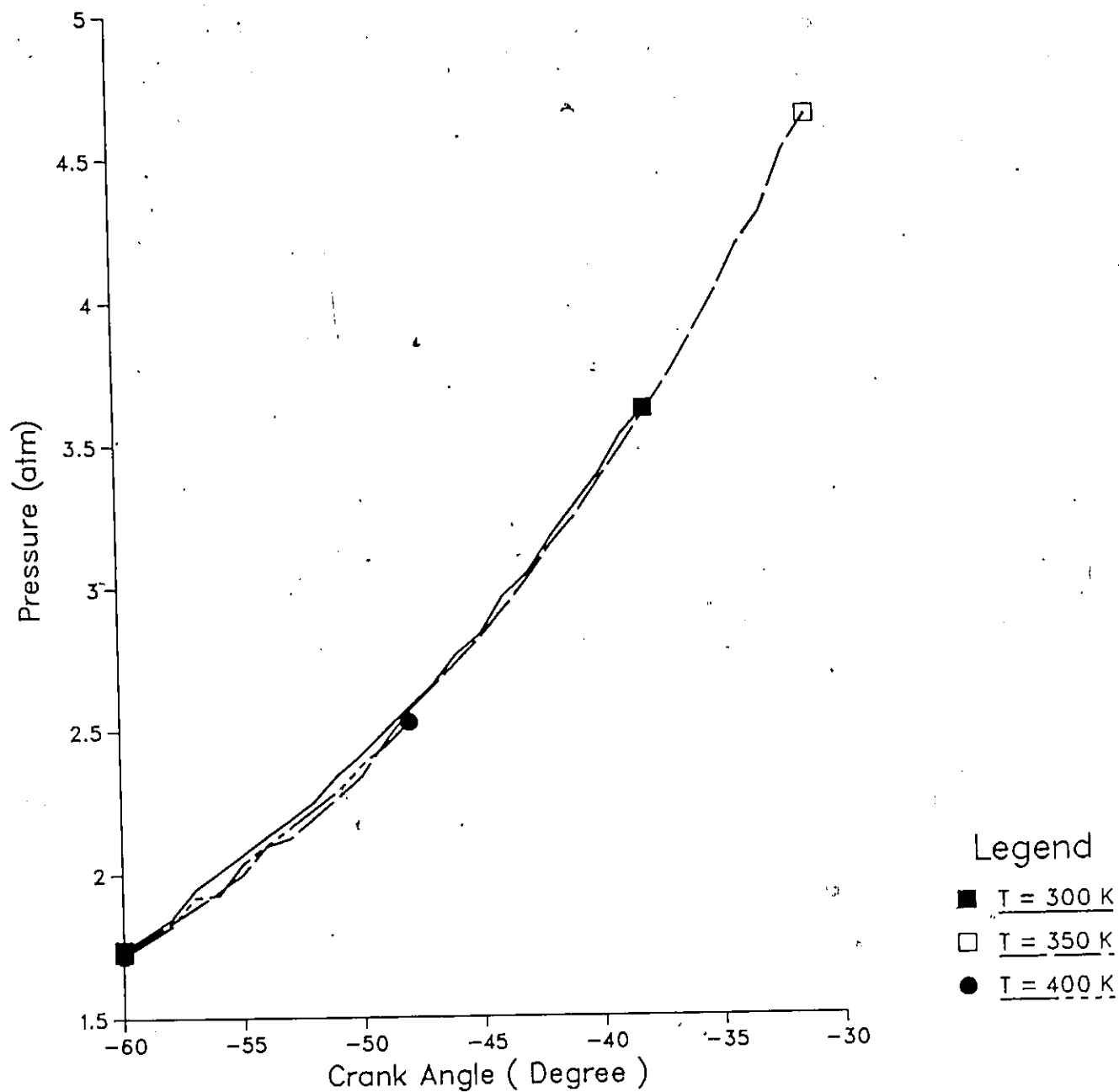


Figure 11. Mass Burn Fraction versus Crank Angle for different Equivalence Ratio

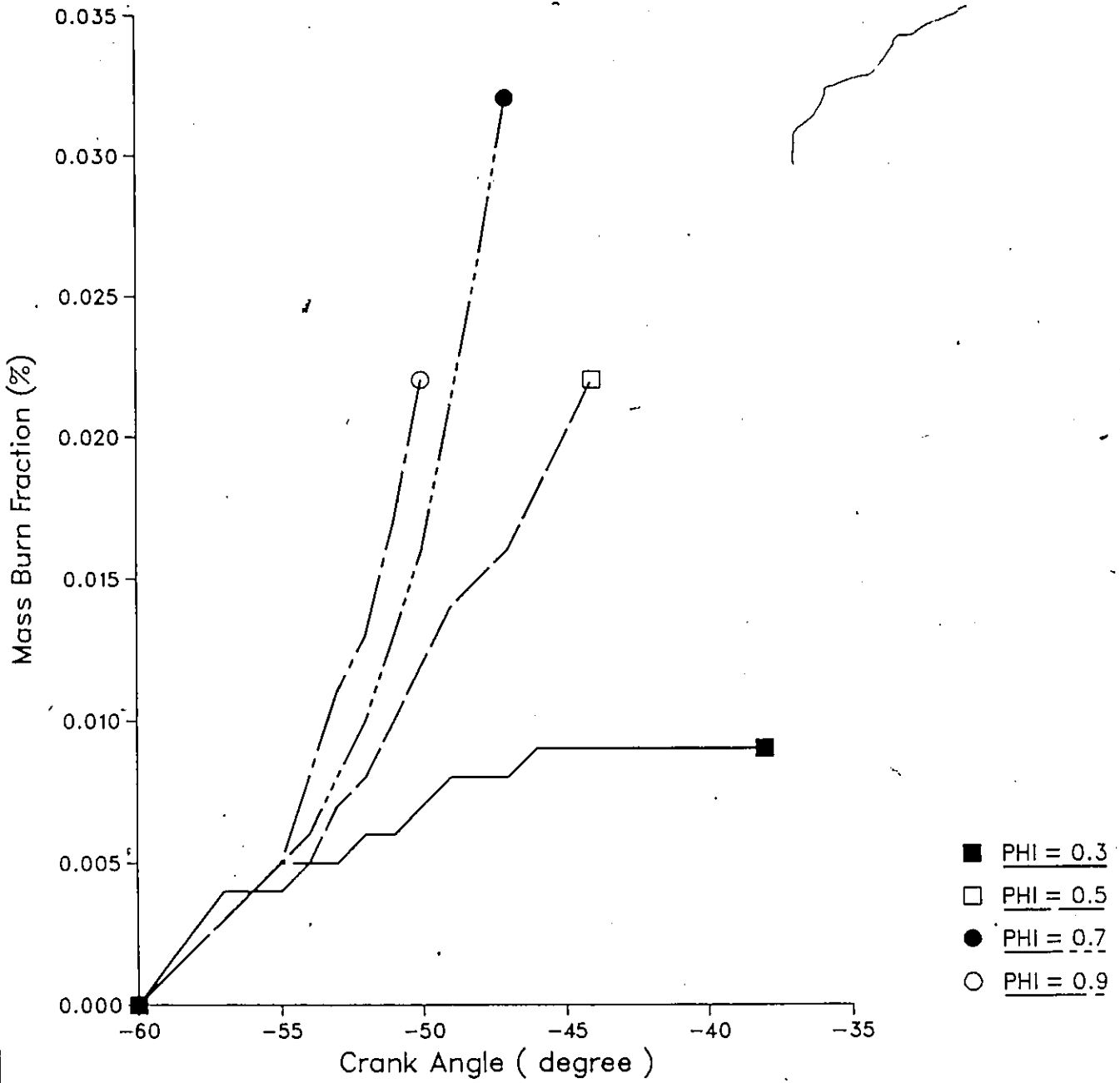


Figure 12. Pressure versus Crank Angle for different Equivalence Ratio

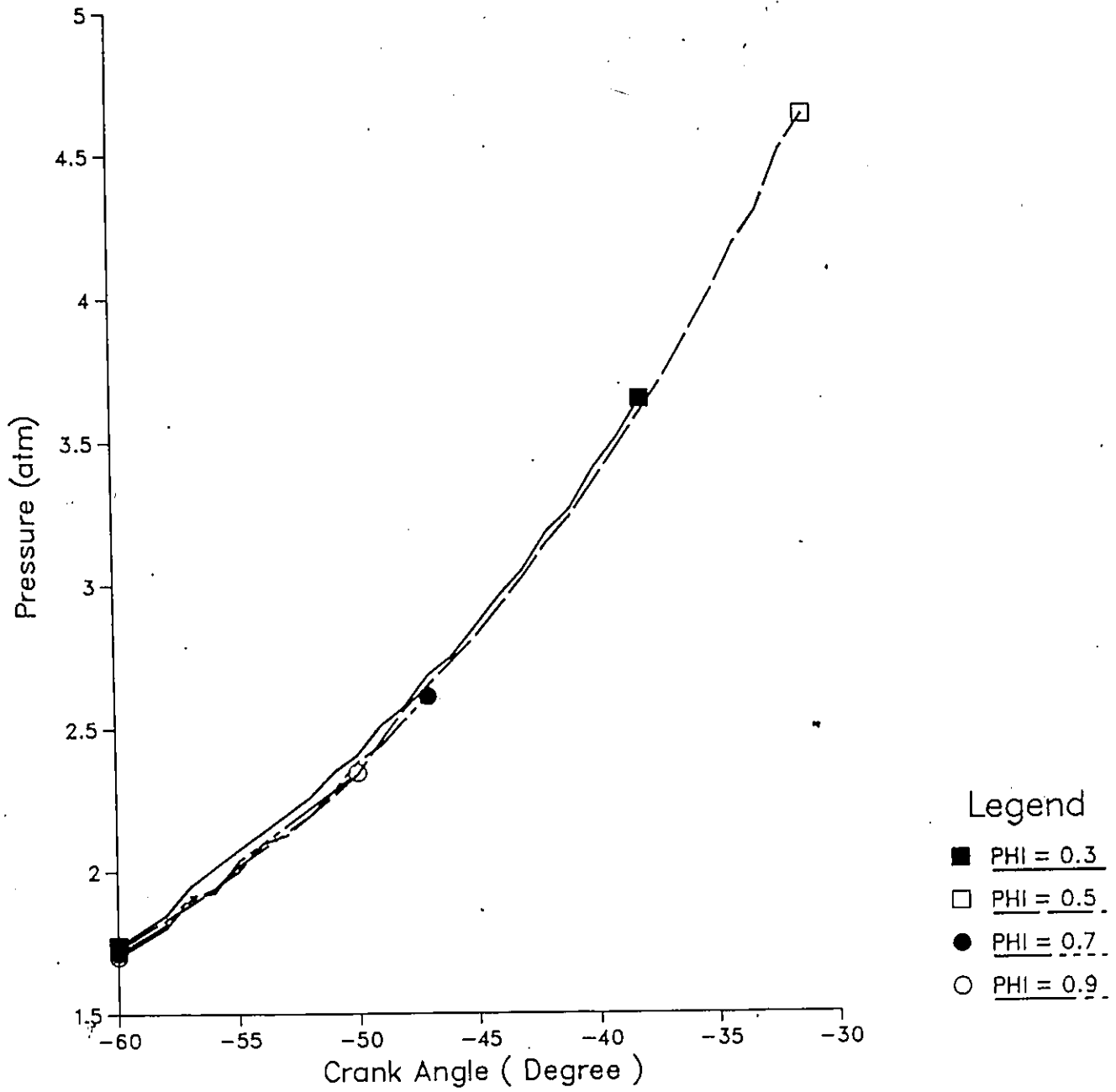


Figure 13. Mass Burn Fraction versus Crank Angle after Ignition for different Spark Advance

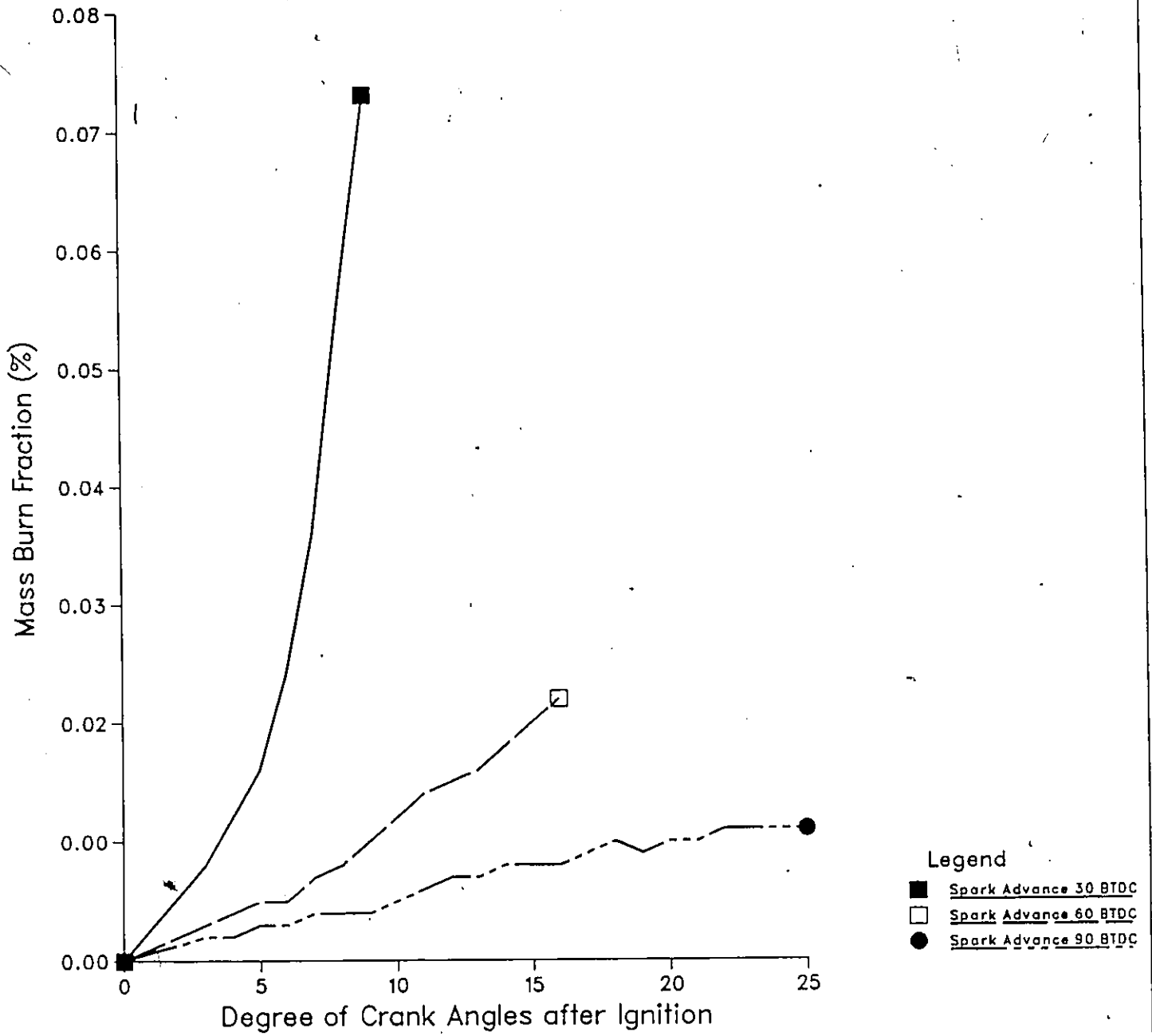


Figure 14. Mass Burn Fraction versus Crank Angle for different Ignition Energy

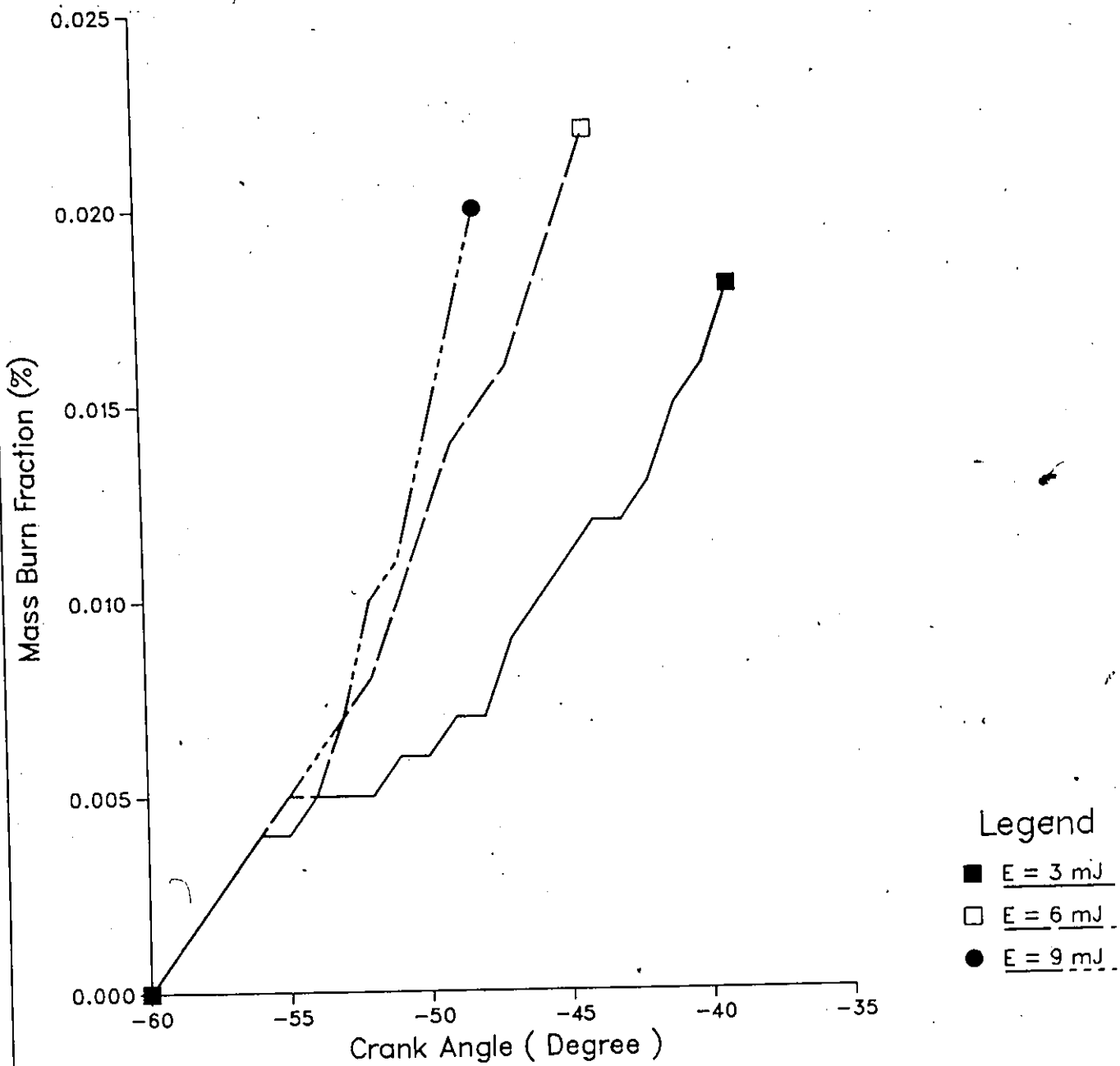


Figure 15. Mass Burn Fraction versus Crank Angle for different Spark Gap Size

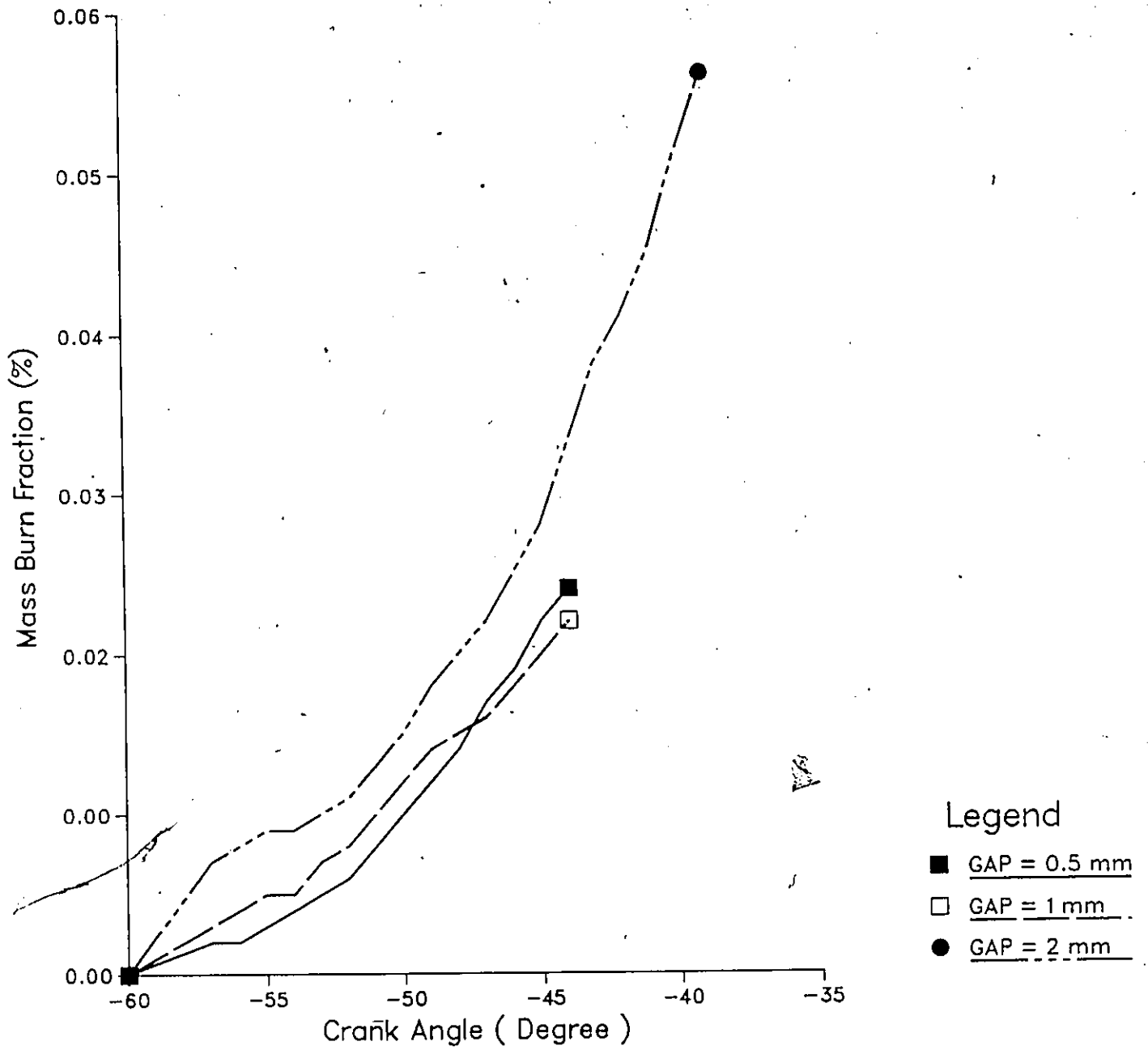


Figure 16. Mass Burn Fraction versus Crank Angle for different Engine Speed

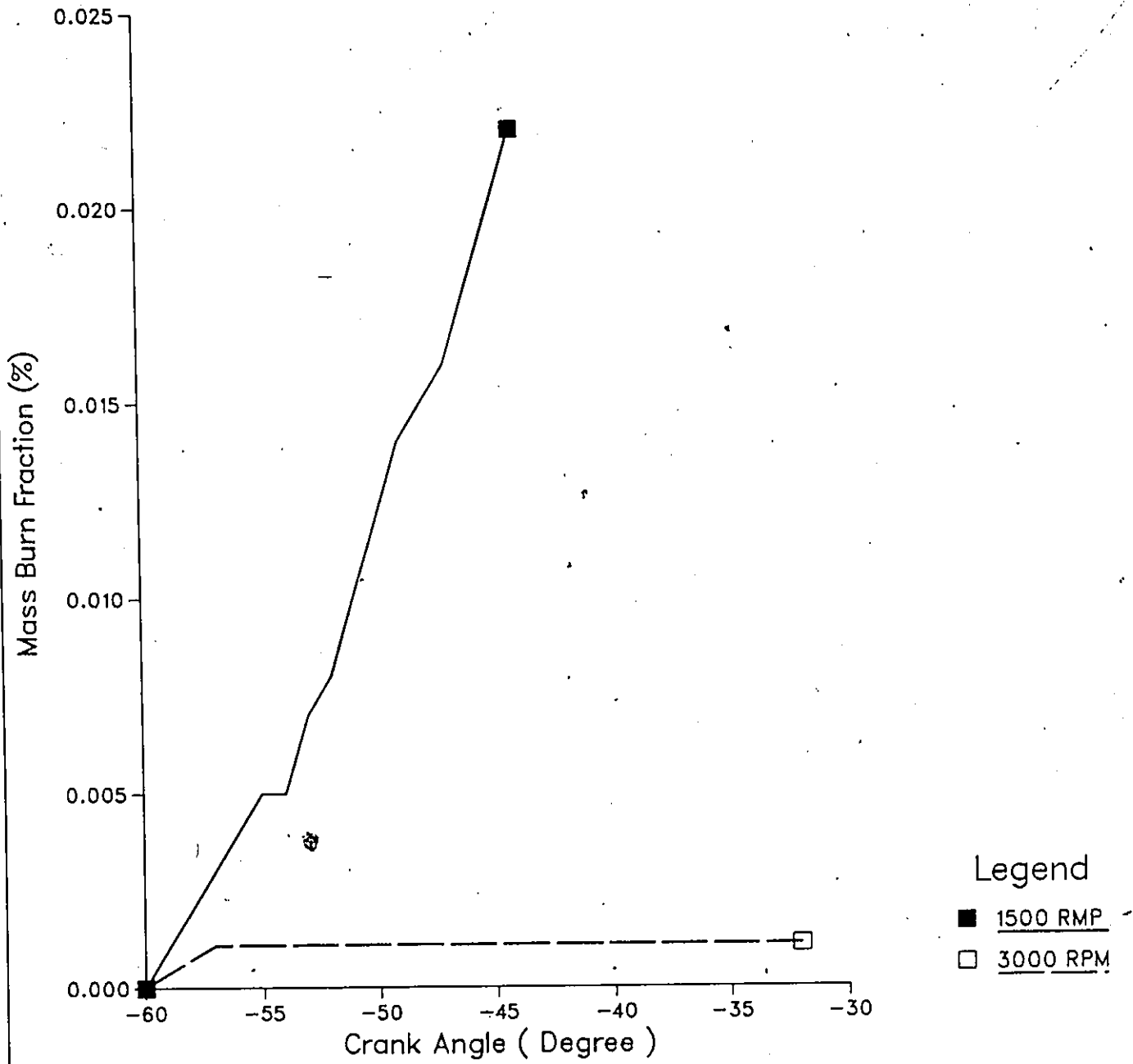


Figure 17. Mass Burn Fraction versus Crank Angle for different Number of Ignited Particles

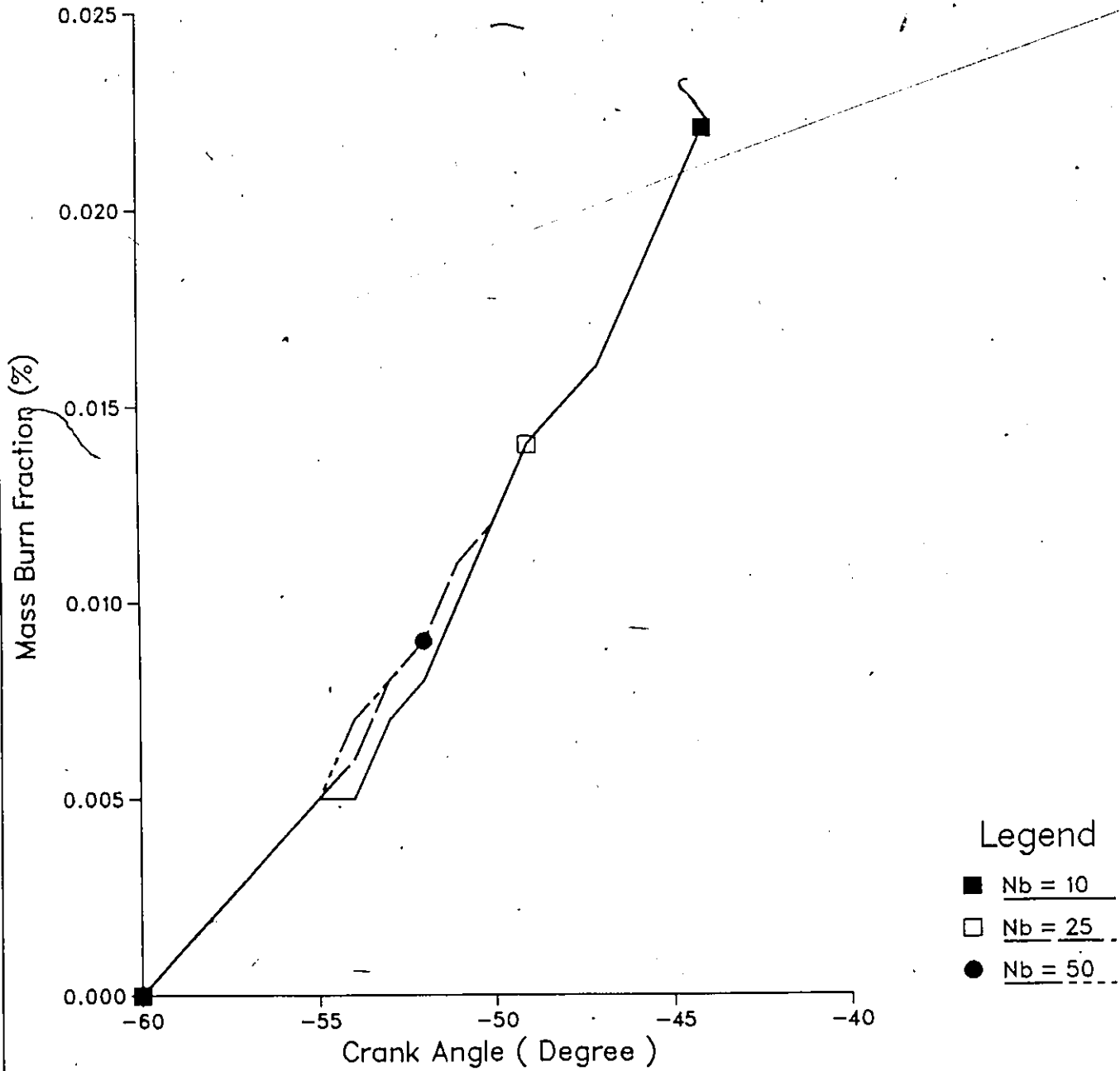


Figure 18. Mass Burn Fraction versus Crank Angle
for a Partial Burn Cycle
Spark Advance : 10 degrees BTDC

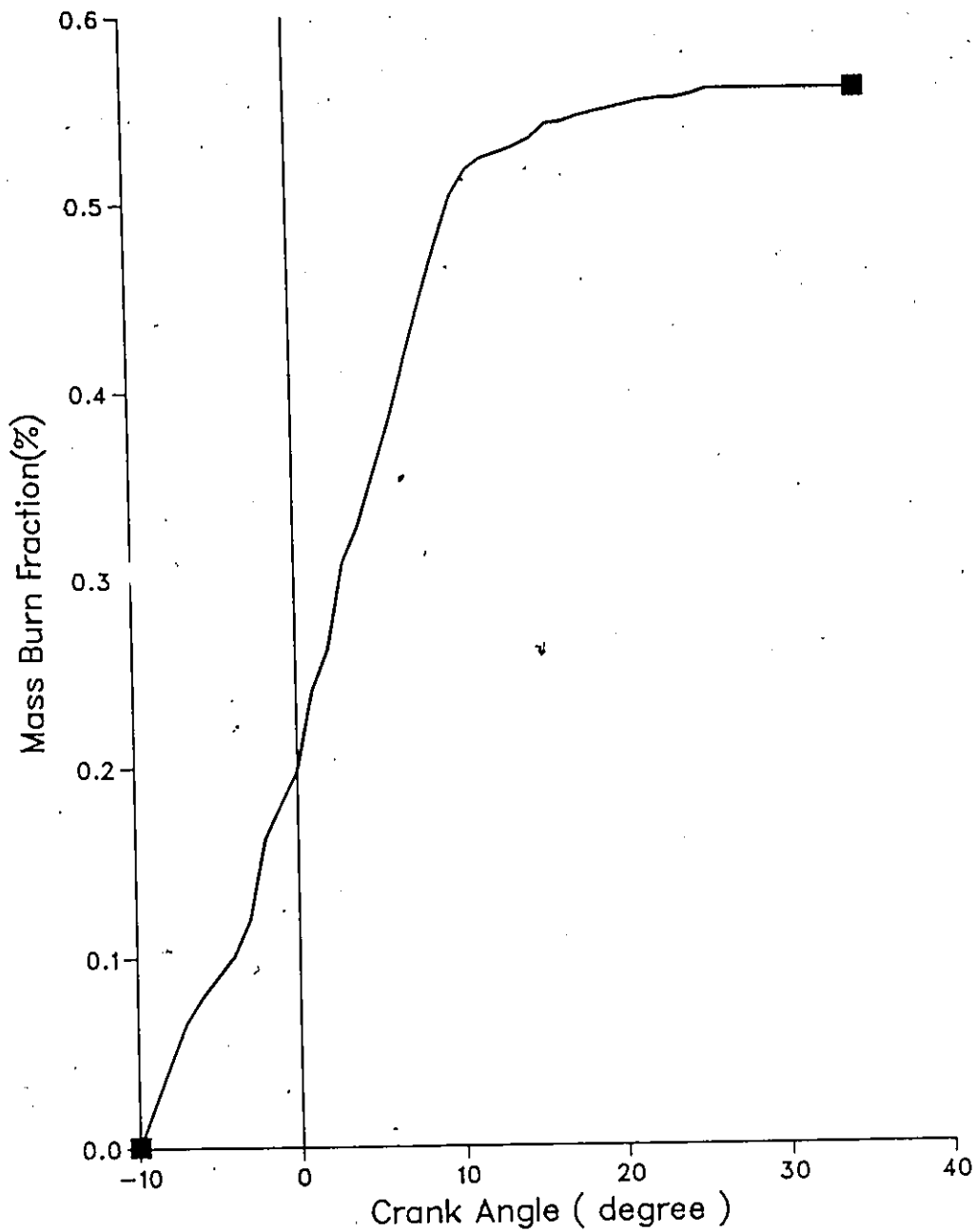


Figure 19. Mass Burn Fraction versus Crank Angle
for a Partial Burn Cycle
Spark Advance : 30 degrees BTDC

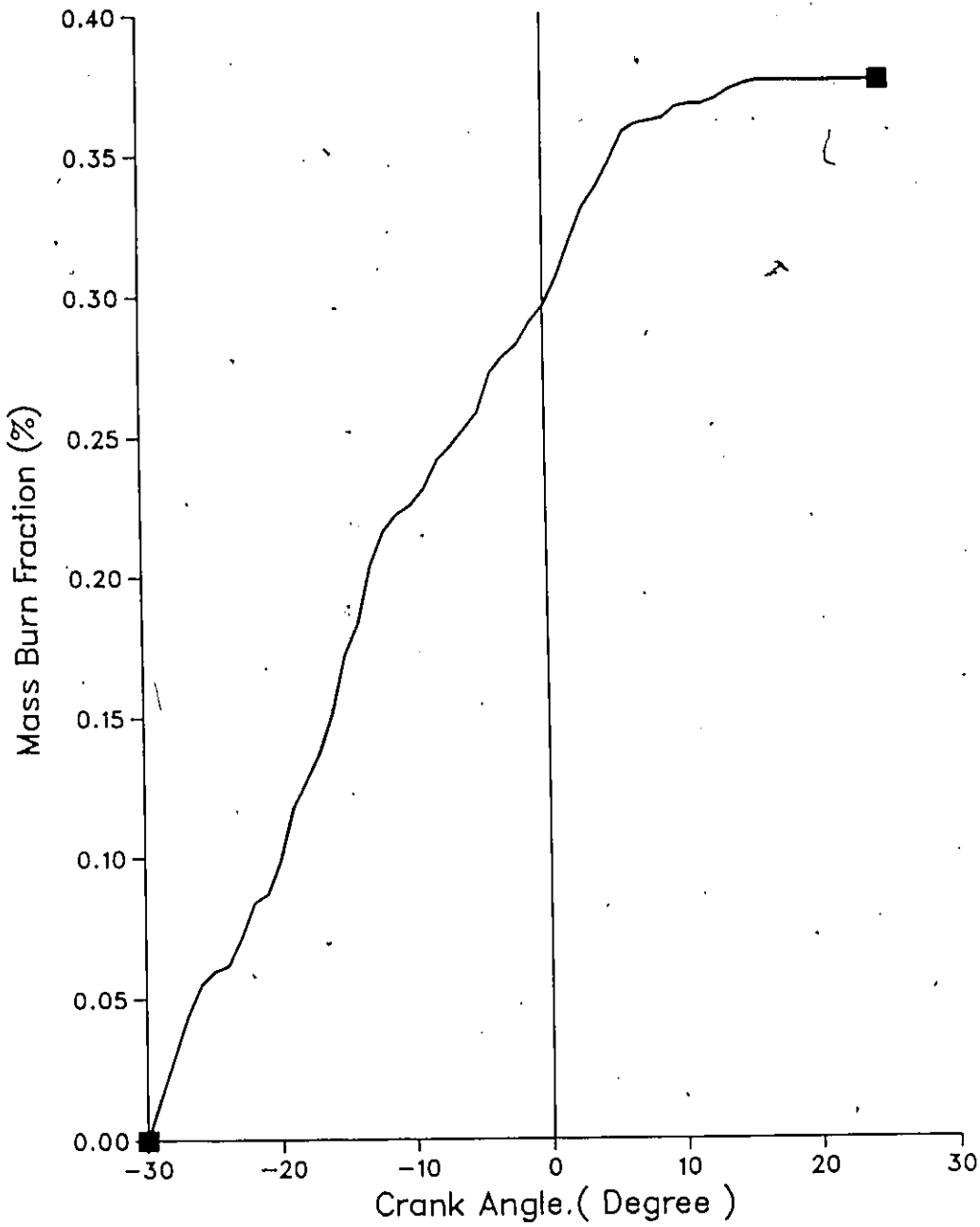


Figure 20. Mass Burn Fraction versus Crank Angle for the inclusion of Age Mixing

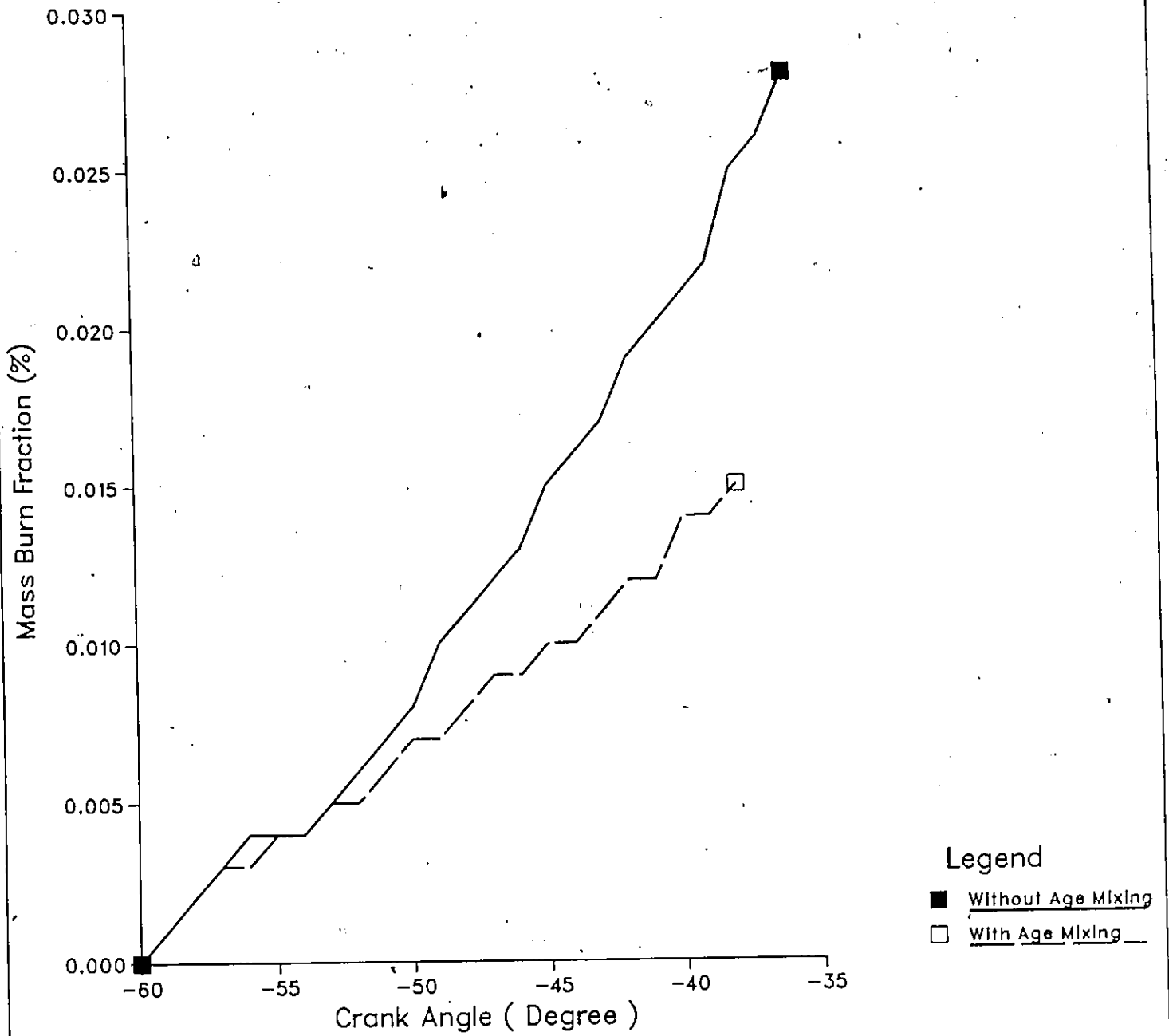


Figure 21. Mass Burn Fraction versus Crank Angle for the inclusion of Age Mixing at Partial Burn

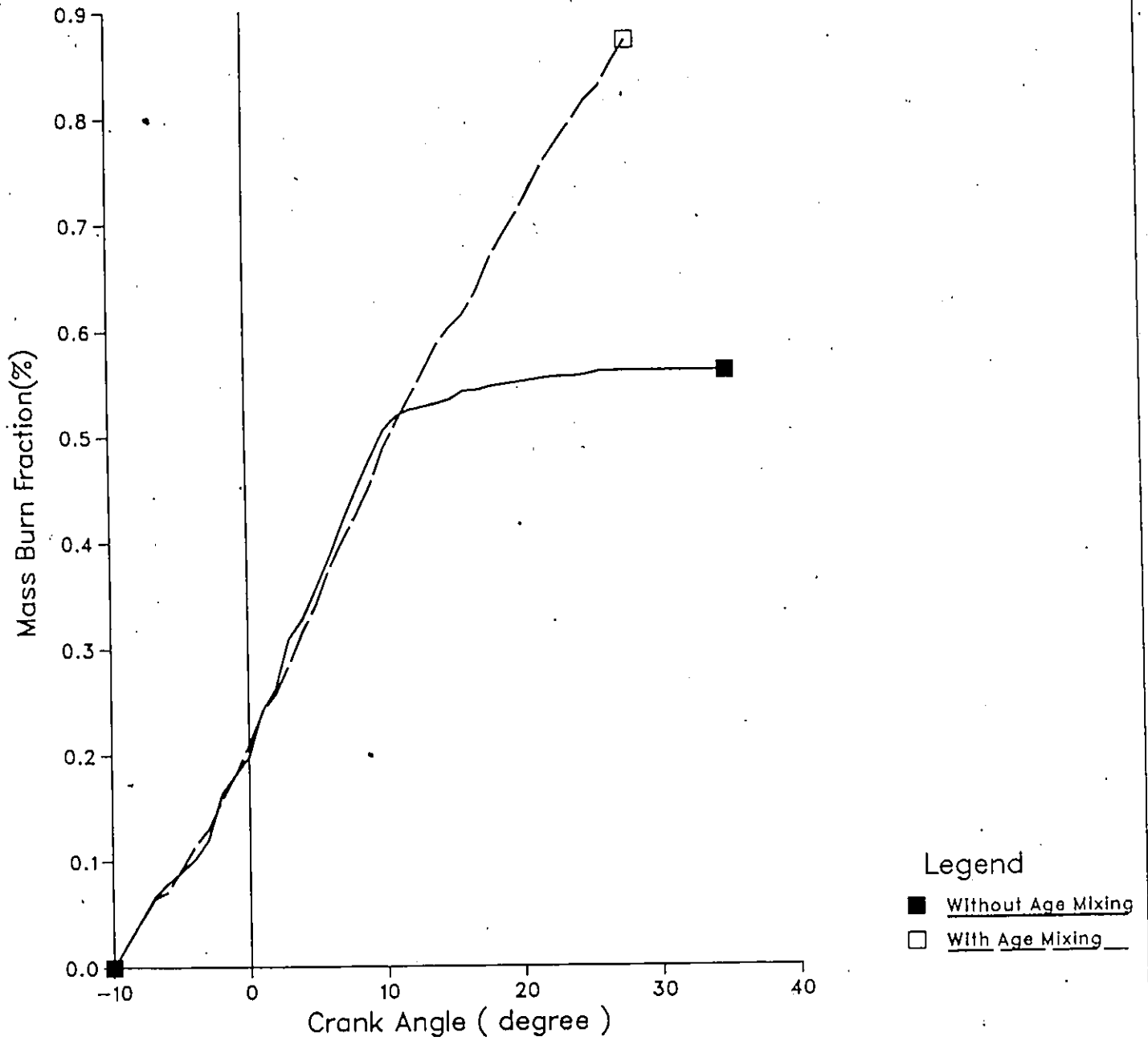
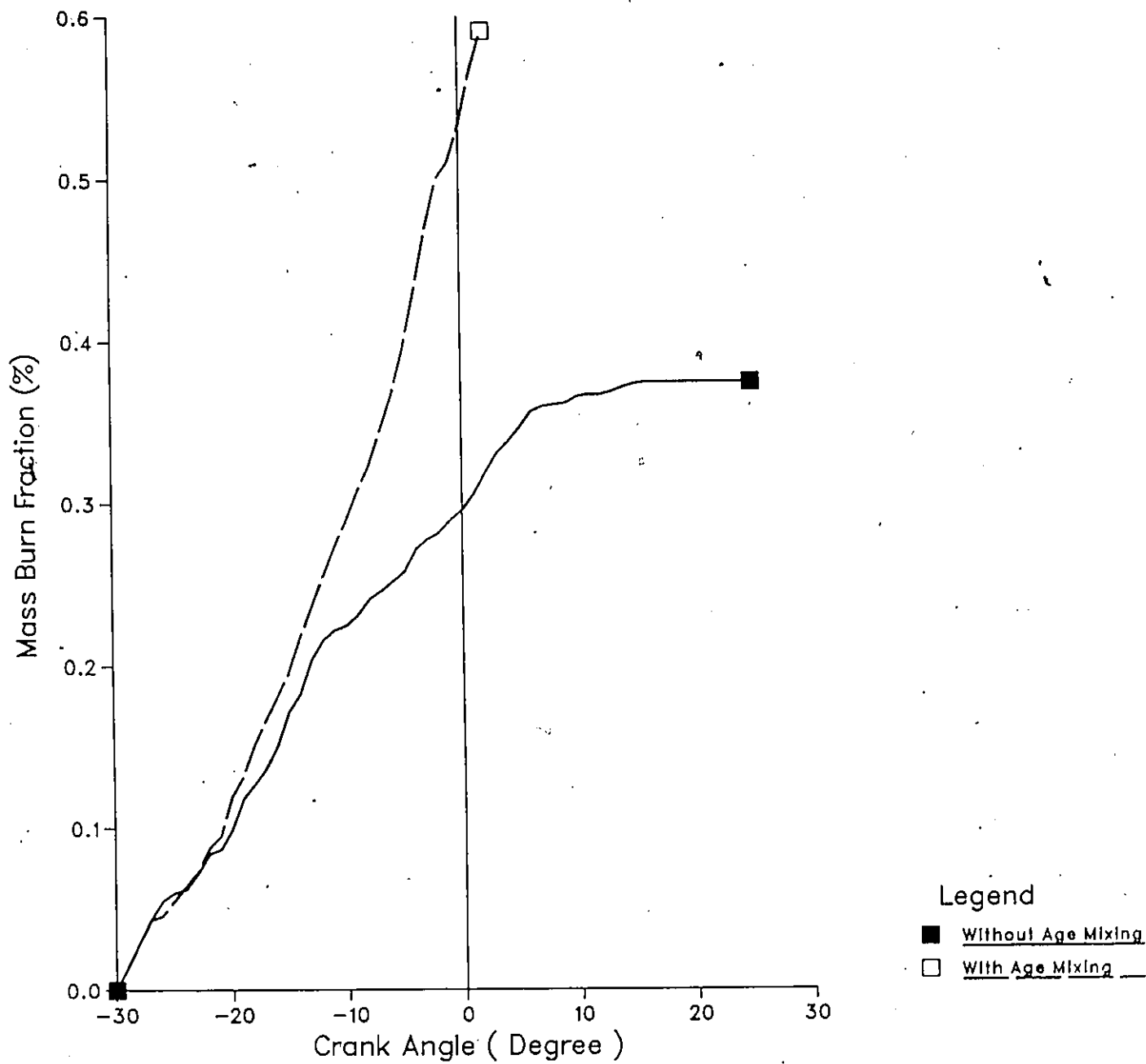


Figure 22. Mass Burn Fraction versus Crank Angle for the inclusion of Age Mixing at Partial Burn



APPENDIX A

```

DIMENSION A(6,8,2)
EQUIVALENCE (A1(1),A(1,1,1))
EQUIVALENCE (A2(1),A(1,1,2))
COMMON/CNT/IUP,ICLD,IKIN
COMMON/CNTF/IF1,IF2,IF3
COMMON/JANAF/ A1(36),A2(36)
COMMON/UGASP/CCU(7),MBARU,RU,GAMU,CPU,HU,TU,RHOU
COMMON/BGASP/CCB(7),MBARB,RB,GAMB,CPB,HB
COMMON/THERMO/R,RGSI,RO2,PSCALE,PSCOR
COMMON/INPRS/PRESS
COMMON /FUEL/ ENW,CX,HY,OZ,AST
COMMON /OXDANT/XI
COMMON/CHARTH/RESFRK,RICH,LEAN
COMMON/CHARU/PHIFR,PHIEGR
COMMON/CHARB/PHI
COMMON/MIX/MASS,F3,VOL3,TO3
COMMON/BURN/FFR(9999),IBURN(9999)
COMMON/IDNUM/IDN(9999)
COMMON/AGE/NAGE,NP(500),FNM(500)
COMMON/PARNUM/N,NT,N1,N2,N3
COMMON/EQNUM/NQ
COMMON/AFRN/V,TOTMX,P,M
COMMON/MOLWT/WM(7)
COMMON/TEMVOL/TEMP(9999),VOL(9999)
COMMON/MOLES/TOTMXU,TOTMXB
COMMON/CRANGL/SA,CRG,CRGSTP
COMMON/STEP/TIMSTP
COMMON/CONST/PEC,B
REAL Y(1000),YPRIM(1000)
REAL X,XEND,INTER,M
REAL MU,MB,MBU,MSG,MBARU,MBARU1,MBARB1,MBARB,MBARAD
REAL MBARBU,MBARAV,MBARIS,MBARB2
REAL MASS,ME,NE,NB,RE,NM
DOUBLE PRECISION DSEED
DATA ERMX,MAXITS/1.E-4,50/

```

```

C-----
C
C TO CALCULATE THE PRESSURE AND TEMPERATURE OF THE MIXTURE BEFORE
C IGNITION, THE INTAKE VALVE IS ASSUMED TO CLOSE AT 120 BTC, WHEN
C THE PRESSURE IS ASSUMED TO BE 0.6 ATM, AND TEMPERATURE TO BE 373 K.
C
C SAI = SPARK ADVANCE
C SAIN = CRANK ANGLE AT CLOSE OF INTAKE VALVE (BTC)
C GAMA = RATIO OF SPECIFIC HEAT
C PIN = PRESSURE AT-CLOSE OF INTAKE VALVE
C TIN = TEMPERATURE AT CLOSE OF INTAKE VALVE
C PO = PRESSURE BEFORE IGNITION
C TO = TEMPERATURE BEFORE IGNITION

```

```

C-----
C IUP=0
C ICLD=0
C IKIN=0
C
C INPUT PARAMETERS ( EQUIVALENCE RATIO INPUT FROM BLOCK DATA )
C
PEC = 4.3E+11
B = 30000.
C = 0.025
PRINT*,' PEC =',PEC,' B =',B,' C =',C
RPM = 3000.
CRGSTP = 1./4.
SAIN = -140.
TIN = 270.
PIN = 0.7
UO = 300.
SAI = -10.
SPDR = 2.
EIGN = 6.E-03/4.184
GAP = 0.10
NB = 5.
SAF = 120.

```

```

APP00010
APP00020
APP00030
APP00040
APP00050
APP00060
APP00070
APP00080
APP00090
APP00100
APP00110
APP00120
APP00130
APP00140
APP00150
APP00160
APP00170
APP00180
APP00190
APP00200
APP00210
APP00220
APP00230
APP00240
APP00250
APP00260
APP00270
APP00280
APP00290
APP00300
APP00310
APP00320
APP00330
APP00340
APP00350
APP00360
APP00370
APP00380
APP00390
APP00400
APP00410
APP00420
APP00430
APP00440
APP00450
APP00460
APP00470
APP00480
APP00490
APP00500
APP00510
APP00520
APP00530
APP00540
APP00550
APP00560
APP00570
APP00580
APP00590
APP00600
APP00610
APP00620
APP00630
APP00640
APP00650
APP00660
APP00670
APP00680
APP00690
APP00700
APP00710
APP00720
APP00730
APP00740
APP00750
APP00760

```



```
DO 25 I = 1,50
TU = TO*(PRESS/PO)**((GAMU-1.)/GAMU)
CALL UPROP(PRESS, TU, ENTHU, CSUBP, RHO)
EU = ENTHU*1000.-RU*TU
EU = EU*MASS*(N-NB)/N
VU = ((N-NB)/N)*VTO(SA)*((PO/PRESS)**(1./GAMU))
WORKU = (PRESS+PO)*PSCALE*(VU-VTO(SA)*(N-NB)/N)/2.
VB = V-VU
TB1 = 2000.
CALL CLDPRD(PRESS, TB1, HB, CSUBP, RHOB, IER)
TB1 = VB*PRESS/(RB/PSCALE)/(MASS*NB/N)
DO 95 J = 1,50
CALL CLDPRD(PRESS, TB1, HB, CSUBP, RHOB, IER)
TB2=TB1
TB1 = VB*PRESS/(RB/PSCALE)/(MASS*NB/N)
IF (ABS(TB2-TB1).LE.0.5) GO TO 96
95 CONTINUE
96 EB = HB*1000.-RB*TB1
EB = EB*MASS*NB/N
WORKB = (PRESS+PO)*PSCALE*(VB-VTO(SA)*NB/N)/2.
EOT = EU+WORKU+EB+WORKB
C PRINT*, ' PRESS,EB+WORKB,EU+WORKU : ',PRESS,EB+WORKB,EU+WORKU
IF (ABS(EB+WORKB-EB1)/EB1.LE.0.010.AND.
1 ABS(EU+WORKU-EU1)/EU1.LE.0.010) GO TO 15
IF (1.GE.50)
1 PRINT*, ' NUMBER OF ITERATION EXCEEDS LIMIT AT IGNITION I '
IF (1.GE.50) STOP
IF (X.EQ.0.AND.(EB+WORKB)/EB1.LT.1.) THEN
PRESS = PRESS + PPLUS
ELSE
X = X + 1.
IF ((EB+WORKB)/EB1.LT.1.) THEN
PRESS = PRESS + (PPLUS/(2.**X))
ELSE
PRESS = PRESS - (PPLUS/(2.**X))
ENDIF
ENDIF
25 CONTINUE
15 SA=SA+SPDR
PRINT*, '+++++ AFTER IGNITION +++++'
PRINT*, ' SA =',SA, ' PRESS = ',PRESS, ' ATM'
PRINT*, ' TU = ', TU, ' TB1 = ',TB1
PRINT*, ' VU1 = ',VU/(N-NB), ' VB1 = ',VB/NB
PRINT*, ' BURNED DIA = ',(6./3.1416*VB)**(1./3.)
PRINT*, ' RHO = ',RHO, ' RHO/RHOB = ',RHO/RHOB
PRINT*, ' EU = ',EU, ' EB = ',EB
PRINT*, ' WORKU = ',WORKU, ' WORKB = ',WORKB
PRINT*, ' EOT1 = ',EOT1, ' EOT = ',EOT
C
C
C TEMP(I) = TEMP OF PARTICAL I
C VOL(I) = VOLUME OF PARTICAL I
C FFR(I) = FUEL FRACTION OF PARTICAL I
C
DO 110 I = 1,NB
TEMP(I) = TB1
VOL(I)=VB/NB
FFR(I)=0.
IDN(I)=0
110 CONTINUE
C
C FO = FUEL FRACTION OF AN UNBURNED PARTICLE
C
FO = 44./((44.+5*(32.+3.76*28.)/PHI)
PRINT*, ' UNBURNED FFR = ',FO, ' UBN FUEL CONC. = ',FO/44., ' MOL/G'
DO 120 I = NB+1,MIN(N,9999)
TEMP(I) = TU
VOL(I)=VU/(N-NB)
FFR(I)=FO
IDN(I)=0
120 CONTINUE
NT=NB
M = MASS/N
ME=NT*M
CALL COUNT(NT)
```

APP01510
APP01520
APP01530
APP01540
APP01550
APP01560
APP01570
APP01580
APP01590
APP01600
APP01610
APP01620
APP01630
APP01640
APP01650
APP01660
APP01670
APP01680
APP01690
APP01700
APP01710
APP01720
APP01730
APP01740
APP01750
APP01760
APP01770
APP01780
APP01790
APP01800
APP01810
APP01820
APP01830
APP01840
APP01850
APP01860
APP01870
APP01880
APP01890
APP01900
APP01910
APP01920
APP01930
APP01940
APP01950
APP01960
APP01970
APP01980
APP01990
APP02000
APP02010
APP02020
APP02030
APP02040
APP02050
APP02060
APP02070
APP02080
APP02090
APP02100
APP02110
APP02120
APP02130
APP02140
APP02150
APP02160
APP02170
APP02180
APP02190
APP02200
APP02210
APP02220
APP02230
APP02240
APP02250
APP02260

```

WM(1)=44.
WM(2)=18.
WM(3)=28.
WM(4)=2.
WM(5)=32.
WM(6)=28.
WM(7)=44.

```

C

```

FF1=FO
X1=FF1/44.
Y1=(M*(1.-FO)/(1.+3.76*WM(6)/WM(5))
-5.*(FO-FF1)*M*WM(5)/WM(7))/WM(5)/M
V1=3.76*M*(1.-FO)/WM(5)/(1.+3.76*WM(6)/WM(5))/M
TOTMXU=X1+Y1+V1

```

```

FF1=0
V1=3.76*M*(1.-FO)/WM(5)/(1.+3.76*WM(6)/WM(5))/M
Z1=3.*(FO-FF1)*M*WM(1)/WM(7)/WM(7)/M
W1=4.*(FO-FF1)*M*WM(2)/WM(7)/WM(2)/M
TOTMXB=V1+W1+Z1

```

C

```

PRINT*, 'CRGSTP =', CRGSTP, 'TIMSTP =', TIMSTP
WRITE(6,600)
600 FORMAT(/,4X,'SA',7X,'VTO',6X,'PCOM',5X,'PRESS',
1 4X,'UPRIM',4X,'VER(%)',4X,'BMF(%)',6X,'NT',5X,'N1',5X,'N3',
1 3X,'ETOTAL',3X,'T1AV',5X,'T3AV',6X,'TU')

```

C

```

P1=PO
T1=TO
DP=0.
WORK=0.
HLAST=0.
IUPT=0
ICLDT=0
IKINT=0
FNT=0.
DO 998 IAGE = 1,500
FNM(IAGE)=0.
998 CONTINUE
NAGE=0.
DSEED=1234567.000

```

C

DO 999 CRNGL = SA,SAF,CRGSTP

C

C TO CALCULATE PRESSURE AND TEMP FOR MOTORED CYCLE

C

```

DO 101 SS=SAI,SA+CRGSTP,CRGSTP
CALL UPROP(P1,T1,ENTHU,CSUBP,RHO)
PCOM=(VTO(SS)/VTO(SAI))*(-GAMU)*P1
TCOM=(PCOM/P1)**((GAMU-1)/GAMU)*T1
DPIS=(PCOM-P1)/TIMSTP
P1=PCOM
T1=TCOM
SAI=SS

```

101

CONTINUE

C

```

PRESS1=PRESS
DPDT=DP*PSCALE
XEND=TIMSTP

```

C

```

IF(N1.EQ.0) THEN
CALL ISCOMP(VTO(SA),VTO(SA+CRGSTP),PRESS,POUT)
PRESS=POUT
ENDIF
IF(N1.EQ.0) GO TO 19

```

C

```

IF1=0
IF2=0
IF3=0
IUP=0
ICLD=0
IKIN=0
CALL KINET(X,XEND,DPDT,Y,YPRIM,HLAST)
IUPT=IUPT+IUP
ICLDT=ICLDT+ICLD
IKINT=IKINT+IKIN

```

```

APP02290
APP02300
APP02310
APP02320
APP02330
APP02340
APP02350
APP02360
APP02370
APP02380
APP02390
APP02400
APP02410
APP02420
APP02430
APP02440
APP02450
APP02460
APP02470
APP02480
APP02490
APP02500
APP02510
APP02520
APP02530
APP02540
APP02550
APP02560
APP02570
APP02580
APP02590
APP02600
APP02610
APP02620
APP02630
APP02640
APP02650
APP02660
APP02670
APP02680
APP02690
APP02700
APP02710
APP02720
APP02730
APP02740
APP02750
APP02760
APP02770
APP02780
APP02790
APP02800
APP02810
APP02820
APP02830
APP02840
APP02850
APP02860
APP02870
APP02880
APP02890
APP02900
APP02910
APP02920
APP02930
APP02940
APP02950
APP02960
APP02970
APP02980
APP02990
APP03000
APP03010
APP03020
APP03030

```

```
CALL COUNT(NT)
DO 131 I = 1,NT
  IF (IBURN(I).NE.1) IDN(I)=0
131 CONTINUE
C... PRINT*, ' N1 =',N1,' N3 =',N3
19 SA=SA+CRGSTP
  DP=(PRESS-PRESS1)/TIMSTP
C PRINT*, ' DPDT OF COMPRESSION =',DPIS,' DPDT OF COMBUSTION =',DP
  IF(N1+N3.EQ.0) PRINT*, ' FLAME IS QUENCHED 1'
  IF(N1+N3.EQ.0) STOP
C
  T1AV=0.
  T3AV=0.
  DO 29 I = 1,NT
    IF (IBURN(I).EQ.1) T1AV=T1AV+TEMP(I)
    IF (IBURN(I).EQ.3) T3AV=T3AV+TEMP(I)
29 CONTINUE
  IF(N1.NE.0)THEN
    T1AV=T1AV/N1
  ENDIF
  IF(N3.NE.0)THEN
    T3AV=T3AV/N3
  ENDIF
C
C TO CALCULATE TOTAL INTERNAL ENERGY OF THE SYSTEM
C AND AVERAGE BURNING AND BURNED GAS DENSITY (RHOAVE)
C
  ETOTAL=0.
  IN=0
  VOLB = 0.
  DO 102 J=1,NT
    IF (IBURN(J).EQ.3) THEN
      CALL CLDPRD(PRESS,TEMP(J),HB,CP,RHOB,IER)
      ETOTAL=ETOTAL+M*(HB*1000.-RB*TEMP(J))
      VOLB = VOLB+VOL(J)
    ENDIF
    IF (IBURN(J).EQ.2) THEN
      CALL UPROP(PRESS,TEMP(J),ENTHU,CSUBP,RHO)
      ETOTAL=ETOTAL+M*(ENTHU*1000.-RU*TEMP(J))
    ENDIF
    IF (IBURN(J).EQ.1.AND.IDN(J).EQ.0) THEN
      IN=IN+1
      JUMP=0
      CALL KINTER(Y,IN,WU,WCM,INTER)
302 ETOTAL=ETOTAL+INTER*M*TOTMX
      VOLB = VOLB+VOL(J)
      IF(JUMP.EQ.1) GO TO 102
      DO 301 I = 1,NT
        IF (IDN(I).EQ.J) JUMP=1
        IF (IDN(I).EQ.J) GO TO 302
301 CONTINUE
      ENDIF
102 CONTINUE
    RHOAVE=(N1+N3)*M/VOLB
    CALL UPROP(PRESS,TEMP(NT+1),ENTHU,CSUBP,RHO)
    ETOTAL=ETOTAL+(N-NT)*M*(ENTHU*1000.-RU*TEMP(NT+1))
    DWORK=(PRESS+PRESS1)*PSCALE*(VTO(SA)-VTO(SA-CRGSTP))/2.
    WORK=WORK+DWORK
    ETOTAL=ETOTAL+WORK
    IF (ABS((ETOTAL-EOT)/EOT).GT.0.10)
1 PRINT*, ' EOT =',EOT,' ETOTAL =',ETOTAL,
1 ' ... 1ST LAW IS VIOLATED 1'
    IF (ABS((ETOTAL-EOT)/EOT).GT.0.10) STOP
C
C VE = ENTRAINED VOLUME
C
  VE=0.
  VFL=0.
  DO 18 IE=1,NT+1
    IF (IE.LE.NT) VE=VE+VOL(IE)
    IF (IE.GT.NT) VU=VOL(IE)*(N-NT)
18 CONTINUE
  VD=ABS(VE+VU-VTO(SA))/VTO(SA)
```

APP03090
APP03100
APP03110
APP03120
APP03130
APP03140
APP03150
APP03160
APP03170
APP03180
APP03190
APP03200
APP03210
APP03220
APP03230
APP03240
APP03250
APP03260
APP03270
APP03280
APP03290
APP03300
APP03310
APP03320
APP03330
APP03340
APP03350
APP03360
APP03370
APP03380
APP03390
APP03400
APP03410
APP03420
APP03430
APP03440
APP03450
APP03460
APP03470
APP03480
APP03490
APP03500
APP03510
APP03520
APP03530
APP03540
APP03550
APP03560
APP03570
APP03580
APP03590
APP03600
APP03610
APP03620
APP03630
APP03640
APP03650
APP03660
APP03670
APP03680
APP03690
APP03700
APP03710
APP03720
APP03730
APP03740
APP03750
APP03760
APP03770
APP03780
APP03790
APP03800
APP03810

```

IF(VD.GT.0.05)
1 PRINT*, ' VTO(SA) = ',VTO(SA), ' VE+VU = ',VE+VU,
1 ' ... PERFECT GAS LAW (VOLUME CONSTRAIN) IS VIOLATED !'
IF(VD.GT.0.05) STOP
VER=VE/(VE+VU)*100.
C
CALL SHARE(SA,VE,H,RE,AE)
C
C UO = TURBULENT INTENSITY AT CLOSE OF INTAKE VALVE ( CM/SEC )
C RHO0 = DENSITY (UNBURNED) AT CLOSE OF INTAKE VALVE
C UPRIM = TURBULENT INTENSITY ( CM/SEC)
C
TU=TEMP(NT+1)
CALL SPEED(UO,RHO0,TU,PRESS,UPRIM,SL)
UT=((2.*RHO)/(3.*RHOAVE))*5*UPRIM+SL
DT=TIMSTP
RHO=(N-NT)*M/VU
ME=ME+DT*AE*UT*RHO
NTP=NT
NT=ME/M
FNT=FNT+ME/M-NT
IF(FNT.GE.1.) NT=NT+1
IF(FNT.GE.1.) FNT=FNT-1.
NAGE=NAGE+1
IF(NAGE.GT.500) PRINT*, ' NAGE > 500 !'
IF(NAGE.GT.500) STOP
NP(NAGE)=NT-NTP
C... PRINT*, ' NAGE = ',NAGE, ' NP = ',NP(NAGE)
IF(NT.GT.9999) PRINT*, ' PARTICLES ENTRAINED > 9999 !'
IF(NT.GT.9999) STOP
CALL COUNT(NT)
C
C BMF = BURNED MASS FRACTION OF THE SYSTEM
C
BMF=0.
DO 31 I = 1,NT
BMF = BMF+(1.-FFR(I)/FO)
31 CONTINUE
BMF=BMF/N*100.
C
C ... CONSTANT C IS IN SEC/CM**2
DELT=TIMSTP
W=C*UPRIM**2.
C
C CALL RANMIX WITHOUT AGE MIXING, CALL AGEMIX WITH AGE MIXING
C
C... CALL RANMIX(DELT,W,NM,FNM1,DSEED)
CALL AGEMIX(DELT,W,NM,DSEED)
C... PRINT*, ' W = ',W, ' NM = ',NM
IF(ABS(SA-INT(SA)).EQ.0.) THEN
WRITE(6,601)SA,VTO(SA),PCOM,PRESS,UPRIM,VER,BMF,
1 NT,N1,N3,ETOTAL,T1AV,T3AV,TEMP(NT+1)
601 FORMAT(/3X,F6.2,3X,F6.2,3X,F6.3,3X,F6.3,3X,F6.1,
1 3X,F7.3,3X,F7.3,3X,F6.1,3X,F6.1,3X,F6.2,
1 3X,F6.1,3X,F6.1,3X,F5.1)
ENDIF
999 CONTINUE
STOP
END
C
C SUBROUTINE PRTY
C
SUBROUTINE PRTY(Y,NQ)
REAL Y(NQ)
WRITE(6,601)
601 FORMAT(/6X,'TEMP',16X,'C3H8')
WRITE(6,602)Y
602 FORMAT(5X,F12.7,5X,F12.7)
RETURN
END
C
C SUBROUTINE COUNT(IN)
C
IBURN(I)= 1 FOR BURNING PARTICLES
IBURN(I)= 2 FOR UNBURNED PARTICLES
IBURN(I)= 3 FOR FULLY BURNED PARTICLES

```

```

APP03820
APP03830
APP03840
APP03850
APP03860
APP03870
APP03880
APP03890
APP03900
APP03910
APP03920
APP03930
APP03940
APP03950
APP03960
APP03970
APP03980
APP03990
APP04000
APP04010
APP04020
APP04030
APP04040
APP04050
APP04060
APP04070
APP04080
APP04090
APP04100
APP04110
APP04120
APP04130
APP04140
APP04150
APP04160
APP04170
APP04180
APP04190
APP04200
APP04210
APP04220
APP04230
APP04240
APP04250
APP04260
APP04270
APP04280
APP04290
APP04300
APP04310
APP04320
APP04330
APP04340
APP04350
APP04360
APP04370
APP04380
APP04390
APP04400
APP04410
APP04420
APP04430
APP04440
APP04450
APP04460
APP04470
APP04480
APP04490
APP04500
APP04510
APP04520
APP04530
APP04540
APP04550
APP04560

```

```

SUBROUTINE COUNT(IN)
COMMON/BURN/FFR(9999),IBURN(9999)
COMMON/PARNUM/N,NT,N1,N2,N3
COMMON/CHARB/PHI
N1=0
N2=0
N3=0
FO = 44./((44.+5.*(32.+3.76*28.)/PHI)

```

C

```

DO 125 I=1,IN
IBURN(I)=1
IF(FFR(I).GE.FO*0.95) IBURN(I)=2
IF(FFR(I).EQ.0.) IBURN(I)=3
IF (IBURN(I).EQ.3) THEN
  N3=N3+1
ELSE
  IF (IBURN(I).EQ.2) THEN
    N2=N2+1
  ELSE
    N1=N1+1
  ENDIF
ENDIF
125 CONTINUE
IBURN(NT+1) = 2
RETURN
END

```

C

C

```

BLOCK DATA
DIMENSION A(6,6,2)
EQUIVALENCE (A1(1),A(1,1,1))
EQUIVALENCE (A2(1),A(1,1,2))
COMMON/JANAF/ A1(36),A2(36)
COMMON/THERMO/R,RGSI,RO2,PSCALE,PSCOR
COMMON /FUEL/ ENW,CX,HY,OZ,AST
COMMON /OXDANT/XI
COMMON/CHARTH/RESFRK,RICH,LEAN
COMMON/CHARU/PHIFR,PHIEGR
COMMON/CHARB/PHI

```

C

C

C

C

*** FUEL INFORMATION *****

```

DATA ENW,CX,HY,OZ,AST/ 0., 3., 8., 0., 0.0/
DATA A1/11.94033,2.088581,-0.47029,.037363,-.589447,-97.1418,
1 6.139094,4.60783,-.9356009,6.669498E-02,.0335801,-56.62588,
2 7.099556,1.275957,-.2877457,.022356,-.1598696,-27.73464,
3 5.555680,1.787191,-.2881342,1.951547E-02,.1611828,.76498,
4 7.865847,.6883719,-.031944,-2.68708E-03,-.2013873,-.893455,
5 6.807771,1.453404,-.328985,2.561035E-02,-.1188462,-.331835/
DATA A2/4.737305,16.65283,-11.23249,2.828001,6.76702E-03,-93.75793
7 7.809672,-.2023519,3.418708,-1.179013,1.43629E-03,-57.08004,
8 6.97393,-.8238319,2.942042,-1.176239,4.132409E-04,-27.19597,
9 6.991878,.1617044,-.2182071,.2968197,-1.625234E-02,-.118189,
& 6.295715,2.388387,-.0314788,-.3267433,4.35925E-03,.103637,
\ 7.0922,-1.2958,3.2069,-1.2022,-3.458E-04,-.013967/

```

C

C

C

C

C

C

C

*** CHEMICAL INFO *****

```

DATA RESFRK,PHI,PHIFR,PHIEGR/0.,0.5,0.5,0.5/

```

*** MOLAR N-O RATIO OF OXDANT ***

```

DATA XI /3.76/

```

```

DATA R,RGSI,RO2,PSCALE,PSCOR
& /1.9869,8.3143E7,.99345,2.42173E-2,1.2187E-2/
END

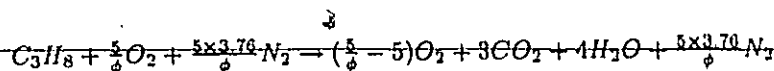
```

- APP04590
- APP04600
- APP04610
- APP04620
- APP04630
- APP04640
- APP04650
- APP04660
- APP04670
- APP04680
- APP04690
- APP04700
- APP04710
- APP04720
- APP04730
- APP04740
- APP04750
- APP04760
- APP04770
- APP04780
- APP04790
- APP04800
- APP04810
- APP04820
- APP04830
- APP04840
- APP04850
- APP04860
- APP04870
- APP04880
- APP04890
- APP04900
- APP04910
- APP04920
- APP04930
- APP04940
- APP04950
- APP04960
- APP04970
- APP04980
- APP04990
- APP05000
- APP05010
- APP05020
- APP05030
- APP05040
- APP05050
- APP05060
- APP05070
- APP05080
- APP05090
- APP05100
- APP05110
- APP05120
- APP05130
- APP05140
- APP05150
- APP05160
- APP05170
- APP05180
- APP05190
- APP05200
- APP05210
- APP05220
- APP05230
- APP05240
- APP05250
- APP05260

APPENDIX B

THEMODYNAMIC PROPERTIES OF PARTICLES

The thermodynamic properties of particles are functions of the temperatures and compositions. The overall reaction mechanism for the combustion of propane in air is assumed.



Equation (37)

where ϕ is the equivalence ratio defined as

$$\phi = \frac{\text{actual air fuel ratio}}{\text{stoichiometric air fuel ratio}}$$

The enthalpy, internal energy, specific heat at constant pressure and specific heat at constant volume are calculated using polynomial curve fitting of thermodynamic properties of the JANAF Table (1971). The polynomial function and coefficients are taken from Hire et al (1976). The specific enthalpy is calculated using the following function,

$$h = \sum_{i=1}^6 X_i \left(\sum_{j=1}^4 [a_{ij} T^j / j] - [a_{5j} / T] + a_{6j} \right)$$

where h is the specific enthalpy in $Kcal/g$, X_i is the number of moles of species i (i is 1 for CO_2 , 2 for H_2O , 3 for CO , 4 for H_2 , 5 for O_2 , and 6 for N_2), T is the temperature, and a_{ij} are the coefficients of the polynomial function. These coefficients are shown in Table 13. The internal energy in $cal/mole$ of fuel is calculated by the following expression,

$$u = R(0.233361 \times 10^{-10} T^5 / 5 - 0.545131 \times 10^{-7} T^4 / 4 + 0.351709 \times 10^{-4} T^3 / 3 + 0.0157505 T^2 / 2 + 1.31841 T - 14091.3) + 201.1 M_f$$

where R is the universal gas constant and M_f is the molecular weight of propane. The internal energy U in $Kcal$ is obtained by the relation,

$$U = H - RT$$

where H is the enthalpy in $Kcal$. The specific heat at constant pressure is calculated using the following polynomial function,

$$C_p = \sum_{i=1}^6 X_i \sum_{j=1}^4 (a_{ij} T^{j-1} + a_{5j} / T^2)$$

where C_p is the specific heat at constant pressure in $cal/g^{\circ}K$. The specific heat at constant pressure of fuel is calculated by the following expression,

$$C_p = R/M_f (0.233361 \times 10^{-10} T^4 - 0.545131 \times 10^{-7} T^3 + 0.351709 \times 10^{-4} T^2 + 0.0157505 T + 1.31841) + R/M_f$$

The specific heat at constant volume C_v is obtained using the relation,

$$C_v = C_p - R$$

where R is the universal gas constant. The ratio of specific heat can be calculated as,

$$\gamma = \frac{C_p}{C_v}$$

For an unburned particle, the above calculations are performed by subroutine UPROP, assuming the presence of the species on the left hand side of the reaction equation (37). For a burned particle, subroutine CLDPRD assumes that dissociation of products is negligible and that the species on the right hand side of the reaction equation are present. For particles with frozen composition consist of all the species in the reaction equation, the above calculation is performed within the subroutine MIXFRO.

APPENDIX C

```

C----- SUBROUTINE SPEED(UO,RHOO,TU,PRESS,UPRIM,SL) -----
C
C   GIVEN : UO = TURBULENT INTENSITY BEFORE IGNITION
C           RHOO = DENSITY (UNBURNED) BEFORE IGNITION
C           TU = UNBURNED TEMPERATURE
C           PRESS = PRESSURE IN ATM
C
C   RETURN : UPRIM = TURBULENT INTENSITY
C           SL = LAMINAR FLAME SPEED
C
C   NOTE : UO,UPRIM,CM,SL ARE IN CM/SEC
C-----
C
C   SUBROUTINE SPEED(UO,RHOO,TU,PRESS,UPRIM,SL)
C   COMMON /UGASP/ X(7),MBAR,RU,GAMU,CPU,HU,TU1,RHOU
C   COMMON/THERMO/R,RGSI,RO2,PSCALE,PSCOR
C   REAL MR,K
C   DATA MR,ALPHA,A,B,E/31.,-0.06,-0.46,1.46,37.7/
C   DATA ERMAX,MAXITS/0.01,25/
C
C   CALL UPROP(PRESS,TU,ENTHLP,CSUBP,RHO)
C   TGUSS=1900.
C   CALL TEMPB(PRESS,TGUSS,ENTHLP,TB,ERMAX,MAXITS,IER)
C   IF (IER.EQ.1)
C     1 PRINT*, ' ... NUMBER OF ITERATION EXCEEDS LIMIT IN "SPEED" 1'
C     IF (IER.EQ.1) STOP
C     TM=UO+0.74*(TB-TU)
C     CM=(8.*R*(4.184E7)*TM/(3.1416*MR))**(1./2.)
C     K=(2.*TU/(3.07*TM))*((PRESS/1.)**ALPHA)
C     YFOL=X(5)**B
C     YFFL=X(7)**A
C     SL=K*CM*(YFOL*YFFL*EXP(-E*1000./(R*TM)))**(1./2.)
C     UPRIM=UO*(RHO/RHOO)**(1./3.)
C
C   RETURN
C   END
C
C   CTEMPB ***** VERSION 1.0 *** 5/29/74 *****
C   SUBROUTINE TEMPB
C
C   PURPOSE
C   TO CALCULATE THE TEMPERATURE OF THE PRODUCTS OF HC-AIR
C   COMBUSTION, FOR GIVEN SPECIFIC ENTHALPY OF THE PRODUCT
C   FOR GIVEN ABSOLUTE PRESSURE
C
C   USAGE
C   CALL TEMPB(P,TGUSS,ENTHLP,T,ERMAX,MAXITS,IER)
C
C   DESCRIPTION OF PARAMETERS
C   GIVEN
C   P - ABSOLUTE PRESSURE OF THE PRODUCTS (ATM)
C   TGUSS- INITIAL GUESS FOR T (DEG K)
C   PHI - EQUIVALENC RATIO OF THE PRODUCTS
C   DEL - MOLAR C H RATIO OF THE PRODUCTS
C   PSI - MOLAR N O RATIO OF THE PRODUCTS
C   ENTHLP- ENTHALPY OF THE PRODUCTS (KCAL/G)
C   ERMAX - MAXIMUM ALLOWABLE RELATIVE ERROR IN RESULTANT T
C   MAXITS- MAXIMUM NUMBER OF ALLOWABLE ITERATIONS WITHOUT
C           SUCCESS
C   IER - FLAG, SET TO 1 IF NO SUCCESS WITHIN MAXITS ITERATIONS
C   RETURNS
C   T - TEMPERATURE OF THE PRODUCTS (DEG K)
C
C   SUBROUTINES AND FUNCTION SUBPROGRAMS REQUIRED
C   HPROD
C
C   METHOD
C   NEWTON-RAPHSON ITERATION
C-----

```

APP05260
APP05270
APP05280
APP05290
APP05300
APP05310
APP05320
APP05330
APP05340
APP05350
APP05360
APP05370
APP05380
APP05390
APP05400
APP05410
APP05420
APP05430
APP05440
APP05450
APP05460
APP05470
APP05480
APP05490
APP05500
APP05510
APP05520
APP05530
APP05540
APP05550
APP05560
APP05570
APP05580
APP05590
APP05600
APP05610
APP05620
APP05630
APP05640
APP05650
APP05660
APP05670
APP05680
APP05690
APP05700
APP05710
APP05720
APP05730
APP05740
APP05750
APP05760
APP05770
APP05780
APP05790
APP05800
APP05810
APP05820
APP05830
APP05840
APP05850
APP05860
APP05870
APP05880
APP05890
APP05900
APP05910
APP05920
APP05930
APP05940
APP05950
APP05960
APP05970
APP05980
APP05990
APP06000
APP06010




```

SUBROUTINE HPROD(P,T,H,CP,CT,RHO,CCT,CCP)
LOGICAL RICH, LEAN, NOTHOT, NOTWRM, NOTCLD
REAL MCP, MWT, K1, K2
COMMON/CHARB/PHI
COMMON/CHARTH/RESFRK,RICH,LEAN
COMMON /PRODMR/DEL,CHI,DUM,DUMY,EPS0,EPS
COMMON /BGASP/CCB(7),MWT,RB,GAMMAB,CPB,HB
COMMON/THERMO/RGAS,RGSI,ROVER2,PSCALE,PSCOR
COMMON/FUEL/ENW,CX,HY,OZ,AST
COMMON/OXDANT/PSI
DATA I1/0/

```

```

APP06770
APP06780
APP06790
APP06800
APP06810
APP06820
APP06830
APP06840
APP06850
APP06860
APP06870
APP06880
APP06890
APP06900
APP06910
APP06920
APP06930
APP06940
APP06950
APP06960
APP06970
APP06980
APP06990
APP07000
APP07010
APP07020
APP07030
APP07040
APP07050
APP07060
APP07070
APP07080
APP07090
APP07100
APP07110
APP07120
APP07130
APP07140
APP07150
APP07160
APP07170
APP07180
APP07190
APP07200
APP07210
APP07220
APP07230
APP07240
APP07250
APP07260
APP07270
APP07280
APP07290
APP07300
APP07310
APP07320
APP07330
APP07340
APP07350
APP07370
APP07380
APP07390
APP07400
APP07410
APP07440
APP07450
APP07460
APP07470
APP07480
APP07490
APP07500
APP07510

```

```

C
C
C
INITIALIZE PARAMETERS USED IN THE CALCULATION
DATA TCOLD, THOT /1000., 1100./

```

```

C
NOTHOT = T .LT. THOT
NOTCLD = T .GT. TCOLD
NOTWRM = .NOT. (NOTCLD .AND. NOTHOT)
IF(T.GE.2800.) T=2800.

```

```

C
C
C
USE SIMPLE ROUTINE FOR LOW TEMPERATURE MIXES

```

```

IF (NOTCLD) GO TO 1
CALL CLDPRD(P,T,H,CP,RHO,IER)
RETURN
1 IF(I1) 3,2,3

```

```

C
C
C
*** DO THIS ONLY FIRST TIME

```

```

2 I1=1
DEL=CX/HY
EPS=(4.*DEL)/(1. + 4.*DEL)
C5 = 2.- EPS + PSI
C6 = EPS + 2.*C5
C3 = (121.5 + 29.59*EPS)*1000.
C4 = 1.175E5
T5 = 3.*C5
TV = (3256.- 2400.*EPS + 300.*PSI)/(1.- .5*EPS + .09*PSI)

```

```

3 DEL=3./B.
EPS=(4.*DEL)/(1. + 4.*DEL)
HFO=PHI*(20372.*EPS-114942.)
MCP = (8.*EPS + 4.)*PHI + 32. + 28.*PSI
RO2MCP=ROVER2/MCP
LEAN=PHI.LE.1.
IF (LEAN) GO TO 4

```

```

C
RICH CASE
HFO=HFO + 1000.*(134.39 - 6.5/EPS)*(PHI - 1.)
C10= 2. + 2.*(7.- 4.*EPS)*PHI + 7.*PSI
C20= 8. + 2.*(2.- 3.*EPS)*PHI + 2.*PSI
DO=PHI*(2.-EPS)+PSI
GO TO 5

```

```

C
LEAN CASE
4 C10= 7. + (9.- 8.*EPS)*PHI + 7.*PSI
C20= 2. + 2.*(5.- 3.*EPS)*PHI + 2.*PSI
DO=1.+PHI*(1.-EPS)+PSI

```

```

C
C
C
*** ENTRY AFTER FIRST CALL

```

```

C
C
C
CALCULATE EQUILIBRIUM CONSTANTS FOR DISSOCIATION
(NOTE THAT THESE HAVE UNITS ATM**( .5 ) )

```

```

5 K1 = 5.819E-6 * EXP(.9674*EPS + 35810./T)
K2 = 2.961E-5 * EXP(2.593*EPS + 28980./T)

```

```

C
C
C
CALCULATE A, X, Y, & U

```

```

C
IF ((4.*P*K1*K1*EPS).EQ.0.)STOP
A = ( C5/(4.*P*K1*K1*EPS) )**( .33333333)
AA=T5*(1.+A+A)+2.*C6*A*A

```

```

C
X = A*EPS*(T5+C6*A)/AA

```

```

C
Z = ABS((1.- PHI)/X)

```



```
C      IF CALCULATING FOR AN INTERMEDIATE TEMPERATURE, USE A WEIGHTED
C      AVERAGE OF THE RESULTS FROM THIS ROUTINE AND THOSE FROM THE
C      SIMPLE ROUTINE
C      IF (NOTWRM) RETURN
C      CALL CLDPRD(P,T,TH,TCP,TRHO,IER)
C      W1 = (T - TCOLD)/(THOT - TCOLD)
C      W2 = 1.0 - W1
C      H   = W1*H   + W2*TH
C      RHOB = W1*RHO + W2*TRHO
C      CP   = W1*CP  + W2*TCP
C      CT   = W1*CT
C      CCT=W1*CCT+W2
C      CCP=W1*CCP+W2
C      MYT=(RHO*T)/(PSCOR*P)
C      CPB=CP
C
C      IF (GAMMAB.LT.1..OR.GAMMAB.GT.2.) THEN
C      PRINT*,
C      PRINT*, '***** EXECUTION STOPPED AT HPROD *****'
C      PRINT*,
C      PRINT*, 'T =',T,' P =',P
C      PRINT*, 'CPB =',CPB,' RB =',RB
C      PRINT*, 'GAMMAB =',GAMMAB
C      PRINT*,
C      PRINT*, '***** EXECUTION STOPPED AT HPROD *****'
C      PRINT*,
C      ENDIF
C      IF (GAMMAB.LT.1..OR.GAMMAB.GT.2.) STOP
C
C      RETURN
C      END
```

```
APP08360
APP08370
APP08380
APP08390
APP08400
APP08410
APP08420
APP08430
APP08440
APP08450
APP08460
APP08470
APP08480
APP08490
APP08500
APP08510
APP08520
APP08530
APP08540
APP08550
APP08560
APP08570
APP08580
APP08590
APP08600
APP08610
APP08620
APP08630
APP08640
APP08650
APP08660
APP08670
APP08680
APP08690
```



```

MX(4,3)=0
MX(5,3)=YO
MX(6,3)=VO
MX(7,3)=XO
TEMP(3)=(TOTMX1*T1+TOTMX2*T2)/(TOTMX1+TOTMX2)

CC
DO 20 I=1,MAXITS
INTER=0.
TCV=0.
T=TEMP(3)
ST=T/1000.
IR = 1
IF(T.LT.500.) IR = 2
DO 50 J = 1,6
TU = (((A(4,J,IR)/4.*ST + A(3,J,IR)/3.)*ST
1 + A(2,J,IR)/2.)*ST + A(1,J,IR))*ST
1 - A(5,J,IR)/ST + A(6,J,IR))*1000. -1.98726*T
INTER=INTER+TU*MX(J,3)*M*2.
TCVS=((A(4,J,IR)*ST+A(3,J,IR))*ST + A(2,J,IR))*ST
1 + A(1,J,IR)+A(5,J,IR)/ST**2 -1.98726
TCV=TCV+TCVS*MX(J,3)*M*2.
50 CONTINUE
C THIS PART IS FOR FUEL PROPANE
FM=44.09
RFV=RGAS/FM
TU=RGAS*(((0.233361E-10/5.*T - 0.545131E-7/4.)*T
+0.351709E-4/3.)*T
1 +0.157505E-1/2.)*T
1 +1.31841)*T
1 -14091.3) + 201.1*FM
INTER=INTER+TU*MX(7,3)*M*2.
TCVF=RFV*(((0.233361E-10*T -0.545131E-7)*T
1 +0.351709E-4)*T +0.157505E-1)*T +1.31841)
TCV=TCV+FM*TCVF*MX(7,3)*M*2.
TO=TEMP(3)
TEMP(3)=TEMP(3)+(U-INTER)/TCV
IF(ABS(U-INTER)/U.LE.ERMAX) GO TO 30
IF(1.GE.MAXITS) PRINT*, '(U-INTER)/U =',(U-INTER)/U
IF(1.GE.MAXITS)
1 PRINT*, '... NUMBER OF ITERATION EXCEEDS LIMIT IN "MIXFRO" '
IF(1.GE.MAXITS) STOP
20 CONTINUE
30 TO=TEMP(3)
RETURN
END

```

- APP10200
- APP10210
- APP10220
- APP10230
- APP10240
- APP10250
- APP10260
- APP10270
- APP10280
- APP10290
- APP10300
- APP10310
- APP10320
- APP10330
- APP10340
- APP10350
- APP10360
- APP10370
- APP10380
- APP10390
- APP10400
- APP10410
- APP10420
- APP10430
- APP10440
- APP10450
- APP10460
- APP10470
- APP10480
- APP10490
- APP10500
- APP10510
- APP10520
- APP10530
- APP10540
- APP10550
- APP10560
- APP10570
- APP10580
- APP10590
- APP10600
- APP10610
- APP10620
- APP10630
- APP10640
- APP10650

APPENDIX F

```

CKINETCCCCCCCCCCCCCCCC10/04/87CCCCCCCCCCCCCCCCCCCCCCCCCCCCCCCCCCCC
C
C SUBROUTINE KINET
C
C PURPOSE
C TO CALCULATE THE EVOLUTION OF SPECIES CONCENTRATION AND TEMPERATURE
C IN A TIME STEP DT. THE EVOLUTION OF SPECIES IS CALCULATED USING
C A SINGLE STEP REACTION MECHANISM DESCRIBED IN WESTBROOK AND DRYER.
C THE 1ST LAW IS USED IN DIFFERENTIAL FORM.
C
C GIVEN:
C
C     X (SECOND) TIME AT WHICH INITIAL VALUES ARE GIVEN
C     XEND (SECOND) TIME AT WHICH VALUES ARE DESIRED
C     P (ATM) PRESSURE AT TIME XEND
C
C GIVEN INITIAL VALUES AT TIME X FOR
C
C     Y(1) (K) TEMPERATURE
C     Y(2) (MOLES/G) CONCENTRATION OF PROPANE FUEL
C
C RETURN VALUES AT XEND FOR
C
C     Y(1) (K) TEMPERATURE
C     Y(2) (MOLES/G) CONCENTRATION OF PROPANE FUEL
C
C SUBROUTINES AND FUNCTION PROGRAM NEEDED
C -SUBROUTINE FCN
C -FUNCTION F2 CALCULATE THE DERIVATIVE OF TEMPERATURE WITH
C RESPECT TO TIME
C -FUNCTION F1 CALCULATE THE RATE OF DEPLETION OF PROPANE FUEL
C -BLOCK DATA CONTAINS COEFFICIENTS USED TO CALCULATE INTERNAL
C ENERGY AND SPECIFIC HEAT (SEE SAE PAPER BY HIRES ET AL )
C
CCCCCCCCCCCCCCCCCCCCCCCCCCCCCCCCCCCCCCCCCCCCCCCCCCCCCCCCCCCCCCCC
C
C SUBROUTINE KINET(X,XEND,DPDT,Y,YPRIM,HLAST)
C
COMMON/CHARU/PHIFR,PHIEGR
COMMON/AFRN/V,TOTMX,P,M
COMMON/TEMVOL/TEMP(9999),VOL(9999)
COMMON/BURN/FFR(9999),IBURN(9999)
COMMON/IDNUM/IDN(9999)
COMMON/PARNUM/N,NT,N1,N2,N3
COMMON/EQNUM/NQ
COMMON/CHARB/PHI
COMMON/CHARTH/RESFRK,RICH,LEAN
COMMON/UGASP/UX(7),MBAR,RU,GAMU,CPU,HU,TU,RHOU
COMMON/BGASP/CCB(7),MWT,RB,GAMB,CPB,HB
COMMON/THERMO/R,RGSI,RO2,PSCALE,PSCOR
COMMON/MOLES/TOTMXU,TOTMXB
COMMON/INPRS/PRESS
COMMON/MOLWT/WM(7)
COMMON/CRANGL/SA,CRG,CRGSTP
COMMON/STEP/TIMSTP
COMMON/CONST/PEC,B
REAL Y(NQ),YPRIM(NQ),X,XEND
REAL MBAR,INEREA,INER,INTER,M
C
C INITIAL VALUES
C
      ITS=0
      B X=0
      IN=0
      DO 10 J=1,NT
      IF(IBURN(J).EQ.1.AND.IDN(J).EQ.0) THEN
        IN=IN+1
        K=(IN-1)*2
        Y(1+K)=TEMP(J)

```

APP11330
APP11340
APP11350
APP11360
APP11370
APP11380
APP11390
APP11400
APP11410
APP11420
APP11430
APP11440
APP11450
APP11460
APP11470
APP11480
APP11490
APP11500
APP11510
APP11520
APP11530
APP11540
APP11550
APP11560
APP11570
APP11580
APP11590
APP11600
APP11610
APP11620
APP11630
APP11640
APP11650
APP11660
APP11670
APP11680
APP11690
APP11700
APP11710
APP11720
APP11730
APP11740
APP11750
APP11760
APP11770
APP11780
APP11790
APP11800
APP11810
APP11820
APP11830
APP11840
APP11850
APP11860
APP11870
APP11880
APP11890
APP11900
APP11910
APP11920
APP11930
APP11940
APP11950
APP11960
APP11970
APP11980
APP11990
APP12000
APP12010
APP12020
APP12030
APP12040
APP12050
APP12060
APP12070

```

Y(2+K)= FFR(J)/44.
ENDIF
10 CONTINUE
NQ=2*IN
C... PRINT*, ' NQ =',NQ
C... CALL PRTY(Y,NQ)
C
EPS1 = ERROR TOLERANCE FOR FIRST STEP SIZE IN "CODE".
C EPS2 = ERROR TOLERANCE FOR CONVERGENCE OF EACH STEP IN "CODE".
C EPS3 = ERROR TOLERANCE FOR CONVERGENCE OF PRESSURE IN "KINET".
C
EPS1=1.E-02
EPS2=1.E-02
EPS3=1.E-02
C
CALL CODE(X,XEND,Y,YPRIM,DPDT,NQ,EPS1,EPS2,HLAST)
C
ITS=ITS+1
FO=44./((44.+5.*(32.+3.76*28)/PHI)
P=PRESS*PSCALE+X*DPDT
PM=(PRESS+P/PSCALE)/2.
IN=0
TOVOL=0.
UNB=0.
DO 4 I = 1,NT
IF (IBURN(I).EQ.1.AND.IDN(I).EQ.0) THEN
IN=IN+1
FF1=Y(2+(IN-1)*2)*44.
T1=Y(1+(IN-1)*2)
X1=FF1/44.
Y1=(M*(1.-FO)/(1.+3.76*WM(6)/WM(5))
-5.*(FO-FF1)*M*WM(5)/WM(7))/WM(5)/M
1 V1=3.76*M*(1.-FO)/WM(5)/(1.+3.76*WM(6)/WM(5))/M
Z1=3.*(FO-FF1)*M*WM(1)/WM(7)/WM(7)/M
W1=4.*(FO-FF1)*M*WM(2)/WM(7)/WM(2)/M
TOTMX=X1+Y1+V1+W1+Z1
TOVOL=TOVOL+M*TOTMX*1.987*T1/P
DO 32 J = 1,NT
IF (IDN(J).EQ.1) TOVOL=TOVOL+M*TOTMX*1.987*T1/P
32 CONTINUE
ENDIF
IF (IBURN(I).EQ.2) THEN
IF (UNB.EQ.0.) THEN
UNB=1.
ENDIF
TOVOL=TOVOL+VU
ENDIF
IF (IBURN(I).EQ.3) THEN
CALL CLDPRD(PM,TEMP(1),ENTHLP,CSUBP,RHOB,IER)
T1=TEMP(1)*(P/PSCALE/PRESS)**((GAMB-1)/GAMB)
TOVOL=TOVOL+M*TOTMXB*1.987*T1/P
ENDIF
4 CONTINUE
CALL UPROP(PM,TEMP(NT+1),ENTHLP,CSUBP,RHO)
TU=TEMP(NT+1)*(P/PSCALE/PRESS)**((GAMU-1)/GAMU)
VU=M*TOTMXU*1.987*TU/P
TOVOL=TOVOL+(N-NT)*VU
C PRINT*, ' VTO =',VTO(SA+1), ' TOVOL =',TOVOL
C
IF (ABS(TOVOL-VTO(SA+1))/VTO(SA+1).LE.EPS3) GO TO 9
IF (ITS.GE.3)
1 PRINT*, ' 4TH ITERATION ON PRESSURE RISE ...'
IF (ITS.GE.4)
1 PRINT*, ' PRESSURE DOES NOT CONVERGE AFTER 4 ITERATIONS 1'
IF (ITS.GE.4) STOP
PNEXT=P*(TOVOL/VTO(SA+1))
DPDT=(PNEXT-PRESS*PSCALE)/TIMSTP
IF (ITS.LT.4) GO TO 8
C
C TO UPDATE FFR(I), TEMP(I) AND VOL(I) FOR ALL PARTICLES
C
9 IN=0.
UNB=0.
DO 2 I=1,NT
IF (IBURN(I).EQ.1.AND.IDN(I).EQ.0) THEN

```

APP12080
APP12090
APP12100
APP12110
APP12120
APP12130
APP12140
APP12150
APP12160
APP12170
APP12180
APP12190
APP12200
APP12210
APP12220
APP12230
APP12240
APP12250
APP12260
APP12270
APP12280
APP12290
APP12300
APP12310
APP12320
APP12330
APP12340
APP12350
APP12360
APP12370
APP12380
APP12390
APP12400
APP12410
APP12420
APP12430
APP12440
APP12450
APP12460
APP12470
APP12480
APP12490
APP12500
APP12510
APP12520
APP12530
APP12540
APP12550
APP12560
APP12570
APP12580
APP12590
APP12600
APP12610
APP12620
APP12630
APP12640
APP12650
APP12660
APP12670
APP12680
APP12690
APP12700
APP12710
APP12720
APP12730
APP12740
APP12750
APP12760
APP12770
APP12780
APP12790
APP12800
APP12810
APP12820


```

RETURN
END
CF1CCCCCCCCCCCCCCCCCCCCCCCCCCCCCCCCCCCCCCCCCCCCCCCCCCCCCCCCCCCCCCCC
C
C   FUNCTION F1(Y,J)
C
C   CALCULATE THE RATE OF DEPLETION OF FUEL PROPANE USING A SINGLE
C   REACTION MECHANISM FROM WESTBROOK AND DRYER.
C
CCCCCCCCCCCCGGCCCCCCCCCCCCCCCCCCCCCCCCCCCCCCCCCCCCCCCCCCCCCCCCCCCC
C

```

```

FUNCTION F1(Y,J)
COMMON/CNTF/IF1,IF2,IF3
COMMON/AFRN/V,TOTMX,P,M
COMMON/CHARB/PHI
COMMON/TEMVOL/TEMP(9999),VOL(9999)
COMMON/BURN/FFR(9999),IBURN(9999)
COMMON/IDNUM/IDN(9999)
COMMON/MOLWT/WM(7)
COMMON/PARNUM/N,NT,N1,N2,N3
COMMON/EQNUM/NQ
COMMON/CRANGL/SA,CRG,CRGSTP
COMMON/INPRS/PRESS
COMMON/THERMO/R,RGS1,RO2,PSCALE,PSCOR
COMMON/CONST/PEC,B
REAL Y(NQ),M
IF1=IF1+1

PO=PRESS*PSCALE
P=PO+TIMSTP*(CRG-SA)/CRGSTP*DPDT
FO=44./(44.+5.*(32.+3.76*28)/PHI)
IN=0
DO 1 I=1,NT
IF (IBURN(I).EQ.1.AND.IDN(I).EQ.0) THEN
IN=IN+1
IF (IN.EQ.J) THEN
FF1=FFR(I)
X01=M*FF1/WM(7)/M
Y01=(M*(1.-FO)/(1.+3.76*WM(6)/WM(5))
-5.*(FO-FF1)*M*WM(5)/WM(7))/WM(5)/M
ENDIF
ENDIF
CONTINUE
1

```

```

C
C   K=(J-1)*2
C   IF(Y(2+K).LE.FO/44.*0.050) Y(2+K)=0.
C   FF1=Y(2+K)*WM(7)
C   Y1=Y01+5.*(Y(2+K)-X01)
C   V1=3.76*M*(1.-FO)/WM(5)/(1.+3.76*WM(6)/WM(5))/M
C   Z1=3.*(FO-FF1)*M*WM(1)/WM(7)/WM(7)/M
C   W1=4.*(FO-FF1)*M*WM(2)/WM(7)/WM(2)/M
C   IF(Y1.LE.Y01*0.050) Y1=0.
C   TOTMXJ=Y(2+K)+Y1+V1+W1+Z1
C   V=TOTMXJ*1.987*Y(1+K)/P
C
C   IF(Y(2+K).LT.0..OR.Y1.LT.0..OR.V.LE.0.)
1 PRINT*, ' Y(2+K) = ',Y(2+K), ' Y1 = ',Y1, ' V = ',V, ' ... IN "F1" '
IF(Y(2+K).LT.0..OR.Y1.LT.0..OR.V.LE.0.) STOP
C
C   F1=-PEC*V*EXP(-B/Y(1+K)/1.987)*((Y(2+K)/V)**.1)*((Y1/V)**1.65)
C
C   RETURN
C   END

```

```

CCCCCCCCCCCCCCCCCCCCCCCCCCCCCCCCCCCCCCCCCCCCCCCCCCCCCCCCCCCCCCCC
C
C   FUNCTION F2(Y,J) = DTDI FOR EACH BURNING PARTICALS
C
CCCCCCCCCCCCCCCCCCCCCCCCCCCCCCCCCCCCCCCCCCCCCCCCCCCCCCCCCCCCCCCC
FUNCTION F2(Y,J,DPDT)
COMMON/CNTF/IF1,IF2,IF3
COMMON/AFRN/V,TOTMX,P,M
COMMON/UGASP/CCU(7),MBARU,RU,GAMU,CPU,HU,TU,RHOU
COMMON/BGASP/CCB(7),MBARB,RB,GAMB,CPB,HB
COMMON/THERMO/R,RGS1,RO2,PSCALE,PSCOR

```

- APP13590
- APP13600
- APP13610
- APP13620
- APP13630
- APP13640
- APP13650
- APP13660
- APP13670
- APP13680
- APP13690
- APP13700
- APP13710
- APP13720
- APP13730
- APP13740
- APP13750
- APP13760
- APP13770
- APP13780
- APP13790
- APP13800
- APP13810
- APP13820
- APP13830
- APP13840
- APP13850
- APP13860
- APP13870
- APP13880
- APP13890
- APP13900
- APP13910
- APP13920
- APP13930
- APP13940
- APP13950
- APP13960
- APP13970
- APP13980
- APP13990
- APP14000
- APP14010
- APP14020
- APP14030
- APP14040
- APP14050
- APP14060
- APP14070
- APP14080
- APP14090
- APP14100
- APP14110
- APP14120
- APP14130
- APP14140
- APP14150
- APP14160
- APP14170
- APP14180
- APP14190
- APP14200
- APP14210
- APP14220
- APP14230
- APP14240
- APP14250
- APP14260
- APP14270
- APP14280
- APP14290
- APP14300
- APP14310
- APP14320
- APP14330

```

COMMON/PARNUM/N,NT,N1,N2,N3
COMMON/EQNUM/NQ
COMMON/INPRS/PRESS
COMMON/STEP/TIMSTP
COMMON/CRANGL/SA,CRG,CRGSTP
REAL Y(NQ),M,INTER
IF2=IF2+1

```

```

C FU1=F1(Y,J)
CALL KINTER(Y,J,WU,WCM,INTER)

```

```

C
C.....P IN DTDI IS IN CAL/CC
PO=PRESS*PSCALE
P=PO+TIMSTP*(CRG-SA)/CRGSTP*DPDT
K=(J-1)*2
T = Y(1+K)

```

```

C DTDI=(FU1*(1.987*T-WU)+TOTMX*1.987*T/P*DPDT)/
1 (WCM+TOTMX*1.987)

```

```

C F2=DTD1

```

```

C RETURN
END

```

```

C CCCCCCCCCCCCCCCCCCCCCCCCCCCCCCCCCCCCCCCCCCCCCCCCCCCCCCCCCCCCC

```

```

C SUBROUTINE KINTER

```

```

C PURPOSE
C TO CALCULATE THE DERATIVE OF TEMPERATURE WITH RESPECT TO
C TIME AND THE INTERNAL ENERGY OF MIXTURE.

```

```

C USAGE
C CALL INTER(Y)

```

```

C DESCRIPTION OF PARAMETERS

```

```

C GIVEN:

```

```

C P (ATM) PRESSURE

```

```

C GIVEN

```

```

C Y(1) (K) TEMPERATURE
C Y(2) (MOLES/G) CONCENTRATION OF PROPANE FUEL
C Y(3) (MOLES/G) CONCENTRATION OF OXYGEN
C Y(4) (MOLES/G) CONCENTRATION OF NITROGEN
C Y(5) (MOLES/G) CONCENTRATION OF CARBON DIOXIDE -
C Y(6) (MOLES/G) CONCENTRATION OF WATER VAPOR

```

```

C GIVEN IN COMMON AREA /FUEL/

```

```

C AF(1) - 6 DIMENSIONAL VECTOR OF ENTHALPY COEFFICIENTS SUCH
C THAT THE ENTHALPY OF FUEL VAPOR AS A FUNCTION
C OF TEMPERATURE ( T DEG K ) IS GIVEN BY
C H(T) = AF(1)*ST + (AF(2)*ST**2)/2 + (AF(3)*ST**3)/3
C + (AF(4)*ST**4)/4 - AF(5)/ST + AF(6)

```

```

C WHERE ST = T/1000 AND H(T) = <KCAL/MOLE>

```

```

C FOR MOST APPLICATIONS THE ENTHALPY FUNCTION H(
C BE VALID OVER AT LEAST THE FOLLOWING TEMPERATURE RAN
C 300 < T < 1000

```

```

C ENTHALPY DATUM STATE IS AT T = 0 ABSOLUTE WITH O2,N2
C AND H2 GASEOUS AND C SOLID GRAPHITE.
C HYDROCARBON-OXIDANT COMBUSTION

```

```

C RETURNS

```

```

C DTDI - DERIVATIVE OF TEMPERATURE WITH RESPECT TO TIME
C (DEG K /SECOND )
C INTER - INTERNAL ENERGY OF MIXTURE (CAL/MOLE OF MIXTURE)

```

```

C REMARKS

```

- 1) ENTHALPY DATUM STATE IS AT T = 0 ABSOLUTE WITH O2,N2,H2 GASEOUS AND C SOLID GRAPHITE
- 2) THE VARIABLES HAVE DIFFERENT INDICES IN THERMO SUBROUTINES AND DGEAR .THEY ARE AS FOLLOWS:

```

APP14340
APP14350
APP14360
APP14370
APP14380
APP14390
APP14400
APP14410
APP14420
APP14430
APP14440
APP14450
APP14460
APP14470
APP14480
APP14490
APP14500
APP14510
APP14520
APP14530
APP14540
APP14550
APP14560
APP14570
APP14580
APP14590
APP14600
APP14610
APP14620
APP14630
APP14640
APP14650
APP14660
APP14670
APP14680
APP14690
APP14700
APP14710
APP14720
APP14730
APP14740
APP14750
APP14760
APP14770
APP14780
APP14790
APP14800
APP14810
APP14820
APP14830
APP14840
APP14850
APP14860
APP14870
APP14880
APP14890
APP14900
APP14910
APP14920
APP14930
APP14940
APP14950
APP14960
APP14970
APP14980
APP14990
APP15000
APP15010
APP15020
APP15030
APP15040
APP15050
APP15060
APP15070

```


C CALCULATE H, CP, AND CT AS IN WRITEUP, USING FITTED
C COEFFICIENTS FROM JANAF TABLES
C

WU=0.
WCM=0.
INTER=0.
ST = T/1000.

C.....TU IS IN CAL/MOLE OF SPECIES
C.....TCV IN CAL/MOLE/K

DO 40 K = 1,6
TU = (((A(4,K,IR)/4.*ST + A(3,K,IR)/3.)*ST
1 + A(2,K,IR)/2.)*ST + A(1,K,IR))*ST
1 - A(5,K,IR)/ST + A(6,K,IR))*1000. -1.98726*T
INTER=INTER+TU*MX(K)/TOTMX
TCV = ((A(4,K,IR)*ST + A(3,K,IR))*ST
1 + A(2,K,IR))*ST + A(1,K,IR)+A(5,K,IR)/ST**2 -1.98726
WU=WU + TU*LEC(K)
WCM=WCM+MX(K)*TCV

C 40 CONTINUE
C THIS PART IS FOR FUEL PROPANE

FM=44.09
RFV=RGAS/FM
TU= RGAS*(((0.233361E-10/5.*T - 0.545131E-7/4.)*T
1 +0.351709E-4/3.)*T
1 +0.157505E-1/2.)*T
1 +1.31841)*T
1 -14091.3) + 201.1*FM
INTER=INTER+TU*MX(7)/TOTMX
TCV=RFV*(((0.233361E-10*T - 0.545131E-7)*T
1 +0.351709E-4)*T
1 +0.157505E-1)*T
1 +1.31841)
TCV=FM*TCV
WU=WU + TU*LEC(7)
WCM=WCM+MX(7)*TCV

C RETURN
END

APP15830
APP15840
APP15850
APP15860
APP15870
APP15880
APP15890
APP15900
APP15910
APP15920
APP15930
APP15940
APP15950
APP15960
APP15970
APP15980
APP15990
APP16000
APP16010
APP16020
APP16030
APP16040
APP16050
APP16060
APP16070
APP16080
APP16090
APP16100
APP16110
APP16120
APP16130
APP16140
APP16150
APP16160
APP16170
APP16180
APP16190
APP16200

APPENDIX G

```

CCCCCCCCCCCCCCCCCCCCCCCCCCCCCCCCCCCCCCCCCCCCCCCCCCCCCCCCCCCCCCCCCCCC
C
C   VTO(CRKINT) IS THE VOLUME OF THE CHAMBER AS A FUNCTION OF
C   THE CRANK ANGLE.
C
CCCCCCCCCCCCCCCCCCCCCCCCCCCCCCCCCCCCCCCCCCCCCCCCCCCCCCCCCCCCCCCCCCCC
C
C   FUNCTION VTO(CRKINT)
C   COMMON/BBORE/BORE
C
C   BORE=4.0
C   STROKE=4.0
C   CONLEN=7.5
C   CR=8.0
C   DATA RADIAN/57.29578/
C   B1=0.39269908*BORE*BORE*STROKE
C   B2=(CONLEN*2./STROKE)**2.-1.
C   B3=1.0+2.*CONLEN/STROKE
C   THBEG=CRKINT
C   AREA=3.14*BORE*BORE/4
C   VTDC=AREA*STROKE/(CR-1.)
C   CAS=COS(THBEG/RADIAN)
C   VTO=VTDC+B1*(B3-CAS-SQRT(CAS**2+B2))
C   RETURN
C   END

```

APP16220
APP16230
APP16240
APP16250
APP16260
APP16270
APP16280
APP16280
APP16290
APP16300
APP16310
APP16320
APP16330
APP16340
APP16350
APP16360
APP16370
APP16380
APP16390
APP16400
APP16410
APP16420
APP16430
APP16440
APP16450
APP16460
APP16470
APP16480
APP16490
APP16500
APP16510


```

ICLD=ICLD+1
C
1 I1 = 2
RICH = PHIFR.GT.1.0
LEAN = .NOT.RICH
DEL = CX/HY
EPS=4.*DEL/(1.+4.*DEL)
MBAR = (8.*EPS + 4.)*PHI + 32. + 28.*PSI
C
C GET THE COMPOSITION IN MOLES/MOLE OXYGEN
C
IF (RICH) GO TO 13
C
*** LEAN CASE SHIFT JUMP TO 35 AFTER THIS
C
I1 = 3
TMOLES = 1.+PSI+PHI*(1.-EPS)
X(1) = EPS*PHI/TMOLES
X(2) = 2.*(1.-EPS)*PHI/TMOLES
X(3) = 0.
X(4) = 0.
X(5) = (1.-PHI)/TMOLES
X(6) = PSI/TMOLES
X(7) = 0.
MBAR = MBAR/TMOLES
DCDT = 0.
GO TO 35
C
*** RICH CASE INITIALIZATION
C
13 TMOLES = PSI+ PHI*(2.-EPS)
X(5) = 0.
X(6) = PSI/TMOLES
X(7) = 0.
MBAR = MBAR/TMOLES
BETA0 = 2.*(1.-EPS*PHI)
CB1 = 2.*(PHI-1.) + EPS*PHI
GA1 = 2.*EPS*PHI*(PHI-1.)
C
*** RICH CASE ENTRY AFTER FIRST TIME
C
20 Z = 1000./T
K = EXP(2.743 + Z*(-1.761 + Z*(-1.611 + Z*.2803)))
DKDT = -K*Z*(-1.761 + Z*(-3.222 + Z*.9409))/T
ALPHA = 1. - K
BETA = BETA0 + CB1*K
GAMMA = GA1*K
C = (- BETA + SQRT(BETA*BETA + 4.*ALPHA*GAMMA))/(2.*ALPHA)
DCDT=DKDT*(C*(CB1+C)-GA1)
DCDT = DCDT/(2.*ALPHA*C + BETA)/TMOLES
X(1) =(EPS*PHI - C)/TMOLES
X(2) = (BETA0 + C)/TMOLES
X(3) = C/TMOLES
X(4) = (2.*(PHI-1.)-C)/TMOLES
C
CONVERT COMPOSITION TO MOLE FRACTIONS AND CALCULATE AVERAGE
MOLECULAR WEIGHT
C
35 IER = 0
IF (T .LT. 100.) IER = 1
IF (T .GT. 6000.) IER = 2
IR = 1
IF (T .LT. 500.) IR = 2
C
CALCULATE H, CP, AND CT AS IN WRITEUP USING FITTED
COEFFICIENTS FROM JANAF TABLES
C
ENTHLP = 0.
CSUBP = 0.
CPFROZ = 0.
ST = T/1000.
DO 40 J = 1,8
TH = ((( A(4,J,IR)/4.*ST + A(3,J,IR)/3. ) *ST
1 + A(2,J,IR)/2. ) *ST + A(1,J,IR) ) *ST
TCP = (( A(4,J,IR)*ST + A(3,J,IR) ) *ST
1 +A(2,J,IR)) *ST+A(1,J,IR)+A(5,J,IR)/ST**2

```

APP17280
APP17290
APP17300
APP17310
APP17320
APP17330
APP17340
APP17350
APP17360
APP17370
APP17380
APP17390
APP17400
APP17410
APP17420
APP17430
APP17440
APP17450
APP17460
APP17470
APP17480
APP17490
APP17500
APP17510
APP17520
APP17530
APP17540
APP17550
APP17560
APP17570
APP17580
APP17590
APP17600
APP17610
APP17620
APP17630
APP17640
APP17650
APP17660
APP17670
APP17680
APP17690
APP17700
APP17710
APP17720
APP17730
APP17740
APP17750
APP17760
APP17770
APP17780
APP17790
APP17800
APP17810
APP17820
APP17830
APP17840
APP17850
APP17860
APP17870
APP17880
APP17890
APP17900
APP17910
APP17920
APP17930
APP17940
APP17950
APP17960
APP17970
APP17980
APP17990
APP18000
APP18010
APP18020
APP18030

```

      TH = TH - A(5,J,IR)/ST + A(6,J,IR)
      ENTHLP = ENTHLP + TH*X(J)
      CPFROZ = CPFROZ + TCP*X(J)
40    CSUBP = CSUBP + 1000.*TH*DCDT*TABLE(J)
      ENTHLP = ENTHLP/MBAR
      CPFROZ=CPFROZ/MBAR
      CSUBP=CPFROZ+CSUBP/MBAR
      CPB=CSUBP

C
C
C
C
      NOW CALCULATE RHO AND ITS PARTIAL DERIVATIVES
      USING PERFECT GAS LAW

      RHOB= PSCOR*MBAR*P/T
      RB=RGAS/MBAR
      GAMB=CPB/(CPB-RB)

C
      IF(GAMB.LT.1..OR.GAMB.GT.2.)THEN
      PRINT*
      PRINT* ..... EXECUTION STOPPED AT CLDPRD .....
      PRINT*
      PRINT* 'T =',T, ' P =',P
      PRINT* 'X(1) =',X(1), ' X(2) =',X(2)
      PRINT* 'X(3) =',X(3), ' X(4) =',X(4)
      PRINT* 'X(5) =',X(5), ' X(6) =',X(6)
      PRINT* 'X(7) =',X(7), ' RB =',RB
      PRINT* 'CPB =',CPB, ' GAMB =',GAMB
      PRINT*
      PRINT* ..... EXECUTION STOPPED AT CLDPRD .....
      PRINT*
      ENDIF
      IF(GAMB.LT.1..OR.GAMB.GT.2.) STOP

C
C
      * ALL DONE
      RETURN
      END
CUPROP ..... VERSION 2.0 1/10/76 .....
C
C
C
C
      SUBROUTINE UPROP
C
C
C
C
      PURPOSE
      TO CALCULATE THE ENTHALPY AND DENSITY OF A HOMOGENOUS MIXTUR
      OF AIR, RESIDUAL GAS, AND FUEL AS A FUNCTION OF
      EQUIVALENCE RATIO, TEMPERATURE, AND PRESSURE
C
C
C
C
      USAGE
      CALL UPROP(P,T,ENTHLP,CSUBP,RHO)
C
C
C
C
      DESCRIPTION OF PARAMETERS
      GIVEN
      P - ABSOLUTE PRESSURE OF PRODUCTS (ATM)
      T - TEMPERATURE OF PRODUCTS (DEG K)
      GIVEN IN COMMON AREA /CHARGE/
      RESFRK- RESIDUAL GAS FRACTION
      PHI - EQUIVALENCE RATIO (FUEL/AIR RATIO DIVIDED BY THE
      CHEMICALLY CORRECT FUEL/AIR RATIO)
      GIVEN IN COMMON AREA /FUEL/
      AF(I) - 6 DIMENSIONAL VECTOR OF ENTHALPY COEFFICIENTS SUCH
      THAT THE ENTHALPY OF FUEL VAPOR AS A FUNCTION
      OF TEMPERATURE ( T DEG K ) IS GIVEN BY
      H(T) = AF(1)*ST + (AF(2)*ST**2)/2 + (AF(3)*ST**3)/3
      + (AF(4)*ST**4)/4 - AF(5)/ST + AF(6)
      WHERE ST = T/1000 AND H(T) = <KCAL/MOLE>
      FOR MOST APPLICATIONS THE ENTHALPY FUNCTION H(
      BE VALID OVER AT LEAST THE FOLLOWING TEMPERATURE RAN
      300 < T < 1000
      ENTHALPY DATUM STATE IS AT T = 0 ABSOLUTE WITH O2,N2
      AND H2 GASEOUS AND C SOLID GRAPHITE.
      ENW - AVERAGE NUMBER OF NITROGEN ATOMS PER FUEL MOLECULE
      CX - AVERAGE NUMBER OF CARBON ATOMS PER FUEL MOLECULE
      HY - AVERAGE NUMBER OF HYDROGEN ATOMS PER FUEL MOLECULE
      OZ - AVERAGE NUMBER OF OXYGEN ATOMS PER FUEL MOLECULE
      QLOWER- LOWER HEATING VALUE (KCAL/G)
      GIVEN IN COMMON AREA/OXDANT/
      XI - MOLAR N O RATIO OF THE OXIDANT (FOR AIR XI = 3.76)

```

APP18040
APP18050
APP18060
APP18070
APP18080
APP18090
APP18100
APP18110
APP18120
APP18130
APP18140
APP18150
APP18160
APP18170
APP18180
APP18190
APP18200
APP18210
APP18220
APP18230
APP18240
APP18250
APP18260
APP18270
APP18280
APP18290
APP18300
APP18310
APP18320
APP18330
APP18340
APP18350
APP18360
APP18370
APP18380
APP18390
APP18400
APP18410
APP18420
APP18430
APP18440
APP18450
APP18460
APP18470
APP18480
APP18490
APP18500
APP18510
APP18520
APP18530
APP18540
APP18550
APP18560
APP18570
APP18580
APP18590
APP18600
APP18610
APP18620
APP18630
APP18640
APP18650
APP18660
APP18670
APP18680
APP18690
APP18700
APP18710
APP18720
APP18730
APP18740
APP18750
APP18760
APP18770
APP18780


```

C      GET THE COMPOSITION IN MOLES/MOLE OXYGEN OF OXIDANT
C
PCTRES = RESFRK
PCTNEW = 1.0 - RESFRK
MBAR=(12.+1./DEL)*(PHIFR*PCTNEW+PHIEGR*PCTRES)*EPS+32.+28.*XI
IF (RICH) GO TO 13
C
C *** THE LEAN VALUES NOT DEPENDENT ON TEMP. (CONSTANT)
C
  I1 = 3
  TMOLES=XI+(1.+EPS*PHIFR/CX)*PCTNEW
  &  +(1.+(1.-EPS)*PHIEGR+EPS*PHIEGR*(Z+W/2.))*PCTRES
  X(1) = EPS*PHIEGR*PCTRES/TMOLES
  X(2) = (2.*(1. - EPS) + EPS*Z)*PHIEGR*PCTRES/TMOLES
  X(3) = 0.
  X(4) = 0.
  X(5) = ((1.-PHIEGR)*PCTRES+PCTNEW)/TMOLES
  X(6) = (XI + EPS*PHIEGR*W/2.*PCTRES)/TMOLES
  X(7) = PCTNEW*EPS*PHIFR/CX/TMOLES
C
  MBAR = MBAR/TMOLES
  DCDT = 0.
  GO TO 35
C
C *** THE RICH CASE
C
  13 TMOLES= XI+(1.+EPS*PHIFR/CX)*PCTNEW
  1  +((2.-EPS)*PHIEGR+EPS*PHIEGR*(Z+W/2.))*PCTRES
  X(5) = PCTNEW/TMOLES
  X(6) = (XI+EPS*PHIEGR*W/2.*PCTRES)/TMOLES
  X(7) = PCTNEW*EPS*PHIFR/CX/TMOLES
  MBAR = MBAR/TMOLES
C
C *** THE CALCULATIONS THAT MUST BE PERFORMED EACH TIME
C
  CB1 = 2.*(PHIEGR-1.) + EPS*PHIEGR
  GA1 = 2.*EPS*PHIEGR*(PHIEGR-1.)
  BETA0 = EPS*PHIEGR*Z + 2.*(1.-EPS*PHIEGR)
C
C *** THE RICH CASE ENTRY
C
  20 ZT = 1000./T
  K = EXP(2.743 + ZT*(-1.761 + ZT*(-1.611 + ZT*.2803)))
  DKDT = -K*ZT*(-1.761 + ZT*(-3.222 + ZT*.9409))/T
  ALPHA = 1.0 - K
  BETA = BETA0 + CB1*K
  GAMMA = GA1*K
  XX = BETA*BETA + 4.*ALPHA*GAMMA
  PRINT*,XX
C
  C = (-BETA + SQRT(BETA*BETA + 4.*ALPHA*GAMMA))/(2.*ALPHA)
  DCDT=-DKDT*(C*(CB1+C)-GA1)
  DCDT = DCDT/(2.*ALPHA*C + BETA)/TMOLES
  X(1) = (EPS*PHIEGR - C)*PCTRES/TMOLES
  X(2) = (BETA0 + C)*PCTRES/TMOLES
  X(3) = C*PCTRES/TMOLES
  X(4) = (2.0*(PHIEGR - 1.) - C)*PCTRES/TMOLES
C
C *** ENTRY FOR CALCULATION OF ENTHALPY
C
  35 IR = 1
  IF (T .LT. 500.) IR = 2
C
C      CALCULATE H, CP, AND CT AS IN WRITEUP, USING FITTED
C      COEFFICIENTS FROM JANAF TABLES
C
  ENTHLP = 0.
  CSUBP = 0.
  CSUBT = 0.
  ST = T/1000.
  DO 40 J = 1,6
  TH = ((( A(4,J,IR)/4.*ST + A(3,J,IR)/3. ) *ST
  1  + A(2,J,IR)/2.)*ST + A(1,J,IR) ) *ST
  TCP = (( A(4,J,IR)*ST + A(3,J,IR) ) *ST
  1  + A(2,J,IR))*ST + A(1,J,IR)+A(5,J,IR)/ST**2
  TH = TH - A(5,J,IR)/ST + A(6,J,IR)
  ENTHLP = ENTHLP + TH*X(J)
  40 CSUBP = CSUBP + TCP*X(J)+ 1000.*TH*DCDT*PCTRES*TABLE(J)

```

APP19540
 APP19550
 APP19560
 APP19570
 APP19580
 APP19590
 APP19600
 APP19610
 APP19620
 APP19630
 APP19640
 APP19650
 APP19660
 APP19670
 APP19680
 APP19690
 APP19700
 APP19710
 APP19720
 APP19730
 APP19740
 APP19750
 APP19760
 APP19770
 APP19780
 APP19790
 APP19800
 APP19810
 APP19820
 APP19830
 APP19840
 APP19850
 APP19860
 APP19870
 APP19880
 APP19890
 APP19900
 APP19910
 APP19920
 APP19930
 APP19940
 APP19950
 APP19960
 APP19970
 APP19980
 APP19990
 APP20000
 APP20010
 APP20020
 APP20030
 APP20040
 APP20050
 APP20060
 APP20070
 APP20080
 APP20090
 APP20100
 APP20110
 APP20120
 APP20130
 APP20140
 APP20150
 APP20160
 APP20170
 APP20180
 APP20190
 APP20200
 APP20210
 APP20220
 APP20230
 APP20240
 APP20250
 APP20260
 APP20270
 APP20280

```

C THIS PART IS FOR FUEL PROPANE
  FM=44.09
  RFV=RGAS/FM
  TH= RFV*(((0.233361E-10/5.*T - 0.545131E-7/4.)*T
1      +0.351709E-4/3.)*T
1      +0.157505E-1/2.)*T
1      +1.31841)*T
1      -14091.3) + 201.1 +RFV*T
  TH=TH*1.0E-3*FM
  TCP=RFV*(((0.233361E-10*T - 0.545131E-7)*T
1      +0.351709E-4)*T
1      +0.157505E-1)*T
1      +1.31841) + RFV
  TCP=FM*TCP
  ENTHLP= ENTHLP + TH*X(7)
  CSUBP= CSUBP + TCP*X(7) + 1000.*TH*DCDT*PCTRES*TABLE(7)
  ENTHLP = ENTHLP/MBAR
  CSUBP = CSUBP/MBAR
  CPU=CSUBP

```

```

C NOW CALCULATE RHO AND ITS PARTIAL DERIVATIVES
C USING PERFECT GAS LAW
C

```

```

RHO=PSCOR*MBAR*P/T
RHOU=RHO
RU=RGAS/MBAR
GAMU=CSUBP/(CSUBP-RU)

```

```

C IF (GAMU.LT.1..OR.GAMU.GT.2.) THEN
  PRINT*, '
  PRINT*, '***** EXECUTION STOPPED AT UPROP *****'
  PRINT*, '
  PRINT*, 'T =', T, ' P =', P
  PRINT*, 'X(1) =', X(1), ' X(2) =', X(2)
  PRINT*, 'X(3) =', X(3), ' X(4) =', X(4)
  PRINT*, 'X(5) =', X(5), ' X(6) =', X(6)
  PRINT*, 'X(7) =', X(7), ' RU =', RU
  PRINT*, 'CPU =', CPU, ' GAMU =', GAMU
  PRINT*, '
  PRINT*, '***** EXECUTION STOPPED AT UPROP *****'
  PRINT*, '
  ENDF
  IF (GAMU.LT.1..OR.GAMU.GT.2.) STOP

```

```

C ALL DONE
C RETURN

```

- APP20290
- APP20300
- APP20310
- APP20320
- APP20330
- APP20340
- APP20350
- APP20360
- APP20370
- APP20380
- APP20390
- APP20400
- APP20410
- APP20420
- APP20430
- APP20440
- APP20450
- APP20460
- APP20470
- APP20480
- APP20490
- APP20500
- APP20510
- APP20520
- APP20530
- APP20540
- APP20550
- APP20560
- APP20570
- APP20580
- APP20590
- APP20600
- APP20610
- APP20620
- APP20630
- APP20640
- APP20650
- APP20660
- APP20670
- APP20680
- APP20690
- APP20700
- APP20710
- APP20720
- APP20730
- APP20740


```
IF(I.GE.50) STOP  
IF(ABS(FRE)/VE.LE.1.E-03) GO TO 3.  
2 CONTINUE  
3 IF(RE.GE.((RR+RS)**2.+H**2.))**.5)THEN  
RE = ((RR+RS)**2.+H**2.))**.5  
AE = 0.  
ENDIF  
C  
4 RETURN  
END
```

```
APP21500  
APP21510  
APP21520  
APP21530  
APP21540  
APP21550  
APP21560  
APP21570  
APP21580  
APP21590
```

APPENDIX J

C	----- SUBROUTINE ISCOMP -----	APP21610
C		APP21620
C		APP21630
C		APP21640
C		APP21650
C		APP21660
C		APP21670
C	GIVEN : VOLI = TOTAL VOLUME BEFORE COMPRESSION	APP21680
C	VOLF = TOTAL VOLUME AFTER COMPRESSION	APP21690
C	PIN = PRESSURE BEFORE COMPRESSION	APP21700
C	GIVEN IN COMMON BLOCK :	APP21710
C	TEMP(I) = TEMPERATURE OF EACH PARTICLE BEFORE COMPRESSION	APP21720
C	VOL(I) = VOLUME OF EACH PARTICLE BEFORE COMPRESSION	APP21730
C	FFR(I) = FUEL FRACTION OF EACH PARTICLE	APP21740
C		APP21750
C	RETURN : POUT = PRESSURE AFTER COMPRESSION	APP21760
C	RETURN IN COMMON BLOCK :	APP21770
C	TEMP(I) = TEMPERATURE OF EACH PARTICLE AFTER COMPRESSION	APP21780
C	VOL(I) = VOLUME OF EACH PARTICLE AFTER COMPRESSION	APP21790
C		APP21800
C	SUBROUTINE NEEDED : UPROP, CLDPRD	APP21810
C		APP21820
C	-----	APP21830
C	SUBROUTINE ISCOMP(VOLI,VOLF,PIN,POUT)	APP21840
	COMMON/BURN/FFR(9999),IBURN(9999)	APP21850
	COMMON/TEMVOL/TEMP(9999),VOL(9999)	APP21860
	COMMON/PARNUM/N,NT,N1,N2,N3	APP21870
	COMMON/UGASP/CCU(7),MBARU,RU,GAMU,CPU,HU,TU,RHOU	APP21880
	COMMON/BGASP/CCB(7),MBARB,RB,GAMB,CPB,HB	APP21890
	COMMON/CHARB/PHI	APP21900
	REAL VNEW(9999)	APP21910
C		APP21920
C	FO=44./((44.+5.*(32.+3.76*28)/PHI)	APP21930
C		APP21940
	CALL UPROP(PIN,TEMP(NT+1),ENTHLP,CSUBP,RHO)	APP21950
	POUT = PIN*(VOLI/VOLF)**GAMU	APP21960
	DO 2 ITS = 1,50	APP21970
	TOVOL=0.	APP21980
	UNB=0.	APP21990
	DO 1 I =1,NT+1	APP22000
	IF (IBURN(I).EQ.2) THEN	APP22010
	IF (UNB.EQ.0.) THEN	APP22020
	CALL UPROP(PIN,TEMP(I),ENTHLP,CSUBP,RHO)	APP22030
	UNB=1.	APP22040
	ENDIF	APP22050
	VNEW(I) = VOL(I)*(POUT/PIN)**(-1./GAMU)	APP22060
	TOVOL=TOVOL+VNEW(I)	APP22070
	ELSE	APP22080
	CALL CLDPRD(PIN,TEMP(I),H,CP,RHO,IER)	APP22090
	VNEW(I) = VOL(I)*(POUT/PIN)**(-1./GAMB)	APP22100
	TOVOL=TOVOL+VNEW(I)	APP22110
	ENDIF	APP22120
1	CONTINUE	APP22130
	TOVOL = TOVOL + (N-NT-1.)*VNEW(NT+1)	APP22140
C		APP22150
	POUT=POUT*(TOVOL/VOLF)**GAMB	APP22160
	IF (ABS(TOVOL-VOLF)/VOLF.LE.1.E-05) GO TO 9	APP22170
	IF (ITS.GE.50) PRINT*	APP22180
	1 ... NUMBER OF ITERATION EXCEEDS LIMIT IN "ISCOMP" 1	APP22190
	IF (ITS.GE.50) STOP	APP22200
2	CONTINUE	APP22210
C		APP22220
		APP22230
9	UNB=0.	APP22240
	DO 3 I =1,MIN(N,9999)	APP22250
	IF (I.LE.NT+1) THEN	APP22260
	IF (IBURN(I).EQ.2) THEN	APP22270
	IF (UNB.EQ.0.) THEN	APP22280
	CALL UPROP(PIN,TEMP(I),ENTHLP,CSUBP,RHO)	APP22290
	UNB=1.	APP22300
	ENDIF	APP22310
	VOL(I)=VNEW(I)	APP22320
	TEMP(I)=TEMP(I)*(POUT/PIN)**((GAMU-1.)/GAMU)	APP22330
	ELSE	APP22340
	CALL CLDPRD(PIN,TEMP(I),H,CP,RHO,IER)	APP22350

```
VOL(I)=VNEW(I)  
TEMP(I)=TEMP(I)*(POUT/PIN)**((GAMB-1.)/GAMB)  
ENDIF  
ELSE  
VOL(I) = VOL(NT+1)  
TEMP(I) = TEMP(NT+1)  
ENDIF  
3 CONTINUE  
C  
RETURN  
END
```

```
APP22360  
APP22370  
APP22380  
APP22390  
APP22400  
APP22410  
APP22420  
APP22430  
APP22440  
APP22450  
APP22460
```

APPENDIX K

		APP22480
		APP22490
		APP22500
		APP22510
		APP22520
		APP22530
C		APP22540
C	SUBROUTINE CODE(X,XEND,Y,YPRIM,DPDT,NQ,EPS1,EPS2,HLAST)	APP22550
	COMMON/BURN/FFR(9999),IBURN(9999)	APP22560
	COMMON/TEMVOL/TEMP(9999),VOL(9999)	APP22570
	COMMON/CRANGL/SA,CRG,CRGSTP	APP22580
	REAL YY(1000),YP(1000),YPRIM(1000)	APP22590
	REAL Y(NQ),YPRIM(NQ)	APP22600
C	IF(NQ.GT.1000) PRINT*,'. NUM OF EQUATIONS > 1000 !'	APP22610
	IF(NQ.GT.1000) STOP	APP22620
C	CALL FCN(NQ,X,Y,YPRIM,DPDT)	APP22630
	TERMIN=ABS(Y(1)/YPRIM(1))	APP22640
	DO 7 I = 2,NQ	APP22650
	IF(Y(I).EQ.0..OR.YPRIM(I).EQ.0.) GO TO 7	APP22660
	IF(ABS(Y(I)/YPRIM(I)).LT.TERMIN) TERMIN=ABS(Y(I)/YPRIM(I))	APP22670
7	CONTINUE	APP22680
	H=AMAX1(EPS1*TERMIN,HLAST,XEND/10)	APP22690
C	PRINT*,' FIRST H =',H	APP22700
	NITS=0	APP22710
	NRH=0	APP22720
	NIH=0	APP22730
	DO 10 ISTEP = 1,100	APP22740
	IF(ISTEP.EQ.51) PRINT*,' WRN : NUM OF STEP > 50 AT CRG =',CRG	APP22750
	IF(ISTEP.GT.99) PRINT*,' NUM OF STEP > 99 AT CRG =',CRG	APP22760
	IF(ISTEP.GT.99) STOP	APP22770
	IFLAG = 0	APP22780
	IF(X+H.GT.XEND) HLAST=H	APP22790
	IF(X+H.GT.XEND) H=XEND-X	APP22800
8	ITS = 0	APP22810
	CALL FCN(NQ,X,Y,YPRIM,DPDT)	APP22820
	DO 11 I = 1,NQ	APP22830
	YY(I)=Y(I)	APP22840
	YPRIM(I)=YPRIM(I)	APP22850
	Y(I)=Y(I)+H*YPRIM(I)	APP22860
11	CONTINUE	APP22870
9	DO 12 I = 1,NQ	APP22880
	YP(I)=Y(I)	APP22890
12	CONTINUE	APP22900
	CALL FCN(NQ,X+H,Y,YPRIM,DPDT)	APP22910
	DO 13 I = 1,NQ	APP22920
	Y(I)=YY(I)+H/2.*(YPRIM(I)+YPRIM(I))	APP22930
13	CONTINUE	APP22940
	ITS=ITS+1	APP22950
	NITS=NITS+1	APP22960
	DO 14 I = 1,NQ	APP22970
	IF(Y(I).EQ.0..OR.YP(I).EQ.0.) GO TO 14	APP22980
	DIF=ABS(Y(I)-YP(I))/AMIN1(Y(I),YP(I))	APP23000
	IF(DIF.GE.EPS2.AND.ITS.LT.5) GO TO 9	APP23010
	IF(DIF.GE.EPS2.AND.ITS.GE.5) THEN	APP23020
	IF(IFLAG.EQ.2)	APP23030
1	PRINT*,' WRN : H IS REDUCED THE 3RD TIME AT STEP',ISTEP	APP23040
	IF(IFLAG.GE.3)	APP23050
1	PRINT*,' STEP CONVERGENCE FAILED. DIF/EPS2 =',DIF/EPS2	APP23060
	IF(IFLAG.GE.3) STOP	APP23070
	H=AMAX1(AMIN1(H/2.,H/DIF*EPS2),H/5.)	APP23080
	IFLAG=IFLAG+1	APP23090
	NRH=NRH+1	APP23100
	DO 15 J = 1,NQ	APP23110
	Y(J)=Y(J)	APP23120
15	CONTINUE	APP23130
	IF(IFLAG.LE.3) GO TO 8	APP23140
	ENDIF	APP23150
	IF(ISTEP.EQ.1) THEN	APP23160
	ENDIF	APP23170
14	CONTINUE	APP23180
	X=X+H	APP23190
	IF(X.EQ.XEND) GO TO 20	APP23200
	IF(ITS.LE.2) H=H*1.5	APP23210
		APP23220

```
IF(ITS.LE.2) NIH=NIH+1
10 CONTINUE
C
C 20 PRINT*, ' STEPS TAKEN = ', ISTEP, ' CORRECTOR ITERATION = ', NITS
C PRINT*, ' STEPSIZE REDUCTION = ', NRH, ' STEPSIZE INCREASE = ', NIH
C PRINT*, ' LAST H = ', HLAST
20 RETURN
END
```

```
APP23230
APP23240
APP23250
APP23260
APP23270
APP23280
APP23290
APP23300
```

